Separating the Kinetic and Sorption Parameters of Mixed Chlorinated Solvents in Contact with Granular Iron

Bei Huang
M.S. of China University of Geosciences, 2004

Submitted to the Department of Geology and the Faculty of the Graduate School of the University of Kansas in Partial Fulfillment of the Requirements for The Degree of Doctor of Philosophy

May 2011

Advisory Committee:

_____
J.F. Devlin, Chair

_____
Andrea Brookfield

_____
Gwen L. Macpherson

_____
Edward F. Peltier

_____
George Tsoflias

Date Defended: _____

The Dissertation Committee for Bei Huang certifies that this is the approved version of the following dissertation:

Separating the Kinetic and Sorption Parameters of Mixed Chlorinated Solvents in Contact with Granular Iron

Advisory Committee:

_____
J.F. Devlin, Chair

_____
Andrea Brookfield

_____
Gwen L. Macpherson

_____
Edward F. Peltier

_____
George Tsoflias

Date Approved: _____

Abstract

Chlorinated solvents and nitroaromatic solvents in drinking-water supplies are an important concern for public health. Granular iron, the most common medium in permeable reactive barriers (PRBs), is very effective at removing organic chemicals, such as chlorinated solvents and nitroaromatic compounds, from groundwater. In an effort to improve barrier designs, studies have been undertaken to examine the iron surface, as well as the reaction kinetics of granular iron. The development of the kinetic iron model (KIM) in 2009, which was derived specifically for PRB settings, made it possible for the first time to assess the simultaneous contributions of sorption and reaction to contaminant degradation rates in iron PRBs, providing a new tool to improve PRB design.

This work extended the previous studies that used KIM by applying the kinetic model to study the effects of iron aging on the reaction kinetics of chlorinated solvents and nitroaromatic solvents. It was found that over time and exposure to water and oxidizing organics, iron tended to lose sorption sites associated with the highest reactivities, but gained reactive sorption capacity to sites with lower reactivity. In the short term, the increasing sorption capacity led to overall faster reaction rates than were observed with new iron.

The results also indicated that the KIM parameters were more than simple fitting parameters. As expected, the nitroaromatic compounds tested (4ClNB and 4AcNB) reacted faster than the chlorinated solvents tested (PCE and TCE). Analysis of the data with the KIM indicated the rate differences were due to the surface reaction rate constant, not sorption. This result matched expectations based on earlier studies of these classes of organic chemicals.

To test the accuracy of the estimated kinetic and sorption parameters, determined in this work, a one dimensional transport model with Langmuir sorption and KIM kinetics was developed to generate synthetic data sets. The model was prepared with the ability to assess intra- and interspecies competition between TCE and PCE in the column experiments. Synthetic data were analyzed with the methods used to interpret the laboratory data and accurate estimates of the input parameters were calculated, validating the methodology.

Finally, the activation energy of the 4-chloronitrobenzene reacting with two types of granular iron, Connelly iron and QMP, in batch reactors was obtained to assess the role of mass transfer in controlling the kinetics. Previous work had indicated that mass transfer was not rate controlling with Connelly iron, but QMP was a texturally different form of granular iron that needed further testing. QMP exhibited slower reaction rates compare to Connelly iron. Based on the estimated activation energies (E_a) of the reduction reactions, the reaction mechanism(s) for 4ClNB transformation on Connelly iron and QMP iron were both electron transfer controlled, and the result also suggest that the different transformation rates were therefore related to phases on the solid surface.

Key words: granular iron, chlorinated solvents, kinetic iron model, aging, sorption, competition, transport model

Vita

Bei Huang was born in Shanghai, China on April 1979. After completing her degree at Zhoushan High School, Zhoushan, Zhejiang in 1997, she entered the China University of Geosciences (CUG), received the degree of Bachelor of Civil Engineering in July, 2001. Meanwhile, she also entered the Huazhong University of Science & Technology (HUST) and minored at Computer Science and Technology in July, 2001. She then entered the Graduate School of the School of Environmental Study of CUG and received a Master of Science degree at Environmental Engineering in July, 2004.

Acknowledgements

I would like to express my deepest gratitude to my advisor, Dr. J.F. Devlin, for his guidance, support, care and encouragement through my PhD study. With a very nice personality, Dr. Devlin is dedicated to his students. Besides advising our studies and research, he also looks for every opportunity for us to develop useful skills for our future careers, and set up a model for us to be a person with honor and dignity. His office is always open to us for all kinds of discussions. I really enjoyed my study and research with him at the University of Kansas.

The research was funded by the National Science Foundation (NSF) Carrier Grant 0134545 to Dr. J.F. Devlin. The experiments in this study were performed at the Kansas Geological Survey, University of Kansas. Jaqueline Grunau from the University of Kansas and Tanille Bagy from Haskell Indian Nations University have helped in the experimental works. Dr. Erping Bi (post-doc research associate) from the China University of Geosciences (Beijing) has provided work assistance and valuable discussions. Ian Bowen, Rubina Firdous, Natalie Garven, Peter Schillig and James Taylor Lyons from the University of Kansas also helped and supported this research. I'd like to extend my sincere gratitude to all these people.

I would like to thank my PhD committee members, Dr. Andrea Brookfield, Dr. Gwen L. Macpherson, Dr. George Tsoflias and Dr. Edward F. Peltier for their guidance and help in reviewing this dissertation.

Also I'd like to thank my parents and my husband for their support and understanding throughout my study. Without their assistance and encouragement, I would not be able to go to a foreign country and focus on my research and finish it on time.

Table of Contents

List of Figures

List of Tables

1 Introduction

The goal of this work was to quantify several factors controlling reaction rates of common chlorinated solvents in solutions contacting granular iron (GI), also known as zero valent iron (ZVI). With the introduction of the kinetic iron model (KIM), the ability to uniquely identifying the sorption and kinetic parameters of the solvent reduction reactions was available for the first time. These were examined as a function of organic compound type and GI age. In addition, an evaluation of mass transfer as a rate controlling mechanism was undertaken. The processes were evaluated with novel experimental designs and data interpretation methods, which were verified using a numerical model created as part of this work to simulate transport and reaction according to the KIM assumptions.

1.1 Treating Chlorinated Solvents in Groundwater

Chlorinated solvents are among the most frequently detected contaminants in groundwater (NAS, 1994), as a consequence of their widespread use in industrial cleaning and degreasing processes during the past half century. Many of these compounds are sufficiently toxic at low concentrations (parts per billion) to render groundwater unsuitable for drinking, and most have been found to have long half-lives in natural subsurface environments (Vogel *et al.*, 1987; Campbell *et al.*, 1997). Chlorinated solvents have been designated as priority pollutants by the United States Environmental Protection Agency and are regulated by the Safe Drinking Water Act Amendment of 1987 (Karanfil and Dastgheib, 2004). For example, the Maximum Contaminant Level Goal **(**MCLG) of EPA's drinking water regulations for trichloroethylene is zero, and the

maximum acceptable contaminant level for trichloroethylene is 0.005 mg/L or 5 ppb (Cai *et al.*, 2007).

As a major class of dense non-aqueous phase liquids (DNAPL), chlorinated solvents are heavier than water, low in solubility, and may be highly retarded relative to the rate of groundwater flow in many aquifers (Hueper *et al.*, 2003). So, source zones containing chlorinated solvents can persist in aquifers for many decades, or even centuries. Also since chlorinated solvents can migrate downward through unconsolidated deposits and fractured bedrock, they can form pools on the tops of impermeable layers at various depths in the subsurface. Remediating chlorinated solvent spills may require several years of investigation and significant financial resources, during which time plumes of contaminated water may continue to grow. Therefore, there is an urgent requirement to develop methods of plume control for chlorinated solvents at contaminated sites.

Chlorinated solvent degradation processes involving granular iron involve the replacement of halogen atoms by hydrogen, a chemical reduction. This process may either diminish health risks, as is the case for vinyl chloride transforming to ethene, or increase the health risk, as occurs when trichloroethene transforms through dichloroethene to vinyl chloride. Complete dehalogenation is the only assured way to eliminate the hazard (Arnold, 1999).

The most common approach for dealing with groundwater contaminants involves the collection of contaminated water by pumping, followed by treatment in a facility engineered for that purpose. The approach is so common that it has been colloquially named “pump-and-treat” (Higgins and Olson, 2009; Ko and Lee, 2010). Unfortunately, where DNAPL compounds are concerned, pump-and-treat is lengthy, expensive, and

sometimes ineffective (Mackay and Cherry, 1989; Gillham *et al.*, 2002; Higgins and Olson, 2009). So, researchers over the past several years have looked for alternatives to pump-and-treat system, in particular *in situ* methods have been sought (Gillham and O'Hannesin, 1994).

The basis for *in situ* treatment methods aimed at treating chlorinated solvents is varied and includes physical, biological, and chemical strategies. Physical processes involve taking advantage of the physical properties of chlorinated solvents to effect their removal from contaminated soil and groundwater (Henry *et al.*, 2003). For example, air sparging is used as a source zone remediation technology to volatilize or strip contaminants from groundwater (Adams and Reddy, 1999; Christ *et al.*, 2005; Kim *et al.*, 2007). Adsorbing materials with high surface area materials, such as fibrous and granular activated carbons is sometimes used to remove various synthetic organic contaminants from potable water supplies and industrial waste waters (Snoeyink and Summers, 1999; Karanfil and Dastgheib, 2004). Thermal remediation drives the volatilization of organic contaminants for their removal by gas extraction (Costanza *et al.*, 2005; Friis *et al.*, 2007a; Friis *et al.*, 2007c). Biological processes involve the destruction of organics such as chlorinated solvents using natural or enhanced microbial populations (Aulenta *et al.*, 2006; Kennedy *et al.*, 2006; Rittmann, 2010). Chemical treatment methods include engineered chemical transformations through the introduction of oxidizing or reducing agents to the subsurface (Henry *et al.*, 2003). Examples include permanganate (Li and Schwartz, 2004; Heiderscheidt *et al.*, 2008), manganese oxides (Ukrainczyk and McBride, 1993b; a), and persulfate (Sra *et al.*, 2010). Reductive transformations may also be engineered by reactions with zinc (Jursic and Melara, 1999; Lin and Tseng, 2000; Kim

and Carraway, 2003; Wang *et al.*, 2008), metallic iron, Fe^{2+} ion, or electrochemical means (Lin and Tseng, 2000).

Granular iron permeable reactive barriers (PRBs) have emerged as a viable *in situ* treatment alternative for groundwater contaminated with halogenated organic solvents, replacing pump-and-treat for many situations involving shallow contamination (<20 m) in porous media (EPA, 1997; Gavaskar, 1998; EPA, 1999; Klausen *et al.*, 2003; Cwiertny and Roberts, 2005). PRBs containing iron were first proposed by the University of Waterloo where it was suggested that a subsurface wall, backfilled with granular iron, and transecting the natural groundwater flow direction, could act as a barrier to the progression of contaminants in the water while the water itself passed through unhindered.

1.2 Zero-Valent Iron

Zero-valent iron (ZVI, Fe^0) is a strong reducing agent and is believed to be the active ingredient in granular iron. Granular iron is actually light steel, manufactured as an ingredient for abrasion resistance in flooring (ConnellyQPM, 2011). Compared to pump-and-treat technology, granular iron-based PRBs can be very cost effective because the operation and maintenance costs are very low (Barker *et al.*, 2000; Farrell *et al.*, 2000a; Klausen *et al.*, 2003). The passive nature of PRB operations offers significant environmental advantages by reducing the possibility of accidental human exposure to contaminants, and requiring virtually no energy input during operation (Higgins and Olson, 2009). In addition, a PRB might be expected to last at least a decade, based on at least one published field trial (Henderson and Demond, 2007; Flury *et al.*, 2009; Higgins and Olson, 2009). Studies have also been conducted to characterize surface phases that

form as reaction products from iron corrosion (Farrell *et al.*, 2000a; Gillham *et al.*, 2002; Klausen *et al.*, 2003; Satalanajaru *et al.*, 2003). Other base metals, such as zinc (Fennelly and Roberts, 1998) and magnesium (Gautam and Suresh, 2006; Patel and Suresh, 2006), have been found to be effective at mediating the reductive dehalogenation of chlorinated organic compounds in aqueous systems, but these are more expensive than iron and therefore have not been utilized in PRBs. Full- and pilot-scale granular iron barriers have been installed at hundreds of sites around the world to treat groundwater contaminated with chlorinated solvents, and a variety of other contaminants (EPA, 2000).

The success of PRBs led to research evaluating iron as treatment alternative for a wide variety of contaminants beyond the chlorinated solvents, including nitroaromatics (Devlin *et al.*, 1998; Klausen *et al.*, 2001; Keum and Li, 2004; Cavalotti *et al.*, 2009), munitions (Gui *et al.*, 2000; Odziemkowski *et al.*, 2000; Park *et al.*, 2004; Zhuang *et al.*, 2008), agrochemicals (Gibb *et al.*, 2004; Shea *et al.*, 2004), inorganics such as metals (Lai and Lo, 2008; Zhou *et al.*, 2008; Franco *et al.*, 2009; Shariatmadari *et al.*, 2009), nitrate (Park *et al.*, 2009a; Park *et al.*, 2009b; Rodriguez-Maroto *et al.*, 2009), and arsenic (Su and Puls, 2004). Studies have also been conducted to assess the effects of iron purity, granular size and brands of commercial iron on reactivity (Su and Puls, 1998; Tamara and Butler, 2004); the evaluate the effects of groundwater characteristics, such as pH, temperature, geochemical composition, and cosolvents on reactivity (Munz and Roberts, 1986; Su and Puls, 1998; McMahon *et al.*, 1999; Tamara and Butler, 2004; Devlin and Allin, 2005; Bi *et al.*, 2009a); and to measure and model reaction kinetics (Johnson *et al.*, 1996; Su and Puls, 1999; Arnold and Roberts, 2000c; Arnold and Roberts, 2000a; Scherer *et al.*, 2001; Devlin and March, 2003; Schäfer *et al.*, 2003; Bi *et al.*, 2009c). With

these studies, a better understanding of granular iron has been achieved, but details concerning the processes of reaction and sorption remain poorly understood, and an elucidation of the fundamental controls on iron reactivity remains incomplete.

1.3 Reaction Mechanisms

The oxidation of iron and reduction of chlorinated solvents is thermodynamically very favorable for highly chlorinated compounds (Matheson and Tratnyek, 1994). Electrons for the reduction are thought to come predominantly from the zero-valent iron core in the granular iron grains, although other sources of electrons have also been recognized, such as Fe^{2+} and $H_{2(g)}$ (Johnson *et al.*, 1998; Kober *et al.*, 2002) (Equations 1.1-1.4 and Figure 1.1),

$$Fe^0 \rightleftharpoons Fe^{2+} + 2e^- \quad 1.1$$

$$RCl + 2e^- + H^+ \Leftrightarrow RH + Cl^- \quad 1.2$$

$$Fe^{2+} + 2H_2O \rightleftharpoons Fe(OH)_{2(s)} + 2H^+ \quad 1.3$$

overall,

$$Fe^0 + RCl + 2H_2O \rightleftharpoons Fe(OH)_{2(s)} + RH + H^+ + Cl^- \quad 1.4$$

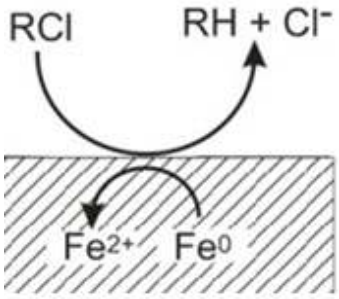

Figure 1.1: Proposed Pathways for Direct Electron Transfer from Iron Metal at the Metal Surface.

In general, reactions involving granular iron have been observed to increase the pH of the solution. For example, the reduction of water results in hydrogen gas

production and the formation of hydroxide ion (Equations 1.5 and 1.6) (Orth and Gillham, 1996; Scherer *et al.*, 1997; Henderson and Demond, 2007). Solution pH is generally seen to rise, sometimes as high as 9 or 10 (Matheson and Tratnyek, 1994; Orth and Gillham, 1996; Henderson and Demond, 2007). As mentioned above, the hydrogen gas produced can serve as a reductant in (Figure 1.2). In this case, the reaction that occurs is hydrogenolysis that may be catalyzed on the solid surface (Equation 1.8) (Matheson and Tratnyek, 1994).

$$Fe^{o} + 2H_2O \Leftrightarrow Fe^{2+} + H_{2(g)} + 2OH^{-} \quad 1.5$$

$$H_{2(g)} + RCl \Leftrightarrow RH + H^{+} + Cl^{-} \quad 1.6$$

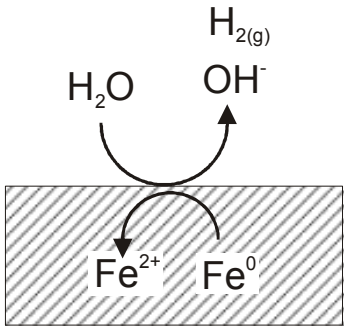

Figure 1.2: Corrosion of Iron by Water to Produce Hydrogen gas.

At elevated pH, Fe^{2+} would be expected to combine with OH^- to form hydroxide or oxy-hydroxide minerals such as $Fe(OH)_2$ or FeOOH. Thus, the iron surface is expected to become coated with these secondary phases, eventually inhibiting further reactions – in particular reactions involving surface catalysis may be profoundly affected (Matheson and Tratnyek, 1994).

1.4 Conceptual Model for Reactions Involving Granular Iron

The granular iron surface is a complex collection of different mineral phases and is generally not smooth. Therefore, the surface may be conceived as a collection of sites that may or may not sorb or react with groundwater pollutants (Burris *et al.*, 1995; Allen-King *et al.*, 1997; Deng *et al.*, 1999; Bi *et al.*, 2009b; Bi *et al.*, 2009c). In this document, the term 'reactive sites' refers to locations on the granular iron surface where reactions have the potential of occurring within a relevant time frame, such as several hours. 'Non-reactive sites' are sites where sorption occurs without the possibility of reaction, or with reactions that occur too slowly to be noticed in the relevant time frame. 'Non-reactive and non-sorptive sites' refers to locations where neither sorption nor reactions have the possibility of occurring. With these definitions in mind, the complexity of the actual surface may be simplified to make a mathematical representation of the surface possible.

The model development begins by postulating the steps leading to and following reactions. The reduction reaction occurs mainly on the iron surface, rather than in the aqueous phase (Burris *et al.*, 1998). So, the attenuation process starts with the adsorption of reactants to reactive and non-reactive sites – both of which remove reactants from the solution – the reaction takes place on the reactive sites and no reaction occurs on the nonreactive sites, then desorption of reactants or products occurs. Under conditions of constant temperature and solution geochemistry, and assuming that mass transfer limitations are either unimportant or can be overcome by efficient mixing (Arnold *et al.*, 1999), the rate of reactant transformation depends only on sorption, desorption and rates of electron transfer (Li and Farrell, 2000; Scherer *et al.*, 2001). The effects of mass transport were investigated in column studies by Bi *et al*. (Bi *et al.*, 2009b) and found to be negligible for trichloroethene and 4-chloronitrobenzene in columns packed with 85%

or more by weight iron (15% or less by weight sand). It is generally expected that the kinetics of sorption and desorption are fast compared to the reaction rate (Lai and Lo, 2008).

A simplified but useful view of the iron surface that recognizes these previous findings considers sorption to three types of sites: fast reactive, slow reactive and nonreactive sites. In addition, there are likely to be locations on the granular iron surface where sorption is negligible, and hence may be considered non-reactive non-sorptive sites (Figure 1.3).

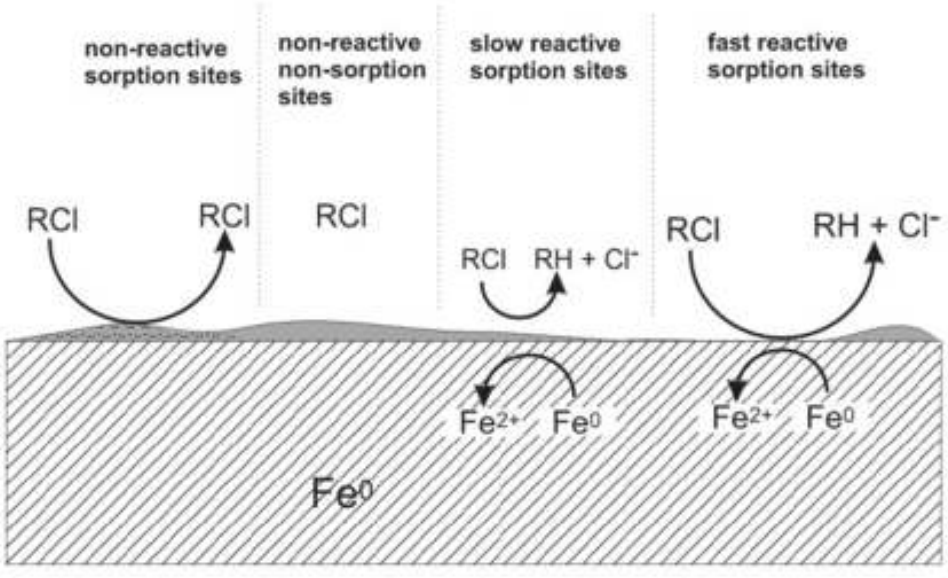

Figure 1.3: Proposed conceptual model for aqueous chlorinated solvent reactions on the granular iron surface.

Fast reactive sites may dominate observed kinetics if present in sufficient numbers. If the contrast in reaction rates at the fast sites and the slow sites is large, a relatively small number of fast reactive sites may be sufficient to dominate the observed kinetics. However, a low number of fast reactive sites could be quickly become coated with oxides, or otherwise become passivated, permitting the more numerous slow

reactive sites to become dominant in the observed reaction rates. Also, according to the conceptual model above, competition for the surface would be expected, because at a certain iron loading and solute concentration, the limited number of available sorption sites could become saturated. When this occurs, reaction rates no longer increase in proportion to reactant concentrations.

The preceding discussion applies to the conventional forms of granular iron that are commercially available, and commonly used in PRBs, such as Connelly iron. However, a newly developed iron product, QMP, consists of grains that are porous in nature. This raises the possibility that intra-grain diffusion might be more pronounced with this product, and reaction rates might be affected by this process. Therefore, additional work is needed to gather the information needed to extend the conceptual model to the QMP product.

1.5 Reaction Kinetics

A key to designing PRB treatment systems is knowledge of the reaction rates of the contaminants of concern. Ideally, a kinetic model that accounts for all experimental observations should be used to correctly design PRBs. In reality, a major component of the literature reports degradation kinetics of chlorinated solvents in terms of a first order kinetic model (Johnson *et al.*, 1996; Gander *et al.*, 2002; Devlin, 2009),

$$\frac{dC}{dt} = -k_{obs}C \qquad 1.7$$

where C is aqueous concentration of chlorinate solvents (M/L^3); k_{obs} is the reported first order observed rate constant (T^{-1}); and t is the time (T). However, experimental evidence clearly shows that the reaction is not truly first order, since reaction rates also depend on the amount of iron present. To account for this observation, some researchers (Johnson *et*

al., 1996; Devlin *et al.*, 1998; Su and Puls, 1999) expanded the pseudo-first order kinetic model with surface area normalized reaction rate constant, k_{SA} ($L^3\ T^{-1}\ M^{-2}$), as showed in the flowing equation:

$$\frac{dC}{dt} = -k_{SA}\rho_a C \qquad 1.8$$

where, ρ_a is the surface area concentration of Fe^0 ($m^2\ L^{-1}$). Alternatively ρ_a can be defined as the mass of Fe^0 per unit of water in the system, k_{SA} is surface area, or mass, normalized reaction rate constant ($L^3\ T^{-1}\ M^{-2}$). Still others have found that the reaction rate depends on the initial aqueous concentration of the aqueous contaminant being treated (Scherer and Tratnyek, 1995; Scherer *et al.*, 1997; Johnson *et al.*, 1998). Langmuir–Hinshelwood kinetics (Equation 1.9) was applied to account for surface limited reactions due to intra-competition, and Langmuir-Hinshelwood-Hougen-Watson kinetics was used to account for inter-species competition (equation not shown) assuming that mass transfer limitations are either unimportant or can be overcome by efficient mixing (Arnold and Roberts, 2000a),

$$\frac{dC_W}{dt} = -\left(\frac{kC_{max}\frac{Fe}{V}}{\frac{1}{J} + C_W}\right)C_W \qquad 1.9$$

where C_W is aqueous concentration of chlorinate solvents (M/L^3), Fe is iron mass (M), V is volume of water (L^3), C_{max} is the surface capacity for sorption (M/M_{solid}), J is the Langmuir sorption parameter describing affinity of solute for solid (L^3/M), k is the first-order rate constant for the reaction on the iron surface (T^{-1}).

The increasing complexity of the models mentioned above lead to the realization that reaction rates depend not only on the rate of electron transfer – represented by the rate constants – but also on the amount of oxidant that can be sorbed – represented by the sorption parameters. Higher sorption means a greater possibility of reaction and faster observed rates. Unfortunately, none of the kinetic models mentioned above can be used to uniquely determine the rate constant and sorption parameters separately. The rate constant is always lumped with at least one of the sorption parameters (Gillham and O'Hannesin, 1994; Vogan *et al.*, 1995; Johnson *et al.*, 1996; Arnold and Roberts, 2000a; Gillham *et al.*, 2002).

Devlin (2009) introduced a kinetic iron model (KIM) that offers the possibility of separating the sorption and reaction contributions to observed rates (Equation 1.10),

$$\frac{dC_W}{dt} = -\frac{kC_{max}\frac{Fe}{V}}{\frac{1}{J} + \frac{C_{max}\frac{Fe}{V}}{1+JC_W} + C_W} C_W \qquad 1.10$$

where the parameters are as previously defined. Unlike the Langmuir–Hinshelwood–Hougen–Watson (LHHW) model, or the Langmuir Hinshelwood (LH) model (Equation 1.9), the KIM accounts for mass sorbed to the solid surface that is in equilibrium, but not necessarily at steady state. Methods of obtaining estimates of J, C_{max}, and k from the KIM include linearization and nonlinear regression methods (Appendix D) (Marietta and Devlin, 2005; Devlin, 2009). Uncertainties in the parameter estimates were obtained from a Monte-Carlo analysis of the fittings (Devlin, 2009).

1.6 Hypothesis and Objectives of this Dissertation

According to the conceptual model presented above, the observed reaction rates between organic compounds and granular iron depend on both sorption (assumed at equilibrium) and electron transfer, provided mass transport rates to the iron surface can be assumed non-limiting. It is hypothesized that the relative roles of these two basic controls on reaction rates changes depend on iron age, compound class, and iron type. The chief objective of this study is to evaluate these hypotheses, taking advantage of the newly developed KIM. Specific objectives of the work are: (1) to evaluate the individual roles of sorption and electron transfer in determining reaction rate changes due to iron aging; (2) to evaluate the individual roles of sorption and electron transfer in determining reaction rates for two classes of organic compounds: chlorinated solvents and nitroaromatics; (3) to evaluate the KIM for reactive sites and Langmuir-type sorption to nonreactive sites as a basis for modeling granular iron column breakthrough curves; (4) to evaluate the effect of iron type on reaction kinetics by comparing conventional Connelly granular iron with a recently developed porous iron product, QMP.

1.7 Organization and Scope of this Dissertation

Each of the objectives stated above form basis of a chapter in the thesis. Chapter 2 presents base case iron kinetics, i.e., reaction rates associated with chlorinated solvents and 'fresh' (a few days of exposure to solution) surfaces, and compares this behavior with that exhibited by iron that has been exposed to solution for several weeks or months. In Chapter 3 the effect of compound class is investigated by comparing chlorinated solvent reaction rates with those of nitroaromatics. The latter compounds are known to react rapidly with granular iron, and it is usually assumed that these reactions rates are

electron transfer controlled, rather than sorption controlled. This assumption will be evaluated and the outcome compared to the chlorinated solvent case. In chapter 4, processes identified in the previous experiments will be quantitatively modeled and compared to the experimental column data. The model will be used to extend earlier KIM-based modeling to include the effects of inter- and intra-competition between TCE and PCE for the iron surface, evaluating the possible effects of competition on the current experiments. In chapter 5, a comparison of iron types is undertaken. The first type is a conventional and commercially available brand of granular iron, Connelly, of the type used in the other chapters of this thesis. The second brand is a newly developed product with a porous texture that raises the possibility of mass transport controlled kinetics due to intra-particle diffusion. Before KIM kinetics can be evaluated with such a material, the role of mass transport must be assessed. This is achieved by conducting temperature-specific kinetic experiments to determine activation energies of the organic transformations on the two iron types.

References

Adams, J. A. and K. R. Reddy (1999). "Laboratory study of air sparging of TCE-Contaminated saturated soils and ground water." Ground Water Monitoring and Remediation 19(3): 182-190.

Allen-King, R. M., R. M. Halket and D. R. Burris (1997). "Reductive Transformation and Sorption of Cis-and Trans-1,2-Dichloroethene in A Metallic Iron-Water System." Environmental toxicology and chemistry 16(3): 424-429.

Arnold, W. A. (1999). Kinetics and Pathways of Chlorinated Ethylene and Chlorinated Ethane Reaction with Zero-Valent Metals. Department of Geography and Environmental Engineering. Baltimore, Maryland Johns Hopkins University. PhD.

Arnold, W. A., W. P. Ball and A. L. Roberts (1999). "Polychlorinated ethane reaction with zero-valent zinc: pathways and rate control." Journal of Contaminant Hydrology 40(2): 183-200.

Arnold, W. A. and A. L. Roberts (2000a). "Inter- and Intraspecies Competitive Effects in Reactions of Chlorinated Ethylenes with Zero-Valent Iron in Column Reactors." Environmental Engineering Science 17(5): 291-302.

Arnold, W. A. and A. L. Roberts (2000b). "Kinetics of chlorinated ethylene reaction with zero-valent iron in column reactors." Abstracts of Papers of the American Chemical Society 219: 12-ENVR.

Aulenta, F., M. Majone and V. Tandoi (2006). "Enhanced anaerobic bioremediation of chlorinated solvents: environmental factors influencing microbial activity and their relevance under field conditions." Journal of Chemical Technology and Biotechnology 81(9): 1463-1474.

Barker, J. F., B. J. Butler, E. Cox, J. F. Devlin, R. Focht, S. M. Froud, D. J. Katic, M. McMaster, M. Morkin and J. Vogan (2000). Sequenced Reactive Barriers for Groundwater Remediation. Boca Rotan, Florida, Lewis Publishers.

Bi, E., I. Bowen and J. F. Devlin (2009). "Effect of Mixed Anions (HCO3--SO42--ClO4-) on Granular Iron (Fe-0) Reactivity." Environmental Science & Technology 43(15): 5975-5981.

Bi, E., J. F. Devlin and B. Huang (2009). "Effects of Mixing Granular Iron with Sand on the Kinetics of Trichloroethylene Reduction." Ground Water Monitoring and Remediation 29(2): 56-62.

Bi, E., J.F. Devlin and B. Huang (2009). "Transport and Kinetic Studies to Characterize Reactive and Non-Reactive Sites on Granular Iron." Environmental Science and Technology.

Burris, D. R., R. M. Allen-King, V. S. Manoranjan, T. J. Campbell, G. A. Loraine and B. Deng (1998). "Chlorinated Ethene Reduction by Cast Iron: Sorption and Mass Transfer." Journal of Environmental Engineering 7: 1012-1019.

Burris, D. R., T. J.Campbell and V. S.Manoranjan (1995). "Sorption of Trichloroethylene and Tetrachloroethylene in A Batch Reactive Metallic Iron-water System." Environmental Science and Technology 29(11): 2850-2855.

Cai, Z. S., D. N. Lerner, R. G. McLaren and R. D. Wilson (2007). "Conceptual analysis of zero-valent iron fracture reactive barriers for remediating a trichloroethylene plume in a chalk aquifer." Water Resources Research 43(3).

Campbell, T. J., D. R. Burris, A. L. Roberts and J. R. Wells (1997). "Trichloroethylene and Tetrachloroethylene Reduction in A Metallic Iron-Water-Vapor Batch System." Environmental Toxicology and Chemistry 16(4): 625-630.

Cavalotti, L. F. R., P. Peralta-Zamora, M. B. Rodrigues and T. C. B. de Paiva (2009). "Degradation of Nitroaromatic Compounds and Remediation of Residues from the Explosive Production by reductive-Oxidative Processes based on Zero-Valent Iron." Quimica Nova 32(6): 1504-1508.

Christ, J. A., C. A. Ramsburg, L. M. Abriola, K. D. Pennell and F. E. Loffler (2005). "Coupling aggressive mass removal with microbial reductive dechlorination for remediation of DNAPL source zones: A review and assessment." Environmental Health Perspectives 113(4): 465-477.

ConnellyQPM (2011). "http://www.connellygpm.com/bldgprod.html."

Costanza, J., E. L. Davis, J. A. Mulholland and K. D. Pennell (2005). "Abiotic Degradation of Trichloroethylene under Thermal Remediation Conditions." Environmental Science and Technology 39(17): 6825-6830.

Cwiertny, D. M. and A. L. Roberts (2005). "On the Nonlinear Relationship between kobs and Reductant Mass Loading in Iron Batch Systems." Environmental Science and Technology 39(22): 8948-8957.

Deng, B., D. R. Burris and T. J. Campbell (1999). "Reduction of Vinyl Chloride in Metallic Iron-Water Systems." Environmental Science & Technology 33(15): 2651-2656.

Devlin, J. F. (2009). "Development and Assessment of A Rate Equation for Chemical Transformations in Reactive Porous Media." Environmental Science and Technology.

Devlin, J. F. and K. O. Allin (2005). "Major Anion Effects on the Kinetics and Reactivity of Granular Iron in Glass-encased Magnet Batch Reactor Experiments." Environmental Science and Technology 39: 1868-1874.

Devlin, J. F., J. Klausen and R. P. Schwarzenbach (1998). "Kinetics of Nitroaromatic Reduction on Granular Iron in Recirculating Batch Experiments." Environmental Science & Technology 32(13): 1941-1947.

Devlin, J. F. and C. March (2003). Investigating the Kinetic Limitations of Granular Iron over A Large Range of 4-chloronitrobenzene Concentrations. National Meeting American Chemical Society Division of Environmental Chemistry. 43.

EPA (1997). Permeable Reactive Subsurface Barriers for the Interception and Remediation of Chlorinated Hydrocarbon and Chromium(VI) Plumes in Ground Water. U. S. E. P. A. O. o. R. a. Development. Ada, OK, National Risk Management Research Laboratory EPA/600/F-97/008.

EPA (1999). Field Applications of In Situ Remediation Technologies: Permeable Reactive Barriers. E. U. S. E. P. Agency). 542-R-99-002.

EPA (2000). Peameable Reactive Barriers Action Team. Remediation Technologies Development Forum, http://www.rtdf.org/public/permbarr/prbsumms/default.cfm.

Farrell, J., M. Kason, N. Melitas and T. Li (2000). "Investigation of the Long-term Performance of Zero-valent Iron for Reductive Dechlorination of Trichloroethylene." Environmental Science and Technology 34: 514-521.

Fennelly, J. P. and A. L. Roberts (1998). "Reaction of 1,1,1-Trichloroethane with Zero-Valent Metals and Bimetallic Reductants." Environmental Science & Technology 32(13): 1980-1988.

Flury, B., J. Frommer, U. Eggenberger, U. Mader, M. Nachtegaal and R. Ketzschmar (2009). "Assessment of Long-term Performance and Chromate Reduction Mechanisms in A Field Scale Permeable Reactive Barrier." Environmental Science and Technology 43(17): 6786-6792.

Franco, D. V., L. M. Da Silva and W. F. Jardim (2009). "Reduction of Hexavalent Chromium in Soil and Ground Water Using Zero-Valent Iron Under Batch and Semi-Batch Conditions." Water Air and Soil Pollution 197(1-4): 49-60.

Friis, A. K., E. A. Edwards, H. J. Albrechtsen, K. S. Udell, M. Duhamel and P. L. Bjerg (2007). "Dechlorination after thermal treatment of a TCE-contaminated aquifer: Laboratory experiments." Chemosphere 67(4): 816-825.

Friis, A. K., J. L. L. Kofoed, G. Heron, H. J. Albrechtsen and P. L. Bjerg (2007). "Microcosm evaluation of bioaugmentation after field-scale thermal treatment of a TCE-contaminated aquifer." Biodegradation 18(6): 661-674.

Gander, J. W., G. F. Parkin and M. M. Scherer (2002). "Kinetics of 1,1,1-Trichloroethane Transformation by Iron Sulfide and a Methanogenic Consortium." Environmental Science & Technology 36(21): 4540-4546.

Gautam, S. K. and S. Suresh (2006). "Dechlorination of DDT, DDD and DDE in soil (slurry) phase using magnesium/palladium system." Journal of Colloid and Interface Science 304(1): 144-151.

Gavaskar, A. R. (1998). Permeable Barriers for Groundwater Remediation: Design, Construction, and Monitoring. Columbus, Ohio, Battelle Press, 1998.

Gibb, C., T. Satapanajaru, S. D. Comfort and P. J. Shea (2004). "Remediating dicamba-contaminated water with zerovalent iron." Chemosphere 54(7): 841-848.

Gillham, R. W. and S. F. O'Hannesin (1994). "Enhanced Degradation of halogenated Aliphatics by Zero-Valent Iron." Ground Water 32(6): 958-967.

Gillham, R. W., K. Ritter, Y. zhang and M. S. Odziemkowski (2002). Factors in the Long-term Performance of Granular Iron PRBs. Groundwater Quality. Sheffield UK.

Gui, L., R. W. Gillham and M. S. Odziemkowski (2000). "Reduction of N-nitrosodimethylamine with granular iron and nickel enhanced iron. 1. Pathways and kinetics." Environmental Science & Technology 34(16): 3489-3494.

Heiderscheidt, J. L., R. L. Siegrist and H. Illangasekare (2008). "Intermediate-scale 2D experimental investigation of in situ chemical oxidation using potassium permanganate for remediation of complex DNAPL source zones." Journal of Contaminant Hydrology 102(1-2): 3-16.

Henderson, A. D. and A. H. Demond (2007). "Long-term performance of zero-valent iron permeable reactive barriers: A critical review." Environmental Engineering Science 24(4): 401-423.

Henry, S. M., C. H. Hardcastle and S. D. Warner (2003). Chlorinated solvent and DNAPL remediation: An overview of physical, chemical, and biological processes. Chlorinated Solvent and Dnapl Remediation - Innovative Strategies for Subsurface Cleanup. S. M. Henry and S. D. Warner. Washington, Amer Chemical Soc. 837: 1-20.

Higgins, M. R. and T. M. Olson (2009). "Life-Cycle Case Study Comparison of Permeable Reactive Barrier versus Pump-and-Treat Remediation." Environmental Science & Technology 43(24): 9432-9438.

Hueper, B. H., G. P. Wealthall, J. W. N. Smith, S. A. Leharne and D. N. Lerner (2003). An Illustrated handbook of DNAPL Transport and Fate in the Subsurface. E. Agency. Almondsbury, Bristol, Environment Agency. R&D Publication 133.

Johnson, T. L., W. Fish, Y. A. Gorby and P. G. Tratnyek (1998). "Degradation of carbon tetrachloride by iron metal: Complexation effects on the oxide surface." journal of contaminant hydrology 29(4): 379-398.

Johnson, T. L., M. M. Scherer and P. G. Tratnyek (1996). "Kinetics of halogenated organic compound degradation by iron metal." Environmental Science & Technology 30(8): 2634-2640.

Jursic, B. S. and C. Melara (1999). "Dechlorination of organic compounds with zinc dust in the presence of alkali metal halides." Abstracts of Papers of the American Chemical Society 218: 526-ORGN.

Karanfil, T. a. and S. A. Dastgheib (2004). "Trichloroethylene Adsorption by Fibrous and Granular Activated Carbons: Aqueous Phase, Gas Phase, and Water Vapor Adsorption Studies." Environmental Science and Technology 38(22): 5834-5841.

Kennedy, L. G., J. W. Everett and J. Gonzales (2006). "Assessment of biogeochemical natural attenuation and treatment of chlorinated solvents, Altus Air Force Base, Altus, Oklahoma." Journal of Contaminant Hydrology 83(3-4): 221-236.

Keum, Y. S. and Q. X. Li (2004). "Reduction of nitroaromatic pesticides with zero-valent iron." Chemosphere 54(3): 255-263.

Kim, H. M., Y. Hyun and K. K. Lee (2007). "Remediation of TCE-contaminated groundwater in a sandy aquifer using pulsed air sparging: Laboratory and numerical studies." Journal of Environmental Engineering-Asce 133(4): 380-388.

Kim, Y. H. and E. R. Carraway (2003). "Dechlorination of chlorinated phenols by zero valent zinc." Environmental Technology 24(12): 1455-1463.

Klausen, J., J. Ranke and R. P. Schwarzenbach (2001). "Influence of solution composition and column aging on the reduction of nitroaromatic compounds by zero-valent iron." Chemosphere 44(4): 511-517.

Klausen, J., P. J. Vikesland, T. Kohn, D. R. Burris, W. P. Ball and A. L. Roberts (2003). "Longevity of Granular Iron in Groundwater Treatment Processes: Solution Composition Effects on Reduction of Organohalides and Nitroaromatic compounds " Environmental Science and Technology 37: 1208-1218.

Ko, N. Y. and K. K. Lee (2010). "Information effect on remediation design of contaminated aquifers using the pump and treat method." Stochastic Environmental Research and Risk Assessment 24(5): 649-660.

Kober, R., O. Schlicker, M. Ebert and A. Dahmke (2002). "Degradation of Chlorinated Ethylenes by Fe0: Inhibition Processes and Mineral Precipitation." Environmental Geology 41: 644-652.

Lai, K. C. K. and I. M. C. Lo (2008). "Removal of chromium (VI) by acid-washed zero-valent iron under various groundwater geochemistry conditions." Environmental Science & Technology 42(4): 1238-1244.

Li, T. and J. Farrell (2000). "Reductive Dechlorination of Trichloroethene and Carbon Tetrachloride Using Iron and Palladized-Iron Cathodes." Environmental Science & Technology 34(1): 173-179.

Li, X. D. and F. W. Schwartz (2004). "DNAPL remediation with in situ chemical oxidation using potassium permanganate. Part I. Mineralogy of Mn oxide and its dissolution in organic acids." Journal of Contaminant Hydrology 68(1-2): 39-53.

Lin, C. H. and S. K. Tseng (2000). "Electrochemically reductive dechlorination of chlorophenol using nickel and zinc electrodes." Water Science and Technology 42(3-4): 167-172.

Mackay, D. M. and J. A. Cherry (1989). "Groundwater Contamination: Pump and Treat Remediation." Environmental Science and Technology 23(6): 630-636.

Marietta, M. and J. F. Devlin (2005). Separating the Kinetic and Sorption Parameters of Nitroaromatic Compounds in Contact with Granular Iron. 4th International Groundwater Quality Conference. waterloo, canada**:** 6.

Matheson, L. J. and P. G. Tratnyek (1994). "Reductive Dehalogenation of Chlorinated Methanes by Iron Metal." Environmental Science and Technology 28(12): 8.

McMahon, P. B., K. F. Dennehy and M. W. Sandstrom (1999). "Hydraulic and Geochemical Performance of a Permeable Reactive Barrier Containing zero-Valent Iron, Denver Federal Center." Ground Water 37(3): 396-404.

Munz, C. and P. V. Roberts (1986). "Effects of Solute Concentration and Cosolvents on the aqueous activity-Coefficient of Halogenated Hydrocarbons." Environmental Science and Technology 20(8): 6.

NAS (1994). Alternatives for ground water cleanup. N. A. o. Sciences. Washington, DC., National Academy Press: Washington, DC.

Odziemkowski, M. S., L. Gui and R. W. Gillham (2000). "Reduction of N-nitrosodimethylamine with granular iron and nickel-enhanced iron. 2. Mechanistic studies." Environmental Science & Technology 34(16): 3495-3500.

Orth, W. S. and R. W. Gillham (1996). "Dechlorination of Trichloroethene in Aqueous Solution Using Fe^{o}." Environmental Science and Technology(30): 66-71.

Park, H., Y. M. Park, S. K. Oh, K. M. You and S. H. Lee (2009a). "Enhanced reduction of nitrate by supported nanoscale zero-valent iron prepared in ethanol-water solution." Environmental Technology 30(3): 261-267.

Park, H., Y. M. Park, K. M. Yoo and S. H. Lee (2009b). "Reduction of nitrate by resin-supported nanoscale zero-valent iron." Water Science and Technology 59(11): 2153-2157.

Park, J., S. D. Comfort, P. J. Shea and T. A. Machacek (2004). "Remediating munitions-contaminated soil with zerovalent iron and cationic surfactants." Journal of Environmental Quality 33(4): 1305-1313.

Patel, U. and S. Suresh (2006). "Dechlorination of chlorophenols by magnesium-silver bimetallic system." Journal of Colloid and Interface Science 299(1): 249-259.

Rittmann, B. E. (2010). "Environmental Biotechnology in Water and Wastewater Treatment." Journal of Environmental Engineering-Asce 136(4): 348-353.

Rodriguez-Maroto, J. M., F. Garcia-Herruzo, A. Garcia-Rubio, C. Gomez-Lahoz and C. Vereda-Alonso (2009). "Kinetics of the chemical reduction of nitrate by zero-valent iron." Chemosphere 74(6): 804-809.

Satalanajaru, T., P. J. Shea, S. D. Comfort and Y. Roh (2003). "Green Rust and Iron Oxide Formation Influences Metolachlor Dechlorination during Zerovalent Iron Treatment." Environmental Science & Technology 37(22): 5219-5227.

Schäfer, D., R. Köber and A. Dahmke (2003). "Competing TCE and cis-DCE Degredation Kinetics by Zero-valent Iron-Experimental Results and Numerical Simulation." Journal of Contaminant Hydrology 65: 183-202.

Scherer, M. M., K. M. Johnson, J. C. Westall and P. G. Tratnyek (2001). "Mass transport effects on the kinetics of nitrobenzene reduction by iron metal." Environmental Science & Technology 35(13): 2804-2811.

Scherer, M. M. and P. G. Tratnyek (1995). Dechlorination of carbon tetrachloride by iron metal: effect of reactant concentrations. 209th ACS National Meeting. Anaheim, California. 35**:** 805-806.

Scherer, M. M., J. C. Westall, M. Ziomek-Moroz and P. G. Tratnyek (1997). "Kinetics of Carbon Tetrachloride Reduction at An Oxide-free Iron Electrode." Environmental Science and Technology 31(8): 6.

Shariatmadari, N., C. H. Weng and H. Daryaee (2009). "Enhancement of Hexavalent Chromium [Cr(VI)] Remediation from Clayey Soils by Electrokinetics Coupled with a Nano-Sized Zero-Valent Iron Barrier." Environmental engineering science 26(6): 1071-1079.

Shea, P. J., T. A. Machacek and S. D. Comfort (2004). "Accelerated remediation of pesticide-contaminated soil with zerovalent iron." Environmental Pollution 132(2): 183-188.

Snoeyink, V. L. and R. S. Summers (1999). Adsorption of Organic Compounds. In Water Quality and Treatment. A Handbook of Community Water Supplies. R. D. Letterman, Ed.; McGraw-Hill. New York: 13.11-13.82.

Sra, K., N. R. Thomson and J. F. Barker (2010). "Persistance of Persulfate in Uncontaminated Aquifer Materials." Environmental Science and Technology 44(8): 3098-3104.

Su, C. and R. W. Puls (1998). Temperature Effect on Reductive Dechlorination of Trichloethene by Zero-Valent Metals. Wickramanayake GB, Hinchee RE, eds. Physical, Chemical, and Thermal Technologies: Proceeding of the First International Conference

on Remediation of Chlorinated and Recalcitrant Compounds. Monterey, CA, Battelle Press. Columbus, OH. 1(5)**:** 317-322.

Su, C. and R. W. Puls (1999). "Kinetics of Trichloroethene Reduction by Zerovalent Iron and Tin: Pretreatment Effect, Apparent Activation Energy, and Intermediate Products." Environmental Science and Technology 33(1): 163-168.

Su, C. and R. W. Puls (2004). "Significance of Iron(II, III) Hydroxycarbonate Green Rust in Arsenic Remediation Using Zerovalent Iron in Laboratory Column Tests." Environmental Science and Technology 38: 7.

Tamara, M. L. and E. C. Butler (2004). "Effects of Iron Purity and Groundwater Characteristics on Rates and Products in the Degradation of Carbon Tetrachloride by Iron Metal." Environmental Science & Technology 38(6): 1866-1876.

Ukrainczyk, L. and M. B. McBride (1993). "The Oxidation and Dechloriantion of Chlorophenols in Dilute Aqueous Suspensions of Manganese Oxides- Reaction-Product." Environmental Toxicology and Chemistry 12(11): 2015-2022.

Vogan, J. L., R. W. Gillham, S. F. O'Hannesin, W. H. Matulewicz and J. E. Rhodes (1995). "Site-Specific Degradation of VOCs in Groundwater Using Zero Valent Iron." Abstracts of Papers of the American Chemical Society 209: 250-ENVR.

Vogel, T. M., C. S. Criddle and P. L. McCarty (1987). "ES Critical Reviews: Transformations of halogenated aliphatic compounds." Environmental Science and Technology 21(8): 722-736.

Wang, Z. Y., W. L. Huang, D. E. Fennell and P. A. Peng (2008). "Kinetics of reductive dechlorination of 1,2,3,4-TCDD in the presence of zero-valent zinc." Chemosphere 71(2): 360-368.

Zhou, H., Y. He, Y. Lan, J. Mao and S. Chen (2008). "Influence of complex reagents on removal of chromium(VI) by zero-valent iron." Chemosphere 72(6): 870-874.

Zhuang, L., L. Gui and R. W. Gillham (2008). "Degradation of pentaerythritol tetranitrate (PETN) by granular iron." Environmental Science & Technology 42(12): 4534-4539.

2 Investigation of Granular Iron Aging on the Kinetics of Trichloroethene Reduction

2.1 Abstract

Column experiments of granular iron with trichloroethene or tetrachloroethene were conducted to examine the effects of aging on granular iron by applying the KIM to analyze kinetic data for the three parameters, k (rate constant), C_{max} (surface capacity for sorption) and J (Langmuir sorption parameter). The results suggested that overall reactivity toward TCE and PCE did not decrease much over a 3 month exposure time. By comparing the KIM parameters, it was indicated that initially the reaction rates were most influenced by a small number of highly reactive sorption sites. Whereas after aging the iron surface, these sites lost reactivity. However, the loss of the highly reactive sites was offset with an increase in the overall reactive sorption capacity on the iron surface, involving somewhat less reactive sites. Therefore, it is possible that the long-term performance of PRB depends on the surfaces with relatively high sorption capacity and moderate reactivity.

2.2 Introduction

Granular iron permeable reactive barrier (PRB) is a technology has received considerable attention in recent years (O'Hannesin and Gillham, 1998; Arnold and Roberts, 2000c; Farrell *et al.*, 2000a; Zhang *et al.*, 2002; Klausen *et al.*, 2003; Jeen *et al.*, 2006). Much progress has been made in lab and in field studies toward understanding the chemistry of granular iron and the mechanisms through which various contaminants are transformed (Gillham and O'Hannesin, 1994; Burris *et al.*, 1998; Arnold and Roberts, 2000c; Grant and Kueper, 2004; Bang *et al.*, 2005; Bransfield *et al.*, 2007; Devlin, 2009;

EPA, July 1997). Hydrochemical and site-specific conditions, such as elapsed time since a spill, pH, temperature, anionic and cationic composition of the groundwater, and the presence of cosolvents all have effects on iron reactivity (Munz and Roberts, 1986; Su and Puls, 1998; McMahon *et al.*, 1999; Tamara and Butler, 2004; Devlin and Allin, 2005; Bi *et al.*, 2009a). In addition, grain-scale mass transfer, grain size, precipitate formation and corrosion, iron purity, and brands of iron (Su and Puls, 1998; Tamara and Butler, 2004), exert influences on granular iron reaction kinetics over the short and long terms (Johnson *et al.*, 1996; Su and Puls, 1999; Arnold and Roberts, 2000c; Arnold and Roberts, 2000a; Scherer *et al.*, 2001; Devlin and March, 2003; Schäfer *et al.*, 2003; Bi *et al.*, 2009c). Since the most detailed and voluminous knowledge of iron behavior comes from lab experiments, which are usually of short duration (Wüst *et al.*, 1999; Arnold and Roberts, 2000a; Butler and Hayes, 2001), additional attention is needed to evaluate likely long-term performance issues.

It is widely accepted that chemical precipitation coats granular iron surfaces, preventing reactive solutes from reaching locations where reactions can occur in a timely fashion (Burris *et al.*, 1995; Bi *et al.*, 2009b). In some unusual cases, such as in the case of magnetite formation, precipitates are not deleterious to the long-term reactivity of granular iron (Lee and Batchelor, 2002b; Kohn and Roberts, 2006). However, in most cases reactivity suffers from precipitate formation, and this has been shown in both laboratory (Mackenzie *et al.*, 1999; Klausen *et al.*, 2003; Vikesland *et al.*, 2003; Devlin and Allin, 2005; Jeen *et al.*, 2006) and field tests (Phillips *et al.*, 2000; Liang *et al.*, 2005).

Precipitates that accumulate inside PRBs may not only affect reactivity, but also the system hydraulics (Mackenzie *et al.*, 1999). Indeed, it has been reported that problems in the long-term performance of PRBs focused on permeability losses due to losses in porosity (Vikesland *et al.*, 2003). Nevertheless, reactivity loss has been identified as the most likely factor that limits long-term performance of iron PRBs (Vikesland *et al.*, 2003; Henderson and Demond, 2007).

In an ongoing attempt to gain insights into the factors controlling granular iron reactivity, Devlin (2009) introduced a kinetic model (KIM) (Equation 2.1), which is capable of separating sorption and reaction parameters, assuming a first-order surface reaction and Langmuir isotherm (Devlin, 2009).

$$\frac{dC_w}{dt} = -\frac{kC_{max}\frac{Fe}{V}}{\frac{1}{J} + \frac{C_{max}\frac{Fe}{V}}{1+JC_w} + C_w} C_w \qquad 2.1$$

Where Fe is iron mass (M) (sometimes represented as iron surface area (Johnson *et al.*, 1996); V is volume of water (L^3); C_w is concentration of reacting solute in water (M/L^3); C_{max} is the surface capacity for sorption (M/M_{solid}), J is the Langmuir sorption parameter describing the affinity of the solute for the solid (L^3/M), k is the first-order rate constant for reaction on the solid surface (T^{-1}), t is time (T).

A purpose of this study is to apply the KIM to obtain the three parameters, k (rate constant), C_{max} (surface capacity for sorption) and J (Langmuir sorption parameter), on samples of iron as it ages. A further goal is to compare sorption to reactive sites, estimated with the KIM, and nonreactive sites, estimated from retardation factors to

examine the changing role of sorption as a function of iron aging in PRBs. To maximize relevance to field applications, the reacting solutes studied in these experiments are trichloroethene and tetrachloroethene, which are among the most commonly treated contaminants using the PRB approach.

2.3 Materials and Methods

2.3.1 Materials

Chemicals including, methanol, hexane, toluene, sodium perchlorate, perchloric acid and sodium hydroxide were obtained in the highest purity available from Fisher Scientific. Trichloroethylene (TCE) and tetrachloroethylene (PCE) were from ACROS Organics. All chemicals were used without purification. Connelly iron was sieved to obtain the 710 μm to 2 mm diameter fraction for use in the experiments. The iron grains were flaky in texture, and used without any pretreatment to best represent the material used in field applications, and to maintain consistency with previously published work (Devlin and Allin, 2005).

A feed solution consisting of 8 mM $NaClO_4$ was prepared daily in deoxygenated, deionized water (Barnstead International Nano Pure Infinity Ultra-pure Water System Series 896), and adjusted pH to 10±0.05 (Accumet PDA pH Meter Module 13-636-PDApHA) by dropwise additions of either 1.1 mM perchloric acid or 0.35 mM sodium hydroxide solution, to simulate the conditions in a PRB (Gillham *et al.*, 2002; Devlin and Allin, 2005), and for consistency with earlier work (Devlin *et al.*, 1998; Devlin and Allin, 2005; Marietta and Devlin, 2005; Bi *et al.*, 2010). The concentration of $NaClO_4$ solution was selected to maintain a solution ionic strength representative of groundwater (Devlin and Allin, 2005).

Deoxygenation of the solutions was achieved by sparging with ultra high purity nitrogen gas (Airgas, Topeka, KS) for 20 minutes. This procedure was verified to reduce the dissolved oxygen (DO) concentration below 0.2 mg/L, based on analysis using a Chemetrics DO kit (K-7512 and K-7501).

Stock solutions of TCE were prepared in HPCL grade methanol at concentrations of 10 mM, 50 mM and 100 mM, and kept in a refrigerator at about 4 ^{o}C for a maximum of 2 months. Stock solutions were prepared in different concentrations, optimized for either standard preparation or source reservoir spiking in the column experiments. Care was taken to minimize the volume of methanol (<0.5% by volume, $<10^{-4}$ mol fraction) introduced to the solution, to avoid cosolvency effects (Staples and Geiselmann, 1988; Imhoff *et al.*, 1995; Devlin and Allin, 2005). Normally, less than 200 µL stock solution was added to the Teflon bag (~2 L total volume) to reach the target initial concentration.

Columns were constructed from Pyrex® glass with a fritted glass funnel tip at the outlet and a Plexiglas® end plug with a machined line port and double Viton® o-rings to seal against the column walls at the inlet. Teflon® bags manufactured by American Durafilm, as showed in Figure 2.1, were used as influent solution reservoirs in all column experiments. They were outfitted with combination Teflon®-stainless steel fittings on top of the bag for filling and emptying. Peek® tubing was used to connect the source bags to the columns. Viton® tubing (Fisher Scientific) was used in the peristaltic pump heads. Control tests showed that sorption by the Viton was negligible (Appendix J). Samples were collected into 2 mL glass sample vials that were sealed with Teflon®-lined caps.

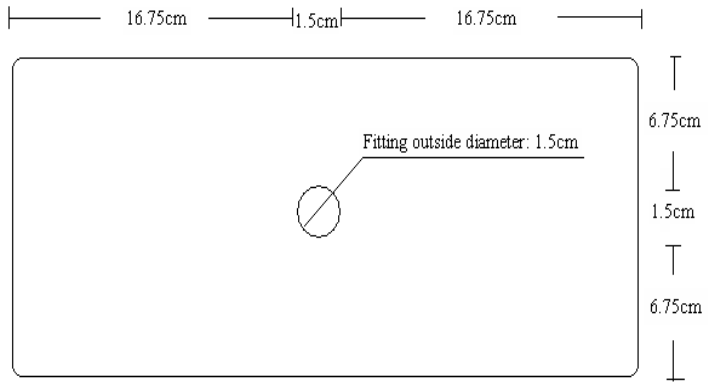

Figure 2.1: Top Surface of the Teflon Bag

2.3.2 Methods

2.3.2.1 Column Test

Columns were 30 cm long with 1.5 cm inside diameters (Figure 2.2 and Figure 2.3). The columns were each packed with 80 ± 1 g of Connelly iron (~18 cm of packed column length). The packing was completed in 15 g lifts. For each lift, iron was poured into the column, which was positioned vertically. The column was then manually shaken for several seconds to promote a reasonably tight and uniform packing of the grains.

Initially, a column was flushed with pure CO_2 gas for 20 minutes to displace atmospheric air. The column was then flushed with deoxygenated 8 mM $NaClO_4$ at pH 10, pumped from a Teflon source bag until the weight of column was stabilized and no air bubbles were visible against the column walls.

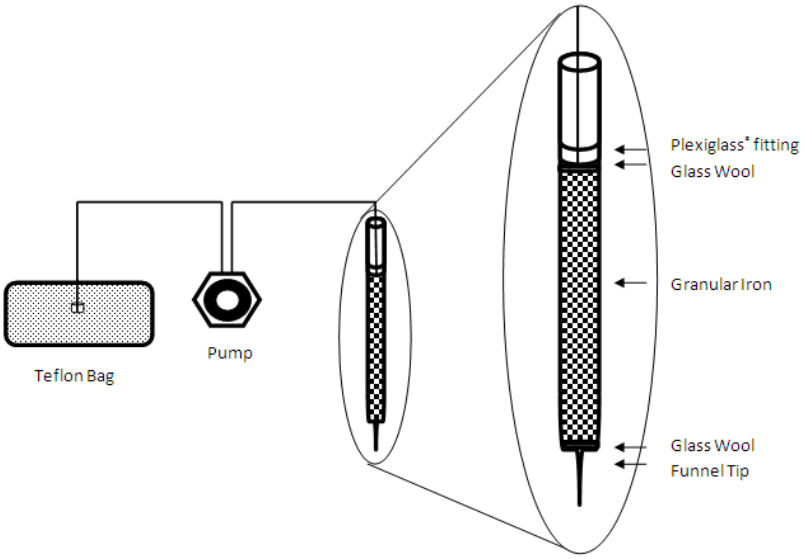

Figure 2.2: Schematic of the Column Experimental Assembly.

Figure 2.3: Photo of Column Experiment with Peristaltic Pump and Glass Column.

Source bags were spiked with TCE stock solution using glass micro-liter syringes (Fisher Scientific) to achieve desired source concentrations. Solutions inside the source bags were stirred at 300 RPM with a Teflon® coated magnetic stir bar. Column experiments were performed over a range of initial concentrations from 10 to 450 μM. Each series began with low concentrations and ended with high concentrations to

minimize changes to the iron surface from experiment to experiment. Samples were collected at the outflow in 2.0 mL sample vials until sufficient time had passed for steady state effluent concentrations to be achieved. Experiments with initial concentration less than 100 μM required 12 hours to complete. For initial concentrations greater than 400 μM, an experiment could be completed in 8 hours or less. During the first hour of each column experiment, samples were collected every 10 to 15 minutes. During the following five hours, samples were collected at intervals of 30 to 45 minutes. After 5 hours, samples were taken every 1 to 1.5 hours.

After each experiment, the columns were flushed with deoxygenated 8 mM $NaClO_4$ solution at pH 10 for at least 12 hours to remove excess reactant and reaction products. Experimental tests showed that after a 12-hour flush, only trace amounts of organic compounds were detectable in the outflow. Following the flush, the reservoir was spiked to the next higher concentration of TCE or PCE in the series and another experiment was initiated. About 10 to 20 days were required to complete a full set of experiments from low influent concentration to high influent concentration. Tests were repeated as the columns aged up to 132 days (Table 2.1).

Table 2.1: Summary of column operating times. Where multiple intervals are shown (C24 and C18), the columns were flushed between intervals with fresh feed solution containing no chlorinated organics at 1mL/min.

column	Experiment time intervals (days)	Total number of Pore Volume passed through the column
C24	1-9	269
	28-43	194
	64-80	228
C15	1-36	545
C16	1-25	360
C20	1-30	207
C18	1-96	881

The dry weight of each column and its weight after saturation (with water) were used to estimate the magnitude of a pore volume, *PV*, and porosity, *n*, (Equation 2.2),

$$PV = \frac{Saturated\ Column\ Weight - Dry\ Column\ Weight}{Water\ Density} \qquad 2.2\ a$$

$$n = \frac{PV}{V} \qquad 2.2\ b$$

where V is total volume of the column. Porosity was found to be within the range 40-70%, which is similar to previously reported granular iron columns (Farrell *et al.*, 2000b; Schäfer *et al.*, 2003; Marietta and Devlin, 2005; Bi *et al.*, 2009b; Bi *et al.*, 2009c). The average linear velocity, *v*, of pumped solution through the column was then calculated from equation 2.3:

$$v = \frac{Q}{An} \qquad 2.3$$

where, *Q* is pumping rate (mL/min), and *A* is column cross-sectional area (1.77 cm^2). The pumping rate *Q* was kept at 1.00 ± 0.03 mL/min at all times, and *Q* was measured at the beginning and at the end of each experiment to ensure the experiment was conducted with a constant flow rate. Therefore, the flow velocity through a column was about 1.5 ± 0.07E-4 m/sec, or 0.9 ± 0.4 cm/min in all experiments, and in the flushes between experiments.

To check the validity of this estimated velocity, a chloride tracer test was conducted (Appendix B). Conditions closely mimicked those of the experiments involving TCE and PCE. The test ran 1 hour with a pumping rate of 1.14 mL/min, in a column with a porosity of 68.6%, and a calculated flow velocity of 0.941 cm/min,

corresponding to a residence time of about 18 minutes. The breakthrough curve of the chloride tracer was fitted with a solution to the advection dispersion equation (Equation 2.4) by optimizing the estimates of dispersivity and velocity (Bear, 1979). The flow velocity was found to be 0.98 cm/min, which is within 5% of the previously estimated velocity, validating the calculation method, which was used for the remainder of the work. An important advantage of the calculation method for general use was that it avoided the introduction of possible surface-active substances, such as chloride, that might cause biases in the column data.

$$C(x,t) = \frac{C_0}{2}\left[exp\left\{\frac{vx}{2D}\left(1 - \sqrt{1+\frac{4kD}{v^2}}\right)\right\} erfc\left\{\frac{Rx - vt\sqrt{1+\frac{4kD}{v^2}}}{2\sqrt{DRt}}\right\} + exp\left\{\frac{vx}{2D}\left(1 + \sqrt{1+\frac{4kD}{v^2}}\right)\right\} erfc\left\{\frac{Rx + vt\sqrt{1+\frac{4kD}{v^2}}}{2\sqrt{DRt}}\right\}\right] \quad 2.4$$

where k is first order rate constant (T^{-1}), assumed zero for chloride; v is flow velocity (L/T), R is retardation factor (dimensionless); x is distance (L); t it time (T); C_o is initial concentration (M/L^3); D is the dispersion coefficient (L^2/T), which is calculated by equation 2.5:

$$D = av + D^*/n \quad 2.5$$

where α is dispersivity (L), n is porosity (dimensionless), and D^* is the effective molecular diffusion coefficient (L^2/T).

2.3.2.2 Analytical Methods

All samples were analyzed within 24 hours of collection. Samples for chlorinated solvents were analyzed using either Gas Chromatograph (GC) or High Performance

Liquid Chromatography (HPLC). GC analyses were conducted with an Agilent 6890 series GC with auto injection, a GC capillary column and a PID detector. The carrier gas was helium (He), flowing at 2 mL/min with a make up flow of 4 mL/min. The analysis time was about 3 min per sample.

HPLC analyses were performed using an Agilent 1100 series HPLC with autosampler and diode array detector, as described in literature (Marietta and Devlin, 2005); (Bi *et al.*, 2009c). Separation of compounds was achieved with a HP Zorbax SB C-18 reversed phase (4.6 mm×25 cm, 5 mM spheres, 4×80 mm 5 mM Zorbax C-18 guard column), giving an analysis time of about 5 minutes per sample (Devlin and Allin, 2005).

Calibration for both the GC and HPLC was accomplished by starting each analytical run with a blank (deionized water) and five to seven standards spanning the concentration range of interest. Standards were also interspersed among the sample vials on the autosampler tray. All standards (before and among sample vials) were considered in generating the calibration curves, and each run was calibrated independently. QAQC was evaluated on the basis of the calibration curve analyses as described by Devlin (Devlin, 1996). Calibration curves were used to assess analytical precision and accuracy (Keith, 1994a; Keith, 1994b; Devlin, 1996), from which the uncertainty on individual measurements was generally within 2% to 10%, depending on the magnitude of the concentration. The detection limit of the GC method was estimated to be not more than 2 μM. The detection limit for HPLC method was estimated to be not more than 0.5 μM.

Chloride in the tracer test was analyzed using a HACH Chloride Test Kit Model 8-P Cat. No. 1440-01. Concentrations were analyzed over the range 50 mg/L to 365.7 mg/L with a method detection limit of about 34.3 mg/L and accuracy of about ± 35 mg/L.

The sensitivity of the method was limited by the necessary sample size of 23 mL. Since only 2 mL samples were collected from the column at the appointed times, each sample was diluted with 21 mL of deionized water (Appendix B).

2.3.3 Kinetic Modeling

The suite of experiments conducted at different initial concentrations was used to quantify the kinetics of TCE disappearance. Breakthrough curves were analyzed by fitting equation 2.4 to the outflow concentrations of reactants, to obtain k_{obs}. Combining the data from the series, a plot of initial rate $(dC/dt)_o$ vs. C_o produced a curve that could be fit with equation 2.1. The initial estimates of the KIM parameters was obtained using a 2-step linearization procedure (Marietta and Devlin, 2005). The kinetic modeling for column experimental data was performed using customized FORTRAN program: KIM2P and KIMPE. Both kinetic and adsorption parameters could be obtained in a single fitting process (Devlin, 2009).

2.4 Results and Discussion

Iron aging is intuitively assessed by considering experiments performed in chronological order. However, unless the water and contaminant fluxes are constant, time alone may not correlate well with rates of change to the iron surface. Therefore, a check on this condition was warranted before adopting a simple chronological analysis of the data. Reactivity was evaluated as a function of cumulative contaminant mass passing through the iron, since this should correlate better to increased corrosion of the iron grains than time. A series from one of the column tests was plotted on a common abscissa showing cumulative time (Figure 2.4) and cumulative TCE mass (Figure 2.5). Reaction rates for TCE increased non-linearly with increasing C_o, as others have observed (note:

C_o increases across each series, but the C_o values are not explicitly shown) (Burris *et al.*, 1998; Arnold and Roberts, 2000b; Bi *et al.*, 2009b). In spite of the different axes, the two graphs show similar patterns of reaction rate change. Therefore, in these experiments, chronological aging appears to be adequate to describe the changes observed.

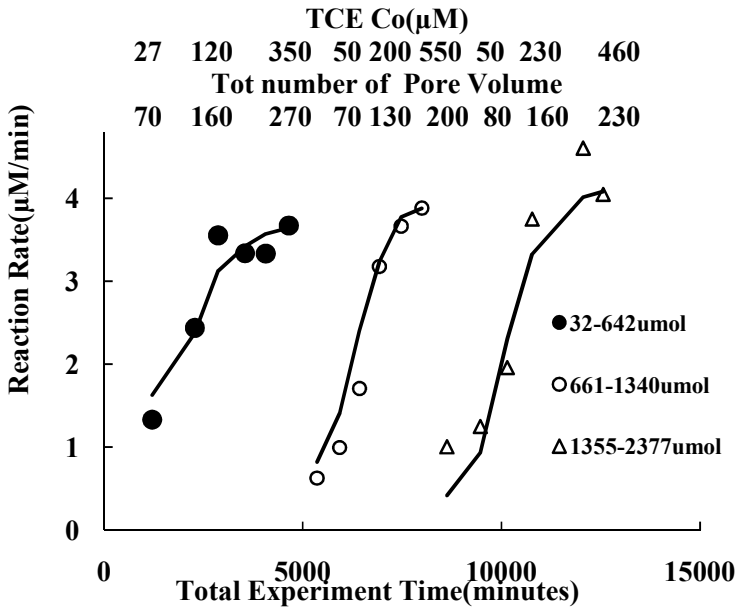

Figure 2.4: Rate for TCE reduction as a function of total experimental time for column (C24). Lines are fitted with KIM (see Table 2.2).

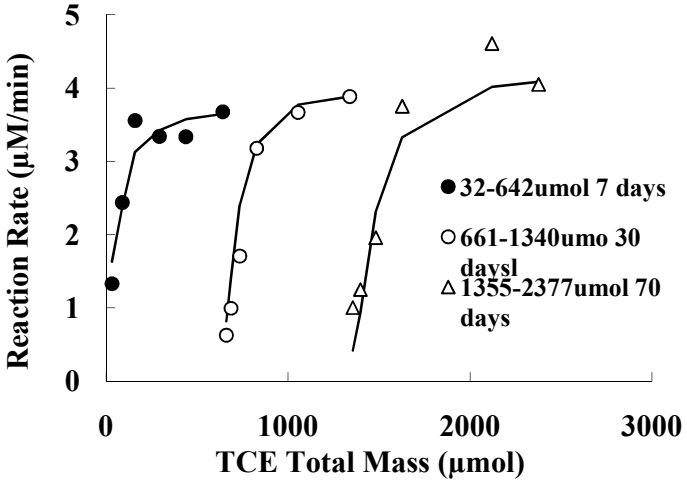

Figure 2.5: Rate of TCE reduction as a function of total TCE mass injected to the column (C24). Lines are fitted with KIM.

Superficially the rate data from column C24 appear not to have changed as the column aged. As discussed below, a more detailed analysis showed that changes did occur. In other columns the changes caused more noticeable differences in the rate vs. C_o curves (Figure 2.6).

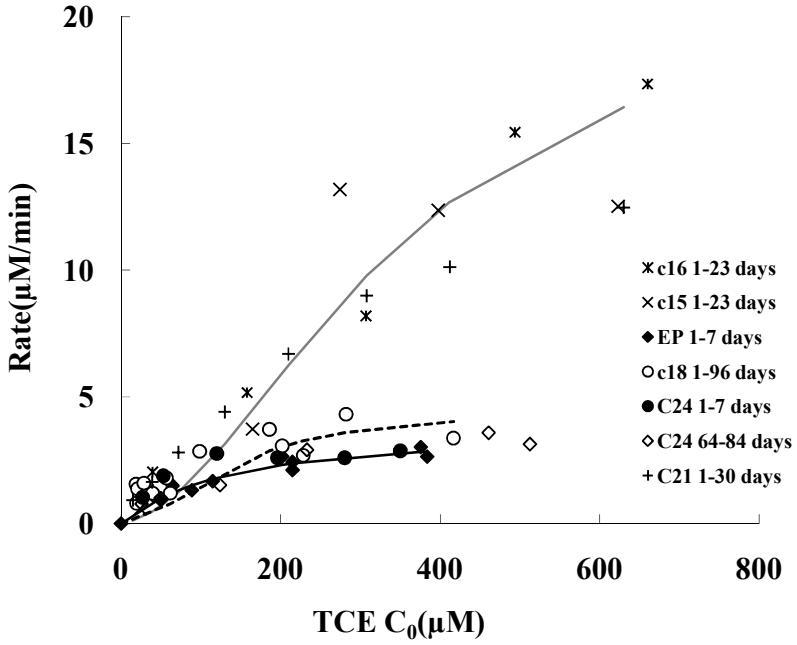

Figure 2.6: Rate of TCE reduction as a function of initial concentration. Data are fitted with KIM (Table 2.2). Solid points(♦) are data from (Bi *et al.*, 2009b). Lines are calculation results of KIM.

In this research, the initial and final column pore volumes were found to vary by less than 10% over the three different periods of investigation. A porosity change greater than this would not have been expected based on the assumption that all corroded iron was transferred to solution and pumped out of the column (Equation 2.6 and 2.7).

$$Fe^0 + RCl + H_2O \rightleftarrows Fe^{2+} + RH + Cl^- + OH^- \qquad 2.6$$

$$Fe^0 + RCl + 2H_2O \rightleftharpoons Fe(OH)_{2(s)} + RH + H^+ + Cl^- \quad 2.7$$

For example, if the TCE concentration of the influent solution was 100 μM, and after 8 hours of pumping the steady state concentration of TCE in the outflow was 50 μM, then about 50 μM of Fe^{2+} would be expected to be produced. With a 1 mL/min pumping rate, this would correspond to a total amount of leached iron not exceeding 2.8 μg/min. Over periods of about 90 days, the maximum iron leached would be about 361 mg, only 0.45% of the total iron in the column (80 g). Moreover, since not all the iron in solution is likely to have been leached out of the column, they formed oxides instead, increases in porosity were not expected to be great. Previous studies have reported effluent concentrations of iron to be low (Gillham and O'Hannesin, 1994). Therefore, it appears that the oxidized iron largely remained in the column, presumably in the form of oxides, such as magnetite, maghemite, and $Fe(OH)_2$.

Within each series, the KIM was fitted to data plotted as initial rate, $(dC/dt)_o$, *vs*. C_o to estimate k, C_{max} and J. Since the parameters were shown to be covariant (in particular k and C_{max}), uncertainties were estimated by implementing a Monte Carlo scheme (Devlin, 2009; Bi *et al.*, 2010). Each rate was estimated to have a ± 15 % error on it by comparing data point deviations from the best fit line. A total of 1000 realizations was generated for each series by randomly varying the data points within the ± 15 % error envelopes, and best fit k, C_{max} and J were estimated for each. The estimates were then examined in histograms to assess the probability distributions of each (Figure 2.7, Figure 2.8 and Figure 2.9). The Monte Carlo scheme was executed in Visual Basic and Excel.

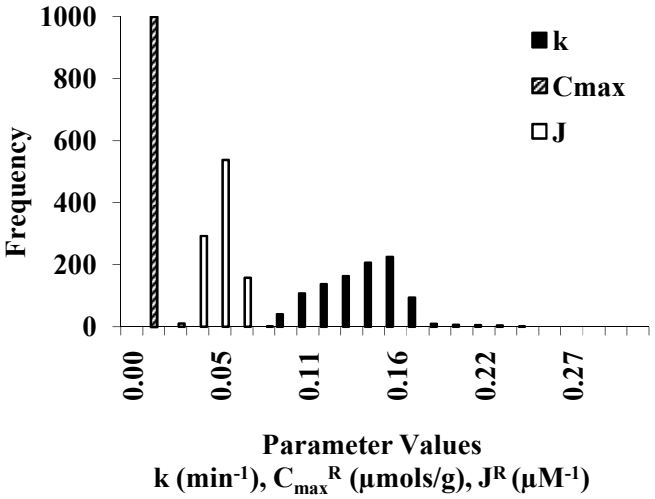

Figure 2.7: Frequency of k, C_{max} and J for TCE contacted iron after a 1-7 days exposure time (column C24).

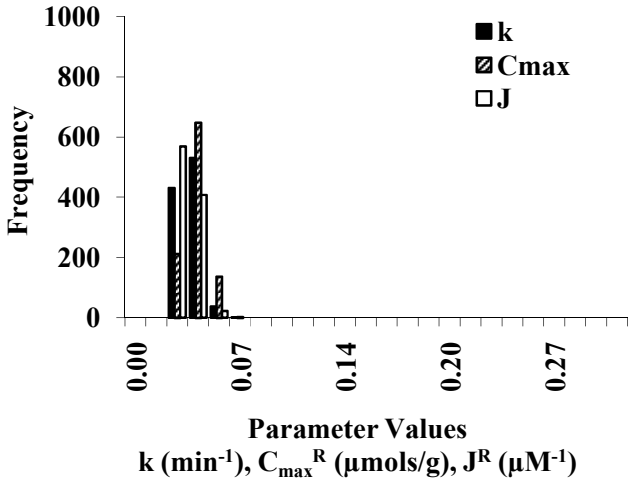

Figure 2.8: Frequency of k, C_{max} and J for TCE contacted iron after a 28-43 days exposure time (column C24).

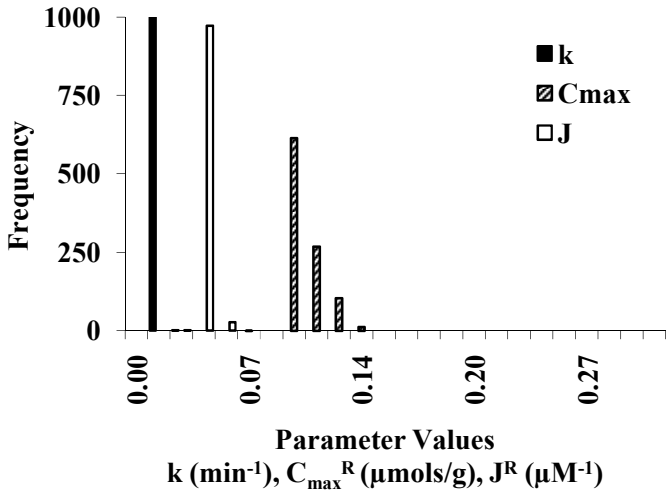

Figure 2.9: Frequency of k, C_{max} and J for TCE contacted iron after a 64-84 days exposure time (column C24).

A comparison of the histograms reveals that, *k* was relatively large and C_{max} was relatively small over the first 7 days of iron exposure to solution. The parameter *J* was of intermediate value. Note that the parameters estimated in this analysis are operational in nature and make no assumptions about the specific chemical moieties responsible for sorption and reaction on the iron surface. As the iron exposure time to aqueous TCE was increased to 30 days, the estimated value of *k* decreased by a factor of 3 to 4, while C_{max} increased by a factor of 2 to 3. The parameter *J* was not significantly altered. The trend continued with the 70-day exposure column. In that case, the *k* estimate was considerably decreased relative to its magnitude in the 7 day column, and C_{max} was considerably increased. Again, *J* was altered a little bit (Table 2.2). These trends were reproduced in combined data from 3 other columns. Columns 15 and 16 were continuously exposed to TCE for 30 days. The experimental data from these two columns were grouped together,

for fitting with the KIM. Column 18 was exposed to TCE from 30 to 90 days (Table 2.2,

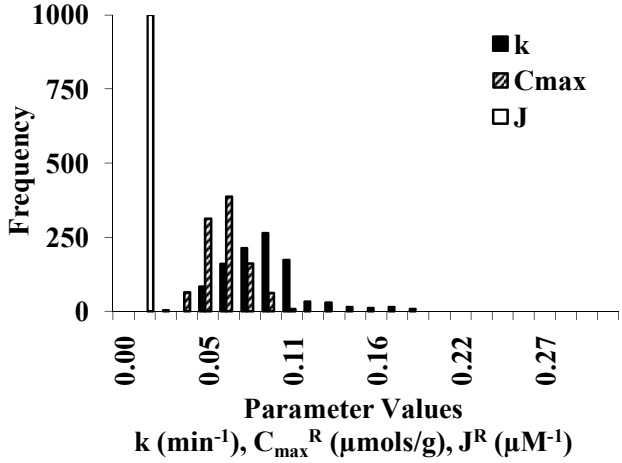

Figure 2.10 and Figure 2.11). The ranges of the three parameters from these three columns are quite close to the parameter ranges from C24 for the same aging periods, establishing reasonable reproducibility in the experiments.

Table 2.2 Ranges of sorption and kinetic parameters for different aged TCE columns

	C24			C15,16,21	C18
	1-7 days	28-43 days	64-84 days	1-30 days	1-96 days
k(min^{-1})	0.1-0.25	0.027-0.068	0.014	0.05-0.19	0.01-0.03
C_{max}(µmol g^{-1})	0.01	0.027-0.068	0.09-0.14	0.03-0.11	0.05-0.3
J(µM^{-1})	0.03-0.08	0.027-0.054	0.04-0.055	0.01	0.01-0.08

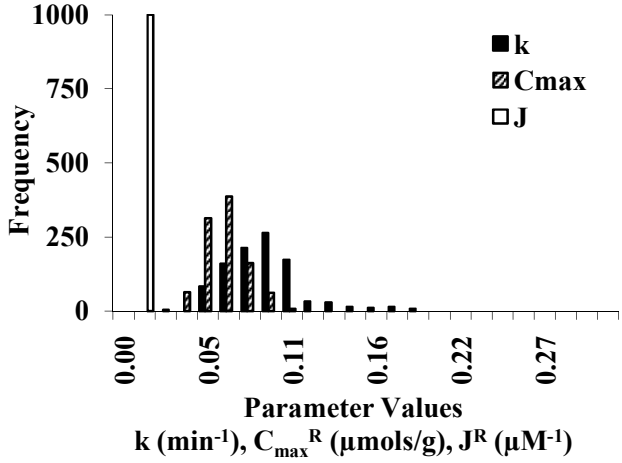

Figure 2.10: Frequency of k, C_{max} and J for TCE 1-30 days experiment set as a function of parameter values (C15, C16 and C21).

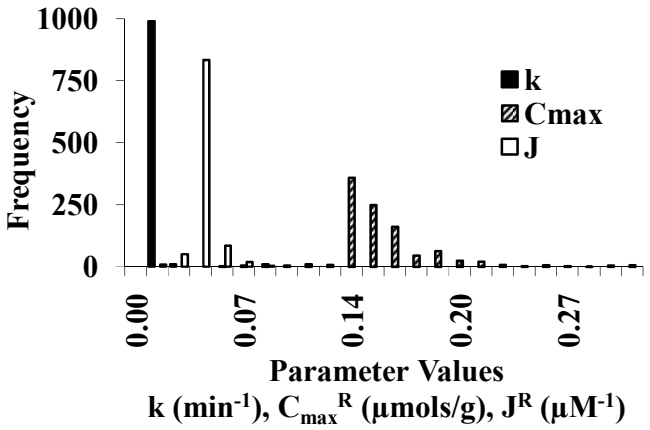

Figure 2.11: Frequency of *k*, C_{max} and *J* for TCE 1-96 days experiment set as a function of parameter values (C18).

A possible interpretation of these results is that young iron reactivity is dominated by a relatively small number (low C_{max}) of highly reactive sites (high *k*), while older iron reactivity becomes dominated by a larger number (high C_{max}) of less reactive sites (low *k*).

Granular iron columns reacting with tetrachloroethylene (PCE) were also analyzed (Appendix F). In independent experiments with different packed columns, the same trends, suggesting losses of high reactivity sites and increasing dominance of lower reactivity sites due to increased sorption to these sites, were noted. This finding suggests the trend may be generally applicable to the chlorinated solvent class of organics. Further work is needed to investigate this applicability to other classes of organic compounds.

2.5 Conclusion

Column experiments were conducted to examine the effects of aging on granular iron. Over the time of the test, about 100 days, reactivity toward TCE and PCE did not decrease significantly. In fact, in some tests reactivity was temporarily enhanced after about a month of exposure to water, and about 200 pore volumes. Despite this apparent

consistency in the reactivity of the iron, analysis of the kinetic data with the KIM indicated that initially the reaction rates were most strongly influenced by a few sorption sites with high associated reactivity. As the iron aged, these sites became less reactive, but the loss in overall reactivity was offset by an increase in the sorption capacity of the iron surface. This finding suggests that the long-term performance of granular iron may depend on surface characteristics that do not resemble those of fresh iron or even iron that has been emplaced for several weeks. The surface that determines long-term reactivity appears to be one with relatively high sorption capacity and low reactivity (compared to the initial material) and evolves over a period of several months. The exact time frames over which the changes occur is not well known, since the conditions of these column tests may depart form field conditions quite significantly. Future investigations of the iron surface should focus on the difference between the young and aged iron surfaces, the field times over which the changes occur, and on a detailed characterization of possible sorption sites on the aged surface, since it is that surface and those sites that may control long-term reactivity.

References

Arnold, W. A. and A. L. Roberts (2000a). "Inter- and Intraspecies Competitive Effects in Reactions of Chlorinated Ethylenes with Zero-valent Iron in Column Reactors." Canadian Geotechnical Journal 17(5): 291-302.

Arnold, W. A. and A. L. Roberts (2000c). "Kinetics of chlorinated ethylene reaction with zero-valent iron in column reactors." Abstracts of Papers of the American Chemical Society 219: 12-ENVR.

Bang, S., M. D. Johnson, G. P. Korfiatis and X. G. Meng (2005). "Chemical reactions between arsenic and zero-valent iron in water." Water Research 39(5): 763-770.

Bear, J. (1979). Hydraulics of Groundwater (Mcgraw-Hill Series in Water Resources and Environmental Engineering) New York, McGraw-Hill Companies.

Bi, E., I. Bowen and J. F. Devlin (2009). "Effect of Mixed Anions (HCO3--SO42--ClO4-) on Granular Iron (Fe-0) Reactivity." Environmental Science & Technology 43(15): 5975-5981.

Bi, E., J. F. Devlin and B. Huang (2009). "Effects of Mixing Granular Iron with Sand on the Kinetics of Trichloroethylene Reduction." Ground Water Monitoring and Remediation 29(2): 56-62.

Bi, E., J.F.Devlin, B. Huang and R. Firdous (2010). "Transport and Kinetic Studies To Characterize Reactive and Nonreactive Sites on Granular Iron." Environmental Science and Technology 44(14): 5564-5569.

Bransfield, S. J., D. M. Cwiertny, K. Livi and D. H. Fairbrother (2007). "Influence of Transition Metal Additives and Temperature on the Rate of Organohalide Reduction by Granular Iron: Implications for Reaction Mechanisms." Applied Catalysis B: Environmental 76: 8.

Burris, D. R., R. M. Allen-King, V. S. Manoranjan, T. J. Campbell, G. A. Loraine and B. Deng (1998). "Chlorinated Ethene Reduction by Cast Iron: Sorption and Mass Transfer." Journal of Environmental Engineering 7: 1012-1019.

Burris, D. R., T. J.Campbell and V. S.Manoranjan (1995). "Sorption of Trichloroethylene and Tetrachloroethylene in A Batch Reactive Metallic Iron-water System." Environmental Science and Technology 29(11): 2850-2855.

Butler, E. C. and K. F. Hayes (2001). "Factors Influencing Rates and Products in the Transformation of Trichloroethylene by Iron Sulfide and Iron Metal." Environmental Science & Technology 35(19): 3884-3891.

Devlin, J. F. (1996). "A Method to Assess Analytical Uncertainties over Large Concentration Ranges with Reference to Volatile Organics in Water." Ground Water Monitoring and Remediation: 179-185.

Devlin, J. F. (2009). "Development and Assessment of A Rate Equation for Chemical Transformations in Reactive Porous Media." Environmental Science and Technology.

Devlin, J. F. and K. O. Allin (2005). "Major Anion Effects on the Kinetics and Reactivity of Granular Iron in Glass-encased Magnet Batch Reactor Experiments." Environmental Science and Technology 39: 1868-1874.

Devlin, J. F., J. Klausen and R. P. Schwarzenbach (1998). "Kinetics of Nitroaromatic Reduction on Granular Iron in Recirculating Batch Experiments." Environmental Science & Technology 32(13): 1941-1947.

Devlin, J. F. and C. March (2003). Investigating the Kinetic Limitations of Granular Iron over A Large Range of 4-chloronitrobenzene Concentrations. National Meeting American Chemical Society Division of Environmental Chemistry. 43.

EPA (July 1997). Permeable Reactive Subsurface Barriers for the Interception and Remediation of Chlorinated Hydrocarbon and Chromium(VI) Plumes in Ground Water. U. S. E. P. A. E. O. o. R. a. Development. National Risk Management Research Laboratory Ada, OK 74820. EPA/600/F-97/008.

Farrell, J., M. Kason, N. Melitas and T. Li (2000). "Investigation of the Long-term Performance of Zero-valent Iron for Reductive Dechlorination of Trichloroethylene." Environmental Science and Technology 34: 514-521.

Farrell, J., N. Melitas, M. Kason and T. Li (2000). "Electrochemical and Column Investigation of Iron-Mediated Reductive Dechlorination of Trichloroethylene and Perchloroethylene." Environmental Science and Technology(34): 2549-2556.

Gillham, R. W. and S. F. O'Hannesin (1994). "Enhanced Degradation of halogenated Aliphatics by Zero-Valent Iron." Ground Water 32(6): 958-967.

Gillham, R. W., K. Ritter, Y. zhang and M. S. Odziemkowski (2002). Factors in the Long-term Performance of Granular Iron PRBs. Groundwater Quality. Sheffield UK.

Grant, G. P. and B. H. Kueper (2004). "The Influence of High Initial Concentration Aqueous-phase TCE on the Performance of Iron Wall Systems
" Journal of Contaminant Hydrology 74: 13.

Henderson, A. D. and A. H. Demond (2007). "Long-term performance of zero-valent iron permeable reactive barriers: A critical review." Environmental Engineering Science 24(4): 401-423.

Imhoff, P. T., S. N. Gleyzer, J. F. McBride, L. A. Vancho, I. Okuda and C. T. Miller (1995). "Cosolvent-Enhanced Remediation of Residual Dense Nonaqueous Phase Liquids: Experimental Investigation." Environmental Science & Technology 29(8): 1966-1976.

Jeen, S.-W., R. W. Gillham and D. W. Blowes (2006). "Effects of Carbonate Precipitates on Long-Term Performance of Granular Iron for Reductive Dechlorination of TCE." Environmental Science and Technology(400): 6432-6437.

Johnson, T. L., M. M. Scherer and P. G. Tratnyek (1996). "Kinetics of halogenated organic compound degradation by iron metal." Environmental Science & Technology 30(8): 2634-2640.

Keith, L. H. (1994b). "Throwaway Data." Environmental Science & Technology 28(8): A389-A390.

Klausen, J., P. J. Vikesland, T. Kohn, D. R. Burris, W. P. Ball and A. L. Roberts (2003). "Longevity of Granular Iron in Groundwater Treatment Processes: Solution Composition Effects on Reduction of Organohalides and Nitroaromatic compounds " Environmental Science and Technology 37: 1208-1218.

Kohn, T. and A. L. Roberts (2006). "The Effect of Silica on the Degradation of Organohalides in Granular Iron Columns." Journal of Contaminant Hydrology 83: 70-88.

Lee, W. and B. Batchelor (2002). "Abiotic Reductive Dechlorination of Chlorinated Ethylenes by Iron-Bearing Soil Minerals. 1. Pyrite and Magnetite. , ." Environmental Science & Technology 35: 5147-5154.

Liang, L., G. R. Moline, W. Kamolpornwijit and O. R. West (2005). "Influence of Hydrogeochemical Processes on Zero-valent Iron Reactive Barrier Performance: A Field Investigation." Journal of Contaminant Hydrology 78: 291-312.

Mackenzie, P. D., D. P. Horney and T. M. J. Sivavec (1999). "Mineral Precipitation and Porosity Losses in Granular Iron Columns." Journal of Hazardous Materials 68: 1-17.

Marietta, M. and J. F. Devlin (2005). Separating the Kinetic and Sorption Parameters of Nitroaromatic Compounds in Contact with Granular Iron. 4th International Groundwater Quality Conference. waterloo, canada**:** 6.

McMahon, P. B., K. F. Dennehy and M. W. Sandstrom (1999). "Hydraulic and Geochemical Performance of a Permeable Reactive Barrier Containing zero-Valent Iron, Denver Federal Center." Ground Water 37(3): 396-404.

Munz, C. and P. V. Roberts (1986). "Effects of Solute Concentration and Cosolvents on the aqueous activity-Coefficient of Halogenated Hydrocarbons." Environmental Science and Technology 20(8): 6.

O'Hannesin, S. F. and R. W. Gillham (1998). "Long-term performance of an in situ "iron wall" for remediation of VOCs." Ground Water 36(1): 164-170.

Phillips, D. H., B. Gu, D. B. Watson, Y. Roh, L. Liang and S. Y. Lee (2000). "Performance Evaluation of A Zerovalent Iron Reactive Barrier: Mineralogical Characteristics." Environmental Science and Technology 34: 4169-4176.

Schäfer, D., R. Köber and A. Dahmke (2003). "Competing TCE and cis-DCE Degredation Kinetics by Zero-valent Iron-Experimental Results and Numerical Simulation." Journal of Contaminant Hydrology 65: 183-202.

Scherer, M. M., K. M. Johnson, J. C. Westall and P. G. Tratnyek (2001). "Mass transport effects on the kinetics of nitrobenzene reduction by iron metal." Environmental Science & Technology 35(13): 2804-2811.

Staples, C. A. and S. J. Geiselmann (1988). "Cosolcent Influences on Organic Solute Retardation Factors." Ground Water 26(2): 192-198.

Su, C. and R. W. Puls (1998). Temperature Effect on Reductive Dechlorination of Trichloethene by Zero-Valent Metals. Wickramanayake GB, Hinchee RE, eds. Physical, Chemical, and Thermal Technologies: Proceeding of the First International Conference on Remediation of Chlorinated and Recalcitrant Compounds. Monterey, CA, Battelle Press. Columbus, OH. 1(5)**:** 317-322.

Su, C. and R. W. Puls (1999). "Kinetics of Trichloroethene Reduction by Zerovalent Iron and Tin: Pretreatment Effect, Apparent Activation Energy, and Intermediate Products." Environmental Science and Technology 33(1): 163-168.

Tamara, M. L. and E. C. Butler (2004). "Effects of Iron Purity and Groundwater Characteristics on Rates and Products in the Degradation of Carbon Tetrachloride by Iron Metal." Environmental Science & Technology 38(6): 1866-1876.

Vikesland, P. J., J. Klausen, H. Zimmermann, A. L. Roberts and W. P. Ball (2003). "Longevity of Granular Iron in Groundwater Treatment Processes: Changes in Solute Transport Properties Over Time." Journal of Contaminant Hydrology 64: 3-33.

Wüst, W. F., R. Kober, O. Schlicker and A. Dahmke (1999). "Combined Zero- and First-order Kinetic Model of the Degradation of TCE and Cis-DCE with Commercial Iron." Environmental Science and Technology 33: 4304-4309.

Zhang, P., X. Tao, Z. Li and R. S. Bowman (2002). "Enhanced Perchloroethylene Reduction in Column Systems Using Surfactant-Modified Zeolite/Zero-Valent Iron Pellets." Environmental Sciences and Technology (36): 3597-3603.

3 Comparison of Kinetic and Sorption Parameters for Chlorinated Solvents and Nitroaromatic Compounds Reacting with Granular Iron

3.1 Abstract

By comparing two chlorinated compounds, trichloroethene (TCE) and tetrachloroethene (PCE), and two nitroaromatic compounds, 4-chloronitrobenzene (4ClNB) and 4-acetylnitrobenzene (4AcNB) in batch and column tests with Connelly granular iron, it was found that the nitroaromatic compounds reacted much more rapidly than the chlorinated solvent compounds. By analyzing KIM parameters, *k,* the first-order rate constant for the reaction on the iron surface of chlorinated solvents has a value of 0.05-0.19 min^{-1} for TCE and 0.03-0.2 min^{-1} for PCE, which are similar. The *k* for nitroaromatic compounds was found to be in the range of 2.73-12.27 min^{-1} for 4ClNB and 1.36-12.95 min^{-1} for 4AcNB, which are significantly higher than those of the chlorinated solvents. It was concluded that the differences in observed rates were due primarily to differences in the inherent chemical differences between compound classes, through the parameter *k*, rather than due to sorption effects as was the case for rate changes as the iron aged.

3.2 Introduction

Granular iron is a commercially available product generally consisting of platy fragments of a light steel ranging in size from <1 mm to about 5 mm in diameter. When used in permeable reactive barriers (PRBs), the PRBs have been shown to be cost effective alternatives to pump-and-treat for groundwater remediation (Gillham and O'Hannesin, 1994; Sivavec and Horney, 1995). The material is known to be reactive with chlorinated hydrocarbons (Gillham and O'Hannesin, 1994; Sivavec and Horney, 1995)),

nitrate (Hwang *et al.*, 2010; Li *et al.*, 2010), chromate (Gui *et al.*, 2009; Liu *et al.*, 2009), and a variety of other substances, both organic and inorganic (Jain *et al.*, 1999; Blowes *et al.*, 2000; Lackovic *et al.*, 2000; Morrison *et al.*, 2002; Lien and Wilkin, 2005). Over the past two decades, considerable research has been focused on describing the kinetics of organic compounds reacting with granular iron and other forms of zero-valent iron (ZVI) (Wüst *et al.*, 1999; Gander *et al.*, 2002; Marietta and Devlin, 2005; Urynowicz, 2007; Wang *et al.*, 2008; Devlin, 2009; Rodriguez-Maroto *et al.*, 2009; Shariatmadari *et al.*, 2009; Bi *et al.*, 2010; Hwang *et al.*, 2010). The most common approach has been to model the kinetics with a simple first order kinetic term. However, because the iron surface is finite in any experiment or application, the first-order models fail when contaminant concentrations grow large, i.e., in excess of 50 to 100 μM. Moreover, because the surface changes as reactions with contaminants proceed, due to corrosion, any relationship between aqueous concentrations and reaction rates is unlikely to be linear with time. To address this, more sophisticated kinetic models have been developed (Burris *et al.*, 1995; Deng *et al.*, 1999; Arnold and Roberts, 2000c; Dries *et al.*, 2004; Cai *et al.*, 2007).

It is commonly assumed that the degradation of chlorinated solvents occurs in three steps, 1) sorption of the contaminant to the granular iron surface, 2) transformation of the contaminant to a reaction product, and 3) desorption of the reaction product from the surface (Arnold, 1999; Arnold and Roberts, 2000b; Marietta and Devlin, 2005; Devlin, 2009) It is the second of these steps that is assumed to be the slowest, and therefore that step that is the primary control on the kinetics of transformation (Arnold, 1999; Devlin, 2009). However, sorption and desorption can also influence the observed reaction rates,

because they determine the number of molecules that can be in the process of reacting at any time. An overall fast reaction rate results when more mass is sorbed on the surface. Therefore, to completely describe the observed kinetics of reactant transformation, it is necessary to parameterize both the sorption and reaction processes. Since different classes of organic compounds are likely to exhibit different inherent reactivities toward granular iron, and different propensities to sorb, the objective of this research is to quantify and compare these characteristics for two different classes.

Most kinetic models that have been applied to granular iron reactions, which account for the finite surface, assume that sorption remains constant throughout time. This assumption works well when the total sorbed reactant mass is low compared to the total reactant mass in a chemically heterogeneous system (solid surface and aqueous solution). However, PRBs and granular iron packed columns contain a high solid surface area to water ratio, and the potential for a high sorbed to total reactant mass fraction, potentially invalidating these models.

Devlin proposed a new kinetic model, that accounted for non-steady state sorption (Devlin, 2009).

$$\frac{dC_W}{dt} = -\frac{kC_{max}\frac{Fe}{V}}{\frac{1}{J}+\frac{C_{max}\frac{Fe}{V}}{1+JC_W}+C_W}C_W \qquad 3.1$$

where C_W is aqueous concentration of chlorinated solvents (M/L^3), Fe is iron mass (M), V is volume of water (L^3), C_{max} is the surface capacity for sorption (M/M_{solid}), J is the Langmuir sorption parameter describing the affinity of the solute for solid (L^3/M), k is the first-order rate constant for the reaction on the iron surface (T^{-1}). In column tests where the Fe/V term is large, the KIM offers the possibility to separate the reaction rate

constant, k, and the Langmuir sorption parameters, J and C_{max}, operating in experimental systems. This will form the basis for the kinetic and sorption parameter estimation in this work.

The two classes selected for comparison were the chlorinated solvents, represented by trichloroethene (TCE) and tetrachloroethene (PCE), and the nitroaromatics, represented by 4-chloronitrobenzene (4ClNB) and 4-acetylnitrobenzene (4AcNB). It was hypothesized that the following trends should be evident in the estimated parameters, based on prior knowledge of these compounds with reactants and sorbents other than granular iron (Arnold, 1999; Arnold *et al.*, 1999; Gautam and Suresh, 2006; Fang and Al-Abed, 2008): 1) the rate constant, k, for the nitroaromatic compounds should be greater than those for the chlorinated solvents; 2) the sorption capacity, C_{max}, of the nitroaromatic compounds should be less than those for the chlorinated solvents because the molecule is larger (and the Langmuir sorption assumption involves monolayer coverage of the solid surface); 3) the affinity parameters are expected to be similar in magnitude for all substances tested, i.e., within about a factor of 10 based on reported K_{oc} values, with an expected trend $J_{4ClNB} \geq J_{PCE} \geq J_{4AcNB} > J_{TCE}$ (ATSDR, 1997; Martin and Axel, 1998; IPCS, 2002; CCME, 2007).

3.3 Experimental Section

3.3.1 Materials

Chemicals including 4-ClNB, 4AcNB, methanol, hexane, toluene, sodium perchlorate, perchloric acid and sodium hydroxide were obtained in the highest purity available from Fisher Scientific. Trichloroethylene (TCE) and tetrachloroethylene (PCE)

were obtained from ACROS Organics. All chemicals were used without additional purification.

Connelly iron was sieved to obtain the 710 μm to 2 mm diameter grains for use in the experiments. The iron grains were platy in texture, and used without any pretreatment to best represent the material used in field applications, and to maintain consistency with previously published work (Devlin and Allin, 2005).

Details of the experiment are the same as those given in Chapter 2. Briefly, an 8 mM $NaClO_4$ feed solution at pH 10±0.05 was prepared daily in deoxygenated, deionized water (Barnstead International Nano Pure Infinity Ultra-pure Water System Series 896). A pH of 10 was selected because it represents conditions inside a granular iron PRB, and for consistency with previous experiments (Gillham *et al.*, 2002; Devlin and Allin, 2005; Marietta and Devlin, 2005; Bi *et al.*, 2009b). Deoxygenation of the feeding solution to reduce the dissolved oxygen below 0.2 mg/L was achieved by sparging with ultra high purity nitrogen gas (Airgas, Topeka, KS) for 20 minutes.

Stock solutions of the organic test compounds were prepared in HPCL grade methanol at concentrations of 10 mM, 50 mM and 100 mM to spike the reservoir solutions to various initial concentrations with minimal addition of methanol – hence cosolvency effects – to the reaction solutions. Each experiment received less than 200 μL of stock solution added to >1000 mL reservoirs. Therefore the methanol concentration in the batch reactor was always below a mole fraction of 10^{-4}, or 1% by volume, (Staples and Geiselmann, 1988; Imhoff *et al.*, 1995; Devlin and Allin, 2005).

Columns used in the experiments were constructed from Pyrex® glass, a fritted glass funnel tip at the outlet, a Plexiglas® end plug at the inlet, a machined influent line

port and double Viton® o-rings were used to seal against the column walls. They were 30 cm long with an internal diameter of 1.5 cm. Teflon bags (American Durafilm) with a 2 liter capacity were used as influent solution reservoirs in all column experiments. Teflon®-stainless steel fittings were attached to the bag for filling and emptying (Figure 3.1). Viton® tubing (Fisher Scientific) was used in the peristaltic pump head, and Peek® tubing was used to connect the columns and Teflon bags on either side of the pump. Samples were collected into 2 mL glass sample vials (Fisher Scientific) that were crimp-sealed with Teflon®-lined caps.

3.3.2 Experimental Methods

Batch and column tests were performed to obtain estimates of the kinetic and sorption parameters necessary to predict compound reduction rates. Batch tests were conducted as described by Devlin and Allin (2005). Series of tests, spanning a range of initial concentrations, C_o, from 10 to 450 μM were conducted with TCE and PCE. Similarly collected data were obtained from the work of Marietta and Devlin (2005) for the compounds 4ClNB and 4AcNB. All batch tests were conducted in GEM reactors with a stirring speed of about 300 rpm (Garvin and Devlin, 2006). Samples of reactor water were sampled at regular intervals and the data fitted with the first order kinetic equation to obtain apparent first order rate constant, k_{obs}.

Columns were packed with 80 ± 1 g of Connelly iron (~18 cm of packed column length). Columns were then flushed with pure CO_2 gas for 20 minutes to displace atmospheric air, and flushed with deoxygenated 8 mM $NaClO_4$ feeding solution until the weight of column stabilized and no air bubbles were visible against the column walls.

A given series was begun with low concentrations and ended with high concentrations so the surface was minimally altered at each step. This procedure was also found to produce datasets with the least noise. For the first hour of each column experiment, samples were collected every 10 to 15 minutes. Through the following 5 hours, samples were taken every 30 to 45 minutes. After 5 hours, samples were taken every 1 to 1.5 hours. Between each test in a series, the columns were flushed with 8 mM $NaClO_4$ feeding solution for at least 12 hours to remove excess reactant and reaction products in advance of the next test.

Figure 3.1 Photo of column experiment with peristaltic pump and glass column.

The total porosity (n) of the columns was found to be in the range of 0.40 to 0.68, which is similar to previously reported granular iron columns (Farrell *et al.*, 2000b; Schäfer *et al.*, 2003; Marietta and Devlin, 2005; Bi *et al.*, 2009b). The pumping rate, Q, was kept at 0.99±0.03 mL/min. The flow velocity was estimated to be $1.5\times10^{-4} \pm 0.1\times10^{-4}$

m/sec, or 0.9 ± 0.4 cm/min in all experiments, based on the pumping rate and porosity measurements, and a tracer test (Appendix B).

3.3.3 Analytical Methods

All samples were analyzed within 24 hours of collection. Samples for chlorinated solvents were analyzed using either gas chromatography (GC) or High Performance Liquid Chromatography (HPLC). GC analyses were conducted with an Agilent 6890 series GC with auto injection, a GC capillary column and a photo-ionization detector **(**PID). The carrier gas was helium (He), flowing at 2 mL/min with a make up flow at 4 mL/min. The analysis time was about 3 min per sample.

HPLC analyses were performed using an Agilent 1100 series HPLC with autosampler and diode array detector, as described by Marietta and Devlin (2005) and Bi *et al.* (2009). Separation of compounds was achieved with a HP Zorbax SB C-18 reversed phase column (4.6 mm % 25 cm, 5 mM spheres, 4 % 80 mm 5 mM Zorbax C-18 guard column), giving an analysis time of about 5 minutes per sample (Devlin and Allin, 2005).

Standards spanning the range of measured concentrations in samples were included in all calibration curves, and each run was calibrated independently. The detection limit of the GC method was estimated to be 2 μM or less. The detection limit for HPLC method was about 0.5 μM or less for most runs (Devlin, 1996). Precision was generally better than ±5% except where sample concentrations approached detection limits.

3.3.4 Kinetic Modeling

For each organic compound studied, apparent first order rate constants, k_{obs}, from fitted breakthrough curves were assembled for a complete experimental series with

varying C_o. Initial rates, $(dC/dt)_o$, were estimated from the product $k_{obs}C_o$, and plotted against C_o for fitting with either the Langmuir-Hinshelwood (L-H) equation (Equation 3.2), in the case of batch test data, or the KIM (Equation 3.1) in the case of column data, as described by Devlin (2009).

$$\frac{dC_W}{dt} = -\left(\frac{kC_{max}\frac{Fe}{V}}{\frac{1}{J} + C_W}\right)C_W \qquad 3.2$$

3.4 Results and Discussion

Batch data were fit with the L-H equation to obtain estimates of *J* and the lumped parameter pair kC_{max} (Table 3.1, Figure 3.2 and Figure 3.3). A comparison of these estimated parameters for PCE and TCE reveals that the PCE value of kC_{max} is 3 times larger than that of TCE, showing PCE reacts faster than TCE. Also, the affinity of PCE for the iron surface, indicated by *J,* is slightly greater than TCE. These trends are consistent with previous findings reported in the literature (Burris *et al.*, 1998).

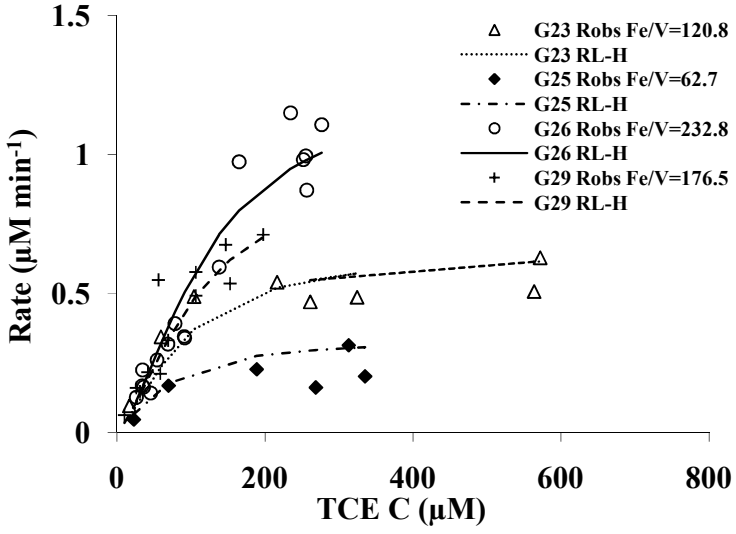

Figure 3.2: Breakthrough of TCE from four granular iron batch sets and associated fits with the L-H model to obtain estimates of *J* and the lumped parameter pair kC_{max}. The best fit parameters estimated are given in Table 3.1.

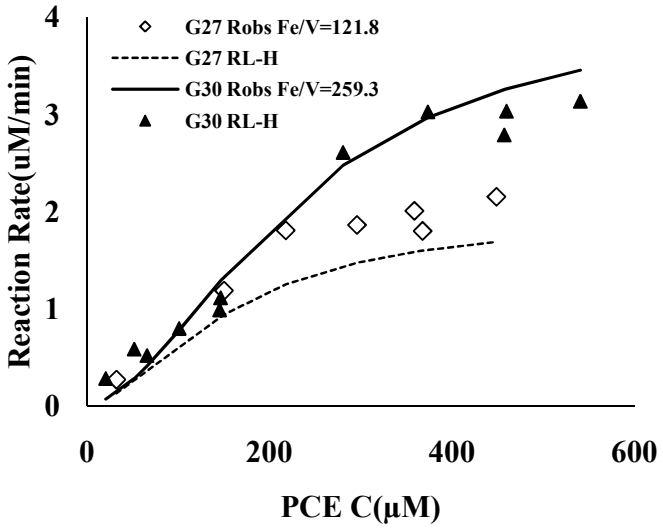

Figure 3.3: Breakthrough of PCE from two granular iron batch sets and associated fit with the L-H model to obtain estimates of *J* and the lumped parameter pair kC_{max}. The best fit parameters estimated are given in Table 3.1.

Table 3.1 Comparison of L-H and KIM kinetic parameters of TCE reacting with iron in column tests.

	L-H		KIM							
	TCE	PCE	TCE			PCE			4ClNB*	4AcNB*
	Batch	Batch	KIM fitting (Figure 3.6)			KIM fitting (Figure 3.7)			KIM fitting	KIM fitting
			C24 (1-7 days)	C15,16,21 (1-30 days)	C18 (1-96 days)	C23 (1-8 days)	C20 (1-38 days)	C25 (63-79 days)	1 day mini-column	1 day mini-column
$k*C_{max}$ ($\mu molg^{-1}min^{-1}$)	0.005	0.016							0.17 -0.23	0.023 -0.76
k (min^{-1})			0.17 ±0.023	0.09 ±0.025	0.007 ±0.0017	0.1 ±0.023	0.1 ±0.023	0.013 ±0.003	4.51 ±1.85	3.5 ±4.43
C_{max} ($\mu mol\ g^{-1}$)			0.005 ±0.001	0.053 ±0.013	0.13 ±0.03	0.01 5±0.002	0.03 ±0.001	0.05 ±0.008	0.038 ±0.013	0.046 ±0.014
J (μM^{-1})	0.034	0.043	0.004 ±0.008	0.003 ±0.001	0.03 ±0.007	0.02 ±0.008	0.024 ±0.001	0.06 ±0.009	0.029 ±0.013	0.07 ±0.03

*: Data from Marietta and Devlin, 2005, analysis from Devlin, 2009.

The breakthrough curves from column tests involving TCE and PCE were similar in several respects. In both cases a delayed rise in concentration, indicating retarded transport, was followed by a plateau in the data that established the onset of the steady state condition. From these curves, best fit k_{obs} and retardation factors, R_f, were calculated (Figure 3.4 and Figure 3.5).

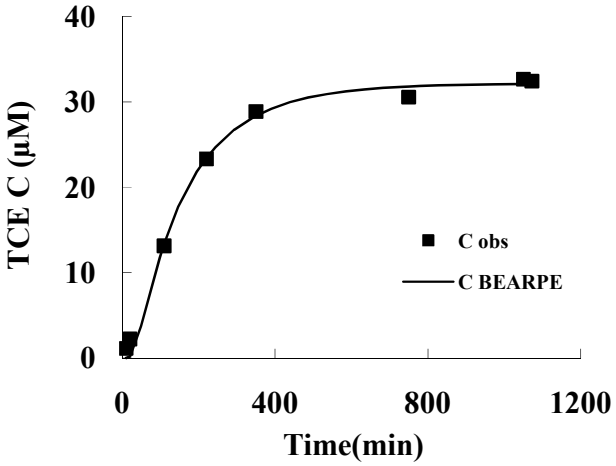

Figure 3.4: Breakthrough of TCE from a granular-iron packed column (C24), and associated fit with the transport code BEARPE. The Fe/V in the column was 4639 g/L and at the time of the test the column was aged 3 days. The best fit parameters estimated are given in Table 3.2.

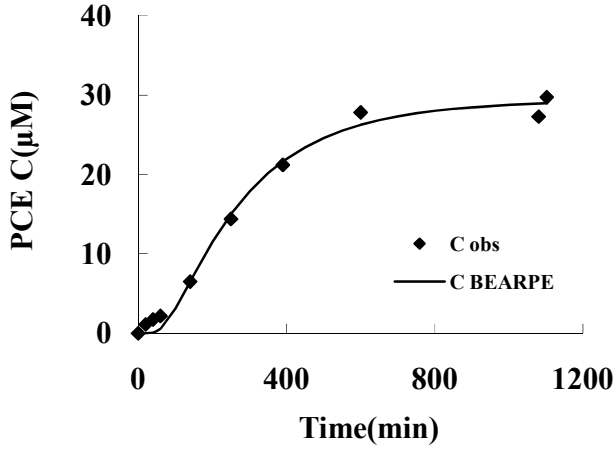

Figure 3.5: Breakthrough of PCE in a granular iron packed column (C25), and associated fit with the transport code BEARPE. The column was packed with a *Fe/V* of 4192 g/L and at the time of the test was aged 3 days. The best fit parameters estimated are given in Table 3.2.

Table 3.2 Parameters of BearPE fitting for TCE and PCE column experiments.

	V (M/sec)	D (M)	C_0 (µM)	L (cm)	Fe/V (g/L)	k_{obs} (min^{-1})	R_f
TCE C24	0.000189	0.1	53	17	4639	0.04	13.89
PCE C25	0.00014	0.1	49	17.5	4192	0.029	13.35

Initial reaction rates ($k_{obs}C_o$) were plotted against initial concentrations for both TCE and PCE column experiments, and the experimental data were fitted well by the

KIM in all cases (Table 3.1, Figure 3.6 and Figure 3.7). The consistency between the KIM and observed data sets for these compounds increases confidence in the values of the estimated kinetic parameters for both TCE and PCE.

In both cases, nonlinear relationships were observed, as expected for surface saturated systems. In some column experiments, the plateau was found to give way to a secondary rise in rates when the concentrations of reactants exceeded approximately 400 μM to 600 μM. The cause of the secondary rise was not explored in these experiments, but has been noted by others (Brunauer, 1943), and attributed to a breakdown of the assumption that the sorption on iron surface is limited to a monolayer. Since concentrations in groundwater are very rarely expected to be in excess of 400 μM, all experiments reported here were conducted with C_o at or below this level.

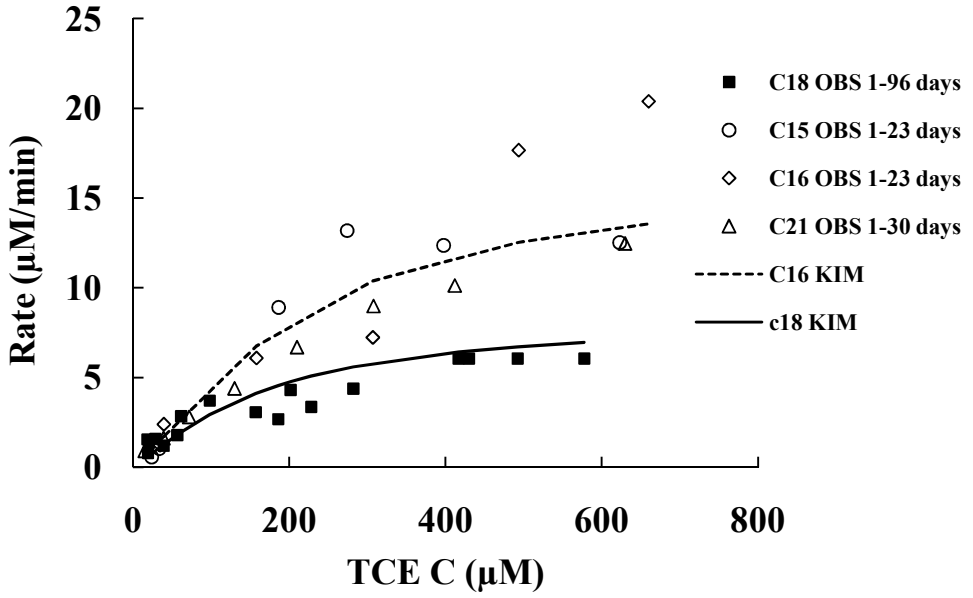

Figure 3.6: TCE rate data from 5 column experiments fitted well with the KIM. Parameters applied in KIM are in Table 3.1.

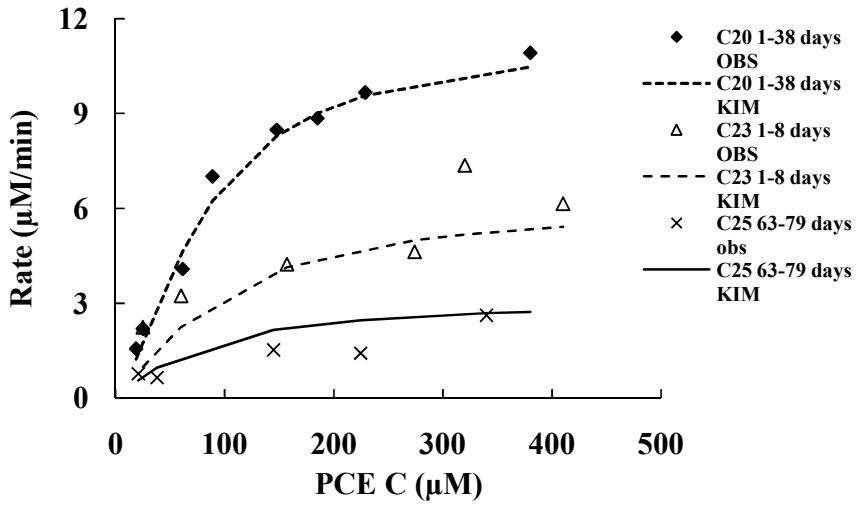

Figure 3.7: PCE column data from 3 column experiments fitted well with the KIM. Parameters applied in KIM are in Table 3.1.

Analysis of the initial rate vs. C_o curves with KIM, estimates could be obtained for each of the parameters *J, k,* and C_{max} (Table 3.1, Figure 3.8 and Figure 3.9). The magnitudes of C_{max} and *k* were similar for TCE and PCE, but the parameter *J* was found to be greater for PCE than it was for TCE, in similarly aged columns. This suggests that the intrinsic reactivity of granular iron with PCE and TCE is similar, but that the higher tendency of PCE to sorb to the iron surface leads to an overall faster apparent reaction rate between the two compounds.

The compound 4ClNB was found to have a *k* similar in magnitude to that of 4AcNB, within the sensitivity of the method. This result is consistent with previous work (Devlin *et al.*, 1998) (Table 3.1). It must be noted that the intrinsic reactivity of 4AcNB is considered greater than that of 4ClNB based on one-electron reduction potentials, as discussed in Devlin *et al.* (1998).

Since 4ClNB and 4AcNB were both found to have *k* values much larger than those determined for TCE and PCE, the fact that the nitroaromatics were found to be

more reactive with granular iron than the chlorinated solvents is largely attributable to electron transfer limitations rather than sorption issues. This notion is further supported by the fact that the magnitudes of C_{max} and J were relatively similar between the two classes of compounds.

In the cases of 4ClNB (Figure 3.10) and 4AcNB (Figure 3.11), C_{max} estimates were similar in magnitude to those of PCE and TCE. This was a bit surprising since the molecular diameter of 4ClNB and 4AcNB is about twice that of TCE and PCE. This might be explained by the aromatic compounds associating with the surface through the nitro group rather than directly with the ring. This could affect the orientation of the molecule in the sorbed state, and the space on the surface it occupies. Further work is needed to evaluate this hypothesis.

Finally, it was hypothesized that the trend in the sorption affinity parameters, J, would be $J_{4ClNB} \geq J_{PCE} \geq J_{4AcNB} > J_{TCE}$. In fact, the experiments found that $J_{4ClNB} \approx J_{PCE} \approx J_{4AcNB} \geq J_{TCE}$, in reasonable agreement with expectations.

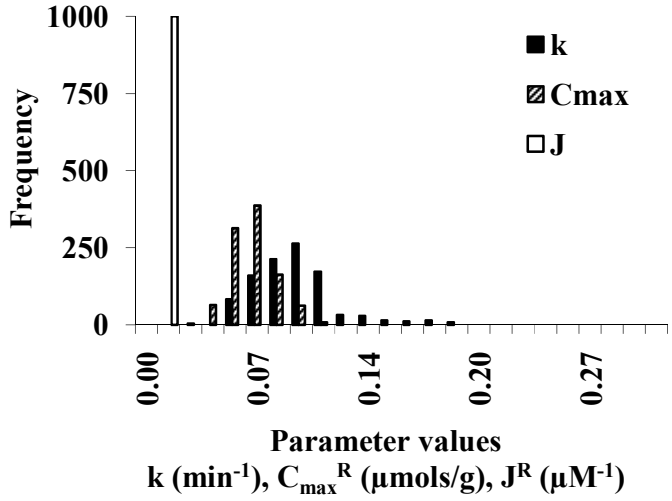

Figure 3.8: Frequency diagram showing the uncertainty range for the parameters *k*, C_{max} and *J* for TCE contacted iron, after 30 days exposure time (column C15, C16 and C21).

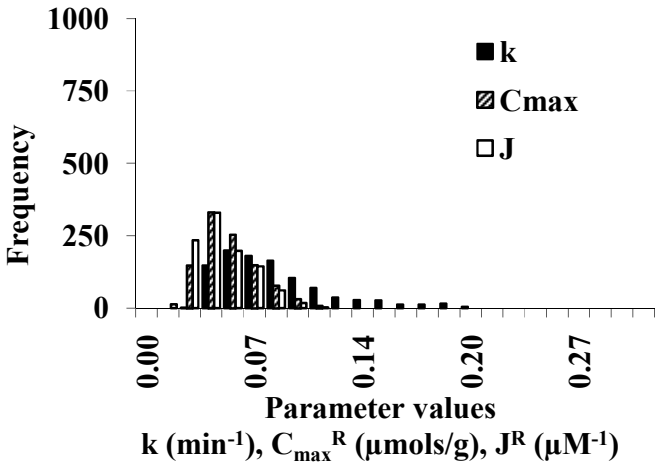

Figure 3.9: Frequency diagram showing the uncertainty range of *k*, C_{max} and *J* for PCE contacted iron after 30 days exposure time (column 20).

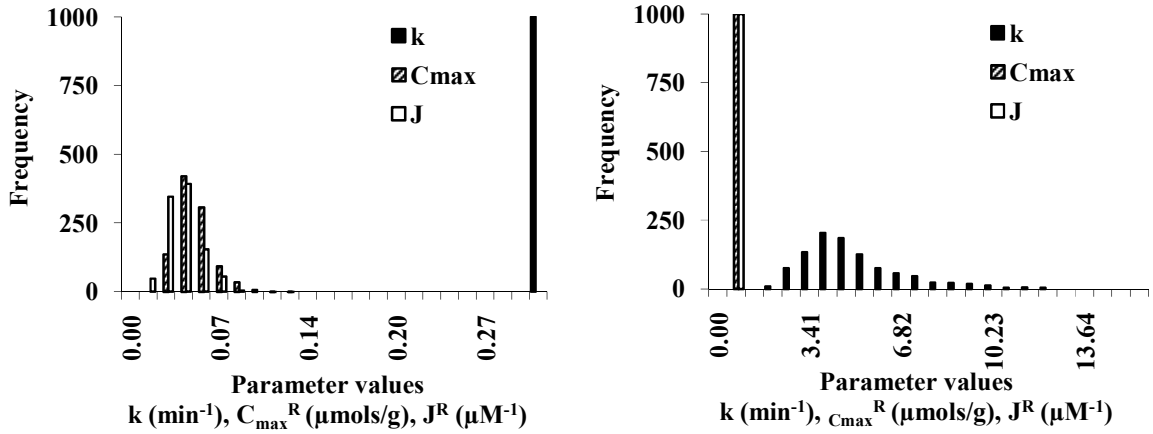

Figure 3.10: Frequency distribution diagrams showing uncertainty range of *k*, C_{max} and *J* for 4ClNB contacted iron after one day exposure time (Marietta and Devlin, 2005). The left figure displays data with maximum parameter values at 0.3. The right figure sets maximum parameter values at 15.

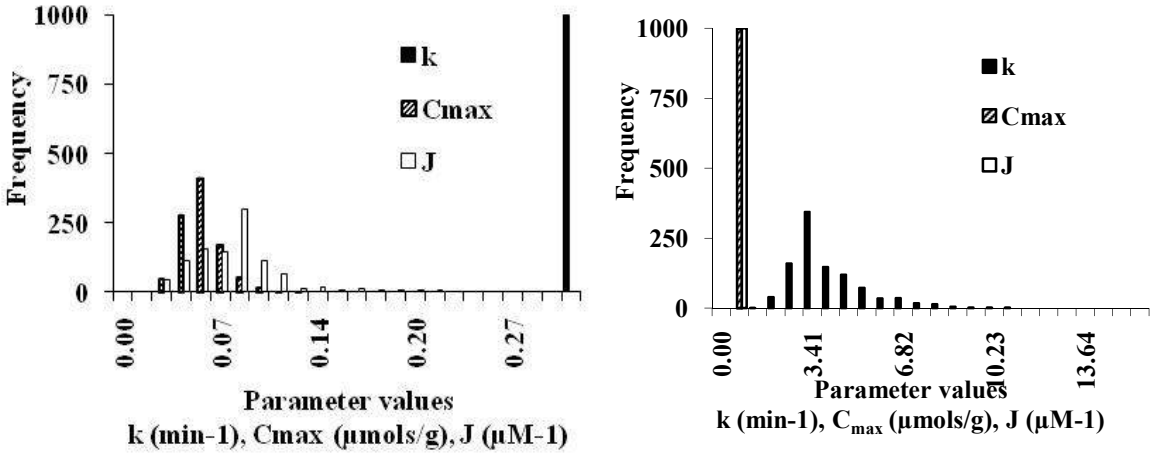

Figure 3.11: Frequency distribution diagrams showing uncertainty range of *k*, C_{max} and *J* for 4AcNB contacted iron after one day exposure time (Marietta and Devlin, 2005). The left figure has maximum parameter values at 0.3. The right figure has maximum parameter values set at 15.

3.5 Conclusions

Two chlorinated compounds, TCE and PCE were reacted with granular iron in batch and column experiments. Analysis with the KIM indicated that the faster rate of PCE degradation was at least partly due to its higher affinity for the iron surface. Rate constants for the reactions of these chemicals were not sufficiently different to evaluate relative intrinsic reactivities. A similar analysis of two nitroaromatic compounds yielded a similar result. It was found that PCE reacted faster than TCE, and 4AcNB reacted faster than 4ClNB with iron. In both cases the higher reactivities could be attributed to higher sorption. Comparing the two classes of chemicals, it was noted that the nitroaromatic compounds reacted much more rapidly than the chlorinated solvent compounds. The KIM analysis indicated that the differences in observed rates were due to differences in electron transfer processes, through the parameter *k*, rather than sorption effects. This result is consistent with expectations based on previously reported thermodynamic and kinetic studies of these compounds, validating the KIM analysis methodology. While

these preliminary results based on the KIM are promising, additional work is needed to further explore other organic groups and contaminant.

References

Arnold, W. A. (1999). Kinetics and Pathways of Chlorinated Ethylene and Chlorinated Ethane Reaction with Zero-Valent Metals. Department of Geography and Environmental Engineering. Baltimore, Maryland Johns Hopkins University. PhD.

Arnold, W. A., W. P. Ball and A. L. Roberts (1999). "Polychlorinated ethane reaction with zero-valent zinc: pathways and rate control." Journal of Contaminant Hydrology 40(2): 183-200.

Arnold, W. A. and A. L. Roberts (2000a). "Inter- and Intraspecies Competitive Effects in Reactions of Chlorinated Ethylenes with Zero-valent Iron in Column Reactors." Canadian Geotechnical Journal 17(5): 291-302.

Arnold, W. A. and A. L. Roberts (2000b). "Kinetics of chlorinated ethylene reaction with zero-valent iron in column reactors." Abstracts of Papers of the American Chemical Society 219: 12-ENVR.

ATSDR (1997). Toxicological Profile for Tetrachloroethylene. A. f. T. S. a. D. Registry. Atlanta, GA 186.

Bi, E., J. F. Devlin and B. Huang (2009). "Effects of Mixing Granular Iron with Sand on the Kinetics of Trichloroethylene Reduction." Ground Water Monitoring and Remediation 29(2): 56-62.

Bi, E., J.F.Devlin and B. Huang (2009). "Transport and Kinetic Studies to Characterize Reactive and Non-Reactive Sites on Granular Iron." Environmental Science and Technology.

Bi, E., J.F.Devlin, B. Huang and R. Firdous (2010). "Transport and Kinetic Studies To Characterize Reactive and Nonreactive Sites on Granular Iron." Environmental Science and Technology 44(14): 5564-5569.

Blowes, D. W., C. J. Ptacek, S. G. Benner, C. W. T. McRae, T. A. Bennett and R. W. Puls (2000). "Treatment of inorganic contaminants using permeable reactive barriers." Journal of Contaminant Hydrology 45(1-2): 123-137.

Brunauer, S. (1943). The Adsorption of Gases and Vapors Vol 1, Physical Adsoprtion, Oxford University Press.

Burris, D. R., R. M. Allen-King, V. S. Manoranjan, T. J. Campbell, G. A. Loraine and B. Deng (1998). "Chlorinated Ethene Reduction by Cast Iron: Sorption and Mass Transfer." Journal of Environmental Engineering 7: 1012-1019.

Burris, D. R., T. J.Campbell and V. S.Manoranjan (1995). "Sorption of Trichloroethylene and Tetrachloroethylene in A Batch Reactive Metallic Iron-water System." Environmental Science and Technology 29(11): 2850-2855.

Cai, Z. S., D. N. Lerner, R. G. McLaren and R. D. Wilson (2007). "Conceptual analysis of zero-valent iron fracture reactive barriers for remediating a trichloroethylene plume in a chalk aquifer." Water Resources Research 43(3).

CCME (2007). Canadian Soil Quality Guidelines TRICHLOROETHYLENE Environmental and Human Health Effects. C. C. o. M. o. t. Environment**:** 4.

Deng, B., D. R. Burris and T. J. Campbell (1999). "Reduction of Vinyl Chloride in Metallic Iron-Water Systems." Environmental Science & Technology 33(15): 2651-2656.

Devlin, J. F. (1996). "A Method to Assess Analytical Uncertainties over Large Concentration Ranges with Reference to Volatile Organics in Water." Ground Water Monitoring and Remediation: 179-185.

Devlin, J. F. (2009). "Development and Assessment of A Rate Equation for Chemical Transformations in Reactive Porous Media." Environmental Science and Technology.

Devlin, J. F. and K. O. Allin (2005). "Major Anion Effects on the Kinetics and Reactivity of Granular Iron in Glass-encased Magnet Batch Reactor Experiments." Environmental Science and Technology 39: 1868-1874.

Devlin, J. F., J. Klausen and R. P. Schwarzenbach (1998). "Kinetics of Nitroaromatic Reduction on Granular Iron in Recirculating Batch Experiments." Environmental Science & Technology 32(13): 1941-1947.

Dries, J., L. Bastiaens, D. Springael, A. Spiros N and L. Diels (2004). "Competition for Sorption and Degradation of Chlorinated Ethenes in Batch Zero-valent Iron Systems." Environmental Science and Technology 38: 2879-2884.

Fang, Y. X. and S. R. Al-Abed (2008). "Dechlorination kinetics of monochlorobiphenyls by Fe/Pd: Effects of solvent, temperature, and PCB concentration." Applied Catalysis B-Environmental 78(3-4): 371-380.

Farrell, J., N. Melitas, M. Kason and T. Li (2000). "Electrochemical and Column Investigation of Iron-Mediated Reductive Dechlorination of Trichloroethylene and Perchloroethylene." Environmental Science and Technology(34): 2549-2556.

Gander, J. W., G. F. Parkin and M. M. Scherer (2002). "Kinetics of 1,1,1-Trichloroethane Transformation by Iron Sulfide and a Methanogenic Consortium." Environmental Science & Technology 36(21): 4540-4546.

Garvin, N. L. and J. F. Devlin (2006). "Minimizing mass transfer effects in granular iron batch tests using GEM reactors." Journal of Environmental Engineering-Asce 132(12): 1673-1676.

Gautam, S. K. and S. Suresh (2006). "Dechlorination of DDT, DDD and DDE in soil (slurry) phase using magnesium/palladium system." Journal of Colloid and Interface Science 304(1): 144-151.

Gillham, R. W. and S. F. O'Hannesin (1994). "Enhanced Degradation of halogenated Aliphatics by Zero-Valent Iron." Ground Water 32(6): 958-967.

Gillham, R. W., K. Ritter, Y. zhang and M. S. Odziemkowski (2002). Factors in the Long-term Performance of Granular Iron PRBs. Groundwater Quality. Sheffield UK.

Gui, L., Y. Q. Yang, S. W. Jeen, R. W. Gillham and D. W. Blowes (2009). "Reduction of chromate by granular iron in the presence of dissolved CaCO3." Applied Geochemistry 24(4): 677-686.

Hwang, Y. H., D. G. Kim, Y. T. Ahn, C. M. Moon and H. S. Shin (2010). "Fate of nitrogen species in nitrate reduction by nanoscale zero valent iron and characterization of the reaction kinetics." Water Science and Technology 61(3): 705-712.

Imhoff, P. T., S. N. Gleyzer, J. F. McBride, L. A. Vancho, I. Okuda and C. T. Miller (1995). "Cosolvent-Enhanced Remediation of Residual Dense Nonaqueous Phase Liquids: Experimental Investigation." Environmental Science & Technology 29(8): 1966-1976.

IPCS (2002). SIDS Initial Assessment Report For SIAM 15. I. P. o. C. Safety. Boston, USA**:** 6.

Jain, A., K. P. Raven and R. H. Loeppert (1999). "Arsenite and arsenate adsorption on ferrihydrite: Surface charge reduction and net OH- release stoichiometry." Environmental Science & Technology 33(8): 1179-1184.

Lackovic, J. A., N. P. Nikolaidis and G. M. Dobbs (2000). "Inorganic arsenic removal by zero-valent iron." Environmental Engineering Science 17(1): 29-39.

Li, J. F., Y. M. Li and Q. L. Meng (2010). "Removal of nitrate by zero-valent iron and pillared bentonite." Journal of Hazardous Materials 174(1-3): 188-193.

Lien, H. L. and R. T. Wilkin (2005). "High-level arsenite removal from groundwater by zero-valent iron." Chemosphere 59(3): 377-386.

Liu, T. Z., P. H. Rao, M. S. H. Mak, P. Wang and I. M. C. Lo (2009). "Removal of co-present chromate and arsenate by zero-valent iron in groundwater with humic acid and bicarbonate." Water Research 43(9): 2540-2548.

Marietta, M. and J. F. Devlin (2005). Separating the Kinetic and Sorption Parameters of Nitroaromatic Compounds in Contact with Granular Iron. 4th International Groundwater Quality Conference. waterloo, canada**:** 6.

Martin, R. and D. Axel (1998). Toolkit for Estimating Physicochemical Properties of Organic Compounds. New York, John Wiley and Sons, Inc.

Morrison, S. J., D. R. Metzler and B. P. Dwyer (2002). "Removal of As, Mn, Mo, Se, U, V and Zn from groundwater by zero-valent iron in a passive treatment cell: reaction progress modeling." Journal of Contaminant Hydrology 56(1-2): 99-116.

Rodriguez-Maroto, J. M., F. Garcia-Herruzo, A. Garcia-Rubio, C. Gomez-Lahoz and C. Vereda-Alonso (2009). "Kinetics of the chemical reduction of nitrate by zero-valent iron." Chemosphere 74(6): 804-809.

Schäfer, D., R. Köber and A. Dahmke (2003). "Competing TCE and cis-DCE Degredation Kinetics by Zero-valent Iron-Experimental Results and Numerical Simulation." Journal of Contaminant Hydrology 65: 183-202.

Shariatmadari, N., C. H. Weng and H. Daryaee (2009). "Enhancement of Hexavalent Chromium [Cr(VI)] Remediation from Clayey Soils by Electrokinetics Coupled with a Nano-Sized Zero-Valent Iron Barrier." Environmental engineering science 26(6): 1071-1079.

Sivavec, T. M. and D. P. Horney (1995). Reductive dechlorination of chlorinated ethenes by iron metal. American Chemical Society. Anaheim, CA.

Staples, C. A. and S. J. Geiselmann (1988). "Cosolcent Influences on Organic Solute Retardation Factors." Ground Water 26(2): 192-198.

Urynowicz, M. A. (2007). "Kinetic approach for modeling TCE chemical oxidation by permanganate." Journal of Advanced Oxidation Technologies 10(1): 196-201.

Wüst, W. F., R. Kober, O. Schlicker and A. Dahmke (1999). "Combined Zero- and First-order Kinetic Model of the Degradation of TCE and Cis-DCE with Commercial Iron." Environmental Science and Technology 33: 4304-4309.

Wang, Z. Y., W. L. Huang, D. E. Fennell and P. A. Peng (2008). "Kinetics of reductive dechlorination of 1,2,3,4-TCDD in the presence of zero-valent zinc." Chemosphere 71(2): 360-368.

4 Transport Kinetic Iron Model for the Reaction and Sorption Competition of Tetrachloroethylene and Trichloroethylene with Granular Iron

4.1 Abstract

A one dimensional finite difference numerical transport model, T-KIM, incorporating the KIM reaction term, was developed and used to extend previous work by considering surface limited reactions and nonlinear sorption to reactive and nonreactive sites, as well as interspecies competition. The model was evaluated against two analytical solutions to the transport equation with first and third type boundaries. The model was used to generate synthetic data sets that were analyzed using the methodology applied in Chapters 2 and 3. The data analysis successfully solved the inverse problem, accurately calculating the KIM and transport parameters used to generate the synthetic data. The T-KIM calculations also revealed that the TCE detected in the column experiments as a result of PCE degradation was insufficient to cause measurable competition effects in the degradation of PCE.

4.2 Introduction

Permeable reactive barriers using zero-valent iron (ZVI) have been applied in numerous cases to treat contaminants in groundwater (O'Hannesin and Gillham, 1998; EPA, 1999; Pulsa *et al.*, 1999; Liang *et al.*, 2005). To improve the performance of ZVI remediation systems, attempts have been made to elucidate the kinetics of the dechlorination process (Su and Puls, 1999; Wüst *et al.*, 1999; Miehr *et al.*, 2004; Marietta and Devlin, 2005; Rodriguez-Maroto *et al.*, 2009). Most of these studies focused on geochemically distinct aqueous systems, changes in mineralogy, transport properties, or loss of reactivity over time. It is now commonly accepted that a pseudo-first-order kinetic

model can describe the disappearance of contaminants from water in both batch and flow-through (column) systems (Burris *et al.*, 1995; Campbell *et al.*, 1997), but that more sophisticated models are required to account processes of importance such as sorption and competition (Wüst *et al.*, 1999; Arnold and Roberts, 2000d; Devlin, 2009).

Reductive dechlorination by granular iron is generally viewed as a surface-mediated reaction (Wüst *et al.*, 1999; Dries *et al.*, 2004). Contaminants are thought to be adsorbed on the iron surface where they are then reduced, with electrons originating primarily from zero-valent iron in the grains. It is therefore not surprising that the observable rate of dechlorination depends both on the total mass of sorbed contaminants on the iron surface and the intrinsic reaction rate. The capacity to sorb depends on the available surface area, which has been found to be linearly related to granular iron mass (Matheson and Tratnyek, 1994). Complete sorption behavior on the iron surface can be described by a Langmuir isotherm expression or by the nonlinear Freundlich equation (Burris *et al.*, 1995; Allen-King *et al.*, 1997; Devlin, 2009). The Langmuir isotherm requires two parameters to be fully described, a sorption capacity term, C_{max}, and an affinity term, J.

Polluted groundwater frequently contains multiple contaminants. If these are reactive with granular iron, each will produce one or more daughter products. These substances may sorb to the iron, competing with the parent compounds for reactive locations on the surface, hereafter referred to as 'reactive sites'. Such competition may occur between different compounds (inter-species competition) or between molecules of the same compound (intra-species competition), limiting parent compound reaction rates. This effect is manifested experimentally as decreasing pseudo-first order rate constants

with increasing concentrations of reacting compound or competing compounds (Johnson *et al.*, 1998; Farrell *et al.*, 2000a; Bi *et al.*, 2009b; Devlin, 2009). A few researchers have developed models that account for competition between species. For example, a mass balance approach was used to develop a modified Langmuir-Hinshelwod-Hougen-Watson kinetic model, which accounted for both inter- and intra-species competition (Arnold and Roberts, 2000a). Also, based on an assumption of limited number of reactive sites on surface, a numerical model, Transport Biochemistry and Chemistry (TBC), was developed in order to identify and quantify the competition between compounds reacting on iron (Schäfer *et al.*, 2003). However, a shortcoming of all models presented before 2009 is that they relied upon lumped parameters that did not permit the quantitative distinction between the contributions of sorption and intrinsic reaction to observable reaction rates. In 2009, a rate expression, referred to as the kinetic iron model (KIM) (Devlin, 2009), was introduced that did permit such a distinction. This model was used to characterize intra-species interactions for nitroaromatic (Devlin, 2009) and chlorinated solvent compounds (Bi *et al.*, 2010) with Connelly granular iron.

The objective of this work is to develop a numerical transport model, T-KIM, which incorporates the KIM reaction term, and extends the earlier work by accounting for inter-species interactions and sorption to both reactive and nonreactive sites. The T-KIM performance is assessed by comparisons with analytical solutions of the advection dispersion equation (Flury *et al.*, 2009) with and without reaction and sorption, and with first and third type boundary conditions. A second objective is to demonstrate consistency between T-KIM and datasets previously reported for in the evaluation of reactive and nonreactive site properties (Bi *et al.*, 2010).

4.3 Theory

4.3.1 Development of the Finite Difference Solution

Reactive transport advection-dispersion equation with sorption is:

$$\frac{\partial C}{\partial t} = D\frac{\partial^2 C}{\partial x^2} - v\frac{\partial C}{\partial x} - k_{obs}C - \frac{\rho_b}{\theta}\frac{\partial \Gamma}{\partial t} \qquad 4.1$$

where ρ_b (=ρ(1-θ)) is the bulk dry density of iron (g L^{-1}) (density ρ of iron is 6.9 g mL^{-1}), θ is porosity, C is the aqueous concentration (M/L^3), v is the average linear velocity (cm min^{-1}), D is the dispersion coefficient (cm^2 min^{-1}) (D= $v\alpha$+D*, α is dispersivity (cm), D* is the effective diffusion coefficient (cm^2 min^{-1})), k_{obs} is the observed first-order rate constant (min^{-1}), Γ is the concentration of sorbed mass of interest on solid surface (M/M), and t is time (T). Units given above are generalized with M representing mass, L length, and T time.

The surface rate constant k in the kinetic iron model KIM (Equation 4.2) is related to the observed rate constant in equation 1.1 as shown in equation 4.3 (Devlin, 2009).

$$\frac{dC}{dt} = -\frac{kC_{max}^R(Fe/V)C}{\frac{1}{J^R} + \frac{C_{max}^R(Fe/V)}{1+J^R} + C} \qquad 4.2$$

$$k_{obs} = \frac{kC_{max}^R(Fe/V)}{\frac{1}{J^R} + \frac{C_{max}^R(Fe/V)}{1+J^R} + C} \qquad 4.3$$

where Fe is iron mass (M) (sometimes represented as iron surface area) (Johnson *et al.*, 1998); V is the volume of water (L^3), and Fe/V is equal to ρ_b/θ in 100% packed granular iron medium. C is the aqueous concentration (M/L^3); C^R_{max} is the capacity of the solid surface to sorb the solute of interest to reactive sites (M/M_{solid}); J^R is a sorption parameter

related to the affinity of a solute for reactive sites (L^3/M); k is the rate constant for the reactions on the solid surface (T^{-1}); t is time (T).

The concentration of mass sorbed to nonreactive sites on the surface is calculated by the Langmuir isotherm sorption:

$$\Gamma = \frac{C^S_{max} C}{\frac{1}{J^S} + C} \tag{4.4}$$

where Γ is the concentration of sorbed mass of interest on solid surface (M/M), C^S_{max} is the capacity of the solid surface to sorb compounds of interest to nonreactive sites (M/M_{solid}), J^S is a sorption parameter related to the affinity of a solute for nonreactive sites (L^3/M), C is the aqueous concentration (M/L^3). If $d\Gamma/dt$ is not assumed to be zero (i.e., steady state does not apply), then differentiating 4.4 yields:

$$\frac{\partial \Gamma}{\partial t} = \frac{C}{\frac{1}{J^S} + C} \frac{\partial C^S_{max}}{\partial t} + \frac{J^S C^S_{max}}{(1 + J^S C)^2} \frac{\partial C}{\partial t} \tag{4.5}$$

Substituting equation 4.5 into equation 4.1 and simplifying,

$$\left(1 + \frac{\rho_b J^S C^S_{max}}{\theta\left(1 + J^S C\right)^2}\right) \frac{\partial C}{\partial t} = D \frac{\partial^2 C}{\partial x^2} - v \frac{\partial C}{\partial x} - k_{obs} C - \frac{\rho_b}{\theta} \frac{C}{\frac{1}{J^S} + C} \frac{\partial C^S_{max}}{\partial t} \tag{4.6}$$

Defining the retardation factor R_f as follows:

$$R_f = 1 + \frac{\rho_b}{\theta} \frac{J^S C^S_{max}}{\left(1 + J^S C\right)^2} \tag{4.7}$$

Bringing equation 4.7 into equation 4.6 and rearranging,

$$\frac{\partial C}{\partial t} = \frac{D}{R} \frac{\partial^2 C}{\partial x^2} - \frac{v}{R} \frac{\partial C}{\partial x} - \frac{k_{obs}}{R} C - \frac{C}{\frac{1 + J^S C}{\frac{\rho_b}{\theta} J^S} + \frac{C^S_{max}}{1 + J^S C}} \frac{\partial C^S_{max}}{\partial t} \tag{4.8}$$

Equation 4.8 can be rewritten to refer specifically to PCE with the addition of appropriate subscripts. For a 100% granular iron column,

$$\frac{\partial C_{PCE}}{\partial t} = \frac{D_{PCE}}{R_{PCE}}\frac{\partial^2 C_{PCE}}{\partial x^2} - \frac{v}{R_{PCE}}\frac{\partial C_{PCE}}{\partial x} - \frac{k_{obs,PCE}}{R_{PCE}}C_{PCE} - \frac{C_{PCE}}{\frac{1 + J_{PCE}^S C_{PCE}}{\frac{Fe}{V}J_{PCE}^S} + \frac{\Gamma_{max,PCE}^S}{1 + J_{PCE}^S C_{PCE}}}\frac{\partial \Gamma_{max,PCE}^S}{\partial t} \quad (4.9)$$

Since TCE is a daughter product of PCE, the degradation of PCE contributes to the formation of TCE for 100% granular iron column.

$$\frac{\partial C_{TCE}}{\partial t} = \frac{k_{obs,PCE} p C_{PCE}}{R_{PCE}}\frac{R_{PCE}}{R_{TCE}} + \frac{D_{TCE}}{R_{TCE}}\frac{\partial^2 C_{TCE}}{\partial x^2} - \frac{v}{R_{TCE}}\frac{\partial C_{TCE}}{\partial x} - \frac{k_{obs,TCE}}{R_{TCE}}C_{TCE} - \frac{C_{TCE}}{\frac{1 + J_{TCE}^S C_{TCE}}{\frac{Fe}{V}J_{TCE}^S} + \frac{\Gamma_{max,TCE}^S}{1 + J_{TCE}^S C_{TCE}}}\frac{\partial \Gamma_{max,TCE}^S}{\partial t}$$

Simplifying,

$$\frac{\partial C_{TCE}}{\partial t} = \frac{k_{obs,PCE} p C_{PCE}}{R_{TCE}} + \frac{D_{TCE}}{R_{TCE}}\frac{\partial^2 C_{TCE}}{\partial x^2} - \frac{v}{R_{TCE}}\frac{\partial C_{TCE}}{\partial x} - \frac{k_{obs,TCE}}{R_{TCE}}C_{TCE} - \frac{C_{TCE}}{\frac{1 + J_{TCE}^S C_{TCE}}{\frac{Fe}{V}J_{TCE}^S} + \frac{\Gamma_{max,TCE}^S}{1 + J_{TCE}^S C_{TCE}}}\frac{\partial \Gamma_{max,TCE}^S}{\partial t} \quad (4.10)$$

Assuming a branching degradation pattern in which TCE forms along one pathway and some other unspecified substance(s) forms along another pathway, the following can also be written,

$$\frac{\partial C_{other}}{\partial t} = \frac{k_{obs,PCE} q C_{PCE}}{R_{other}} + \frac{D_{other}}{R_{other}}\frac{\partial^2 C_{other}}{\partial x^2} - \frac{v}{R_{other}}\frac{\partial C_{other}}{\partial x} - \frac{k_{obs,other}}{R_{other}}C_{other} - \frac{C_{other}}{\frac{1 + J_{other}^S C_{other}}{\frac{Fe}{V}J_{other}^S} + \frac{\Gamma_{max,other}^S}{1 + J_{other}^S C_{other}}}\frac{\partial \Gamma_{max,other}^S}{\partial t} \quad (4.11)$$

where p and q are stoichiometric coefficients relating daughter compound production from PCE ($p + q = 1$ for the branching pattern of degradation, and where concentrations are expressed in μM). Competition for the surface is also possible with other compounds

and daughter products, such as vinyl chloride and dichloroethylene (DCE). Similar equations could be formulated for each of these compounds, but for the purposes of this work, the effects of all other competitors are lumped into the hypothetical substance, 'other' (Equation 4.11).

Substituting the KIM expression for k_{PCE}, k_{TCE}, and k_{other} (Equation 4.3), the final forms of the T-KIM equations are obtained (Equations 4.12, 4.13 and 4.14).

$$\frac{\partial C_{PCE}}{\partial t} = \frac{D_{PCE}}{R_{PCE}}\frac{\partial^2 C_{PCE}}{\partial x^2} - \frac{v}{R_{PCE}}\frac{\partial C_{PCE}}{\partial x} - \frac{\dfrac{k_{PCE} C^R_{max,PCE}(Fe/V)}{\dfrac{1}{J^R_{PCE}} + \dfrac{C^R_{max,PCE}(Fe/V)}{1+J^R_{PCE}} + C_{PCE}}}{R_{PCE}} C_{PCE} - \frac{C_{PCE}}{\dfrac{1+J^S_{PCE}C_{PCE}}{\dfrac{Fe}{V}J^S_{PCE}} + \dfrac{\Gamma^S_{max,PCE}}{1+J^S_{PCE}C_{PCE}}}\frac{\partial \Gamma^S_{max,PCE}}{\partial t} \tag{4.12}$$

$$\frac{\partial C_{TCE}}{\partial t} = \frac{\dfrac{k_{PCE} C^R_{max,PCE}(Fe/V)}{\dfrac{1}{J^R_{PCE}} + \dfrac{C^R_{max,PCE}(Fe/V)}{1+J^R_{PCE}} + C_{PCE}} pC_{PCE}}{R_{TCE}} + \frac{D_{TCE}}{R_{TCE}}\frac{\partial^2 C_{TCE}}{\partial x^2} - \frac{v}{R_{TCE}}\frac{\partial C_{TCE}}{\partial x} - \frac{\dfrac{k_{TCE} C^R_{max,TCE}(Fe/V)}{\dfrac{1}{J^R_{TCE}} + \dfrac{C^R_{max,TCE}(Fe/V)}{1+J^R_{TCE}} + C_{TCE}}}{R_{TCE}} C_{TCE} - \frac{C_{TCE}}{\dfrac{1+J^S_{TCE}C_{TCE}}{\dfrac{Fe}{V}J^S_{TCE}} + \dfrac{\Gamma^S_{max,TCE}}{1+J^S_{TCE}C_{TCE}}}\frac{\partial \Gamma^S_{max,TCE}}{\partial t} \tag{4.13}$$

$$\frac{\partial C_{other}}{\partial t} = \frac{\dfrac{k_{PCE} C^R_{max,PCE}(Fe/V)}{\dfrac{1}{J^R_{PCE}} + \dfrac{C^R_{max,PCE}(Fe/V)}{1+J^R_{PCE}} + C_{PCE}} qC_{PCE}}{R_{other}} + \frac{D_{other}}{R_{other}} \frac{\partial^2 C_{other}}{\partial x^2} - \frac{v}{R_{other}} \frac{\partial C_{other}}{\partial x}$$

$$- \frac{\dfrac{k_{other} C^R_{max,other}(Fe/V)}{\dfrac{1}{J^R_{other}} + \dfrac{C^R_{max,other}(Fe/V)}{1+J^R_{other}} + C_{other}}}{R_{other}} C_{other}$$

$$- \frac{C_{other}}{\dfrac{1+J^S_{other}C_{other}}{\dfrac{Fe}{V}J^S_{other}} + \dfrac{\Gamma^S_{max,other}}{1+J^S_{other}C_{other}}} \frac{\partial \Gamma^S_{max,other}}{\partial t} \qquad 4.14$$

4.3.2 Crank-Nicholson Finite Difference Equation

A finite difference scheme was employed to solve equations 4.9, 4.10 and 4.11 numerically. Crank-Nicholson weighting (ω) was used to minimize errors associated with numerical dispersion and instability. The combined implicit and explicit solutions with the weighting factor are written below. In general, x is the distance from the source (L), Δx is the interval of distance (L); t is time (T), Δt is the interval of time (T); $C_{x,\,t}$ is the aqueous concentration at distance x and time t (M/L^3); R is the retardation factor (unitless); D is the dispersion coefficient (m^2 s^{-1}); ω is Crank-Nicholson weighting, set as 0.5; $\Gamma^S_{max\,x,t}$ is the concentration of sorbed mass of interest on the non-reactive sites on the solid surface at distance x and time t (M/M), C^S_{max} is the capacity of the solid surface to sorb compounds of interest to nonreactive sites (M/M$_{solid}$); J^S is a sorption parameter related to the affinity of a solute for nonreactive sites (L^3/M). Certain terms, such as $C_{x,t}$, R, $\Gamma^S_{max\ x,t}$, C^S_{max}, J^S and D are dropped for specific chemicals (PCE, TCE and other compounds).

$$\frac{C_{x,t}-C_{x,t-\Delta t}}{\Delta t}=\omega\frac{D}{R}\frac{\frac{C_{x+\Delta x,t}-C_{x,t}}{\Delta x}-\frac{C_{x,t}-C_{x-\Delta x,t}}{\Delta x}}{\Delta x}-\omega\frac{v}{R}\frac{C_{x,t}-C_{x-\Delta x,t}}{\Delta x}-\omega\frac{k}{R}C_{x,t}$$

$$-\omega\frac{C_{x,t}}{\frac{1+J^{S}C_{x,t}}{\frac{\rho b}{\theta}J^{S}}+\frac{\Gamma^{S}_{\max x,t}}{1+J^{S}C_{x,t}}}\frac{\Gamma^{S}\max x,t-C^{S}\max x,t-\Delta t}{\Delta t}+(1-\omega)\frac{D}{R}\frac{\frac{C_{x+\Delta x,t-\Delta t}-C_{x,t-\Delta t}}{\Delta x}-\frac{C_{x,t-\Delta t}-C_{x-\Delta x,t-\Delta t}}{\Delta x}}{\Delta x}$$

$$-(1-\omega)\frac{v}{R}\frac{C_{x,t-\Delta t}-C_{x-\Delta x,t-\Delta t}}{\Delta x}-(1-\omega)\frac{k}{R}C_{x,t-\Delta t}-(1-\omega)\frac{C_{x,t-\Delta t}}{\frac{1+J^{S}C_{x,t-\Delta t}}{\frac{Fe}{V}J^{S}}+\frac{\Gamma^{S}_{\max x,t-\Delta t}}{1+J^{S}C_{x,t-\Delta t}}}\frac{\Gamma^{S}\max x,t-C^{S}\max x,t-\Delta t}{\Delta t}$$

Simplifying and solving for the concentration at position *x* and time *t*,

$$C_{x,t}=\gamma(\alpha C_{x+\Delta x,t}+bC_{x-\Delta x,t}+\alpha(\frac{1-\omega}{\omega})C_{x+\Delta x,t-\Delta t}+b(\frac{1-\omega}{\omega})C_{x-\Delta x,t-\Delta t}+eC_{x,t-\Delta t})$$

$$-\gamma(\Gamma^{S}\max x,t-\Gamma^{S}\max x,t-\Delta t)(\frac{\omega C_{x,t}}{\frac{1+J^{S}C_{x,t}}{\frac{Fe}{V}J^{S}}+\frac{\Gamma^{S}_{\max x,t}}{1+J^{S}C_{x,t}}}+\frac{(1-\omega)C_{x,t-\Delta t}}{\frac{1+J^{S}C_{x,t-\Delta t}}{\frac{Fe}{V}J^{S}}+\frac{\Gamma^{S}_{\max x,t-\Delta t}}{1+J^{S}C_{x,t-\Delta t}}})$$

4.15

where,

$$\alpha=\frac{\omega D\Delta t}{\Delta x^{2}R}$$

$$b=\alpha+\frac{\omega v\Delta t}{R\Delta x}$$

$$e=1-\frac{2(1-\omega)D\Delta t}{R\Delta x^{2}}-\frac{(1-\omega)v\Delta t}{R\Delta x}-\frac{(1-\omega)k\Delta t}{R}$$

$$\gamma=\frac{\Delta x^{2}}{\left(\Delta x^{2}+\frac{2\omega D\Delta t}{R}+\frac{\omega v\Delta t\Delta x}{R}+\frac{\omega k\Delta t\Delta x^{2}}{R}\right)}$$

The final forms of the T-KIM equations solved by Crank-Nicholson were obtained (Equations 4.16, 4.17 and 4.18).

$$C_{x,t(PCE)} = \qquad 4.16$$

$$\gamma_{x,t\ PCE}\left(a_{x,t\ PCE}C_{x+\Delta x,t\ PCE} + b_{x,t\ PCE}C_{x-\Delta x,t\ PCE} + a_{x,t\ PCE}\left(\frac{1-\omega}{\omega}\right)C_{x+\Delta x,t-\Delta t\ PCE} + b_{x,t\ PCE}\left(\frac{1-\omega}{\omega}\right)C_{x-\Delta x,t-\Delta t\ PCE} + e_{x,t\ PCE}C_{x,t-\Delta t\ PCE}\right) -$$

$$\gamma_{x,t\ PCE}\left(\Gamma^S_{\max x,t\ PCE} - \Gamma^S_{maxx,t-\Delta t\ PCE}\right)\left(\frac{\omega C_{x,t\ PCE}}{\frac{1+J^S_{PCE}C_{x,t\ PCE}}{\frac{Fe}{V}J^S_{PCE}} + \frac{\Gamma^S_{\max x,t\ PCE}}{1+J^S_{PCE}C_{x,t\ PCE}}} + \frac{(1-\omega)C_{x,t-\Delta t\ PCE}}{\frac{1+J^S_{PCE}C_{x,t-\Delta t\ PCE}}{\frac{Fe}{V}J^S_{PCE}} + \frac{\Gamma^S_{\max x,t\ PCE}}{1+J^S_{PCE}C_{x,t-\Delta t\ PCE}}}\right)$$

$$C_{x,t(TCE)} = \frac{\frac{k_{PCE}C^R_{max,x,t\ (PCE)^{(Fe/V)}}}{\frac{1}{J^R_{PCE}} + \frac{C^R_{max,x,t\ (PCE)^{(Fe/V)}}}{1+J^R_{PCE}}} pC_{x,t\ (PCE)}}{R_{x,t\ TCE}} + \gamma_{x,t\ TCE}\left(a_{x,t\ TCE}C_{x+\Delta x,t\ TCE} + b_{x,t\ TCE}C_{x-\Delta x,t\ TCE} + a_{x,t\ TCE}\left(\frac{1-\omega}{\omega}\right)C_{x+\Delta x,t-\Delta t\ TCE} + b_{x,t\ TCE}\left(\frac{1-\omega}{\omega}\right)C_{x-\Delta x,t-\Delta t\ TCE} + e_{x,t\ TCE}C_{x,t-\Delta t\ TCE}\right) - \gamma_{x,t\ TCE}\left(\Gamma^S_{\max x,t\ TCE} - \Gamma^S_{maxx,t-\Delta t\ TCE}\right)\left(\frac{\omega C_{x,t\ TCE}}{\frac{1+J^S_{TCE}C_{x,t\ TCE}}{\frac{Fe}{V}J^S_{TCE}} + \frac{\Gamma^S_{\max x,t\ TCE}}{1+J^S_{TCE}C_{x,t\ TCE}}} + \frac{(1-\omega)C_{x,t-\Delta t\ TCE}}{\frac{1+J^S_{TCE}C_{x,t-\Delta t\ TCE}}{\frac{Fe}{V}J^S_{TCE}} + \frac{\Gamma^S_{\max x,t\ TCE}}{1+J^S_{TCE}C_{x,t-\Delta t\ TCE}}}\right) \qquad 4.17$$

$$C_{x,t(other)} = \frac{\frac{k_{PCE}C^R_{max,x,t\ (PCE)^{(Fe/V)}}}{\frac{1}{J^R_{PCE}} + \frac{C^R_{max,x,t\ (PCE)^{(Fe/V)}}}{1+J^R_{PCE}}} qC_{x,t\ (PCE)}}{R_{x,t\ other}} + \gamma_{x,t\ other}\left(a_{x,t\ other}C_{x+\Delta x,t\ other} + b_{x,t\ other}C_{x-\Delta x,t\ other} + a_{x,t\ other}\left(\frac{1-\omega}{\omega}\right)C_{x+\Delta x,t-\Delta t\ other} + b_{x,t\ other}\left(\frac{1-\omega}{\omega}\right)C_{x-\Delta x,t-\Delta t\ other} + e_{x,t\ other}C_{x,t-\Delta t\ other}\right) - \gamma_{x,t\ other}\left(\Gamma^S_{\max x,t\ other} - \Gamma^S_{maxx,t-\Delta t\ other}\right)\left(\frac{\omega C_{x,t\ other}}{\frac{1+J^S_{other}C_{x,t\ other}}{\frac{Fe}{V}J^S_{other}} + \frac{\Gamma^S_{\max x,t\ TCE}}{1+J^S_{other}C_{x,t\ other}}} + \frac{(1-\omega)C_{x,t-\Delta t\ other}}{\frac{1+J^S_{other}C_{x,t-\Delta t\ other}}{\frac{Fe}{V}J^S_{other}} + \frac{\Gamma^S_{\max x,t\ other}}{1+J^S_{other}C_{x,t-\Delta t\ other}}}\right) \qquad 4.18$$

4.3.3 Competition for Nonreactive Sites by PCE and TCE

The surface of granular iron can be conceptualized as consisting of locations, or sites, where reactions are possible, and where reactions do not occur (Burris *et al.*, 1995; Bi *et al.*, 2009b). The later type of site is one that sorbs organics that undergo no subsequent reaction. Assuming that the total capacity for sorption to these sites, is quantified as the parameter C^S_{maxTOT}, and that it does not change in time, then at any given time only part of this capacity may be occupied by PCE, TCE, or other competing species (Campbell *et al.*, 1997). A mass balance capturing this concept may be written (Equation 4.19)

$$C^S{}_{\max TOT} = \Gamma^S{}_{TCE} + \Gamma^S{}_{PCE} + \Gamma^S_{other} + \Gamma^S{}_{AV} \qquad 4.19$$

where Γ^S_{TCE} is the concentration of nonreactive sites occupied by TCE (M/M), Γ^S_{PCE} is the concentration of nonreactive sites occupied by PCE (M/M), Γ^S_{other} is the concentration of nonreactive sites occupied by other competing species, and Γ^S_{AV} is the concentration of unoccupied (available) nonreactive sites (M/M).

At any given time, the maximum amount of surface available to sorb a particular substance can be calculated from equation 4.19 as the sum of the substance specific sorption term and the available sorption term. For example, the capacity to sorb PCE, $\Gamma^S_{max\ PCE,}$ is given by the sum of $\Gamma^S_{PCE} + \Gamma^S_{AV}$. With this definition, the mass balances can be rewritten,

$$\Gamma^S_{max\ PCE} = C^S_{maxTOT} - \Gamma^S_{TCE} - \Gamma^S_{other} \qquad 4.20$$

$$\Gamma^S_{max\ TCE} = C^S_{maxTOT} - \Gamma^S_{PCE} - \Gamma^S_{other} \qquad 4.21$$

$$\Gamma^S_{max\ other} = C^S_{maxTOT} - \Gamma^S_{PCE} - \Gamma^S_{TCE} \qquad 4.22$$

In the above equations, the C^S_{maxTOT} term is a prescribed number that is assumed fixed in time. In order to calculate the Γ^S_{max} terms, the sorbed concentrations of each substance

must also be estimated. This can be done through compound specific Langmuir isotherms that relate the equilibrium sorbed concentrations at any time to the measured aqueous concentrations at that same time (Lee and Batchelor, 2002a). For PCE this can be expressed as,

$$\Gamma^{S}{}_{PCE} = \frac{C^{S}{}_{\max PCE} C_{PCE}}{\frac{1}{J^{S}{}_{PCE}} + C_{PCE}} \tag{4.23}$$

where $C^{S}{}_{maxPCE}$ is the nonreactive sorption capacity for PCE (M/M), $J^{S}{}_{PCE}$ is sorption parameter related to the affinity of PCE for nonreactive sites (L^3/M), C_{PCE} is the aqueous concentration of PCE (M/L^3). Similarly, for the other substances being modeled,

$$\Gamma^{S}{}_{TCE} = \frac{C^{S}{}_{\max TCE} C_{TCE}}{\frac{1}{J^{S}{}_{TCE}} + C_{TCE}} \tag{4.24}$$

$$\Gamma^{S}{}_{other} = \frac{C^{S}{}_{\max other} C_{other}}{\frac{1}{J^{S}{}_{other}} + C_{other}} \tag{4.25}$$

where parameters are similarly defined for the subscripted substances. Calculated $C^{S}{}_{max}$ for PCE, TCE and other substances can be used with user defined values of J^{S} to calculate time and location specific retardation factors for each transported substance.

4.3.4 Competition for Reactive Sites by PCE and TCE

In a fashion similar to that described for the nonreactive site cases, mass balances can be written for the reactive sites as follows,

$$C^{R}{}_{\max TOT} = \Gamma^{R}{}_{TCE} + \Gamma^{R}{}_{PCE} + \Gamma^{R}_{other} + \Gamma^{R}{}_{AV} \tag{4.26}$$

$$I^{R}{}_{max\,PCE} = C^{R}{}_{maxTOT} - I^{R}{}_{TCE} - I^{R}{}_{other} \tag{4.27}$$

$$I^{R}{}_{max\,TCE} = C^{R}{}_{maxTOT} - I^{R}{}_{PCE} - I^{R}{}_{other} \tag{4.28}$$

$$\Gamma^{R}_{max\ other}=C^{R}_{maxTOT}-\Gamma^{R}_{PCE}-\Gamma^{R}_{TCE} \quad 4.29$$

where the superscripted R denotes reactive sites and other symbols are as previously defined for nonreactive sites. As before, the compound specific sorption terms can be determined at any time from the measured aqueous concentrations by applying Langmuir isotherms,

$$\Gamma^{R}_{PCE}=\frac{\Gamma^{R}_{\max PCE}C_{PCE}}{\frac{1}{J^{R}_{PCE}}+C_{PCE}} \quad 4.30$$

$$\Gamma^{R}_{TCE}=\frac{\Gamma^{R}_{\max TCE}C_{TCE}}{\frac{1}{J^{R}_{TCE}}+C_{TCE}} \quad 4.31$$

$$\Gamma^{R}_{other}=\frac{\Gamma^{R}_{\max other}C_{other}}{\frac{1}{J^{R}_{other}}+C_{other}} \quad 4.32$$

Calculated Γ^{R}_{max} of PCE, TCE and the other competing species are utilized in the KIM reaction term to calculate reaction rates.

4.3.5 Boundary Conditions

Two different boundary conditions are considered in T-KIM. The first type boundary at x=0 is:

$$vc = vC_0$$

therefore, $C_{(0,t)}=C_0$.

The third type boundary condition (Cauchy) recognizes dispersion at the boundary and is given by:

$$-D\frac{\partial C}{\partial x}+vc=vC_0$$

The finite different form is:

$$-D\frac{C_{x+\Delta x}-C_x}{\Delta x}+vC_x=vC_0$$

rearranging,

$$-D\frac{C_{x+\Delta x}}{\Delta x}+D\frac{C_x}{\Delta x}+vC_x=vC_0$$

leading to an estimated concentration at the boundary given by,

$$C_{0,t}=\frac{vC_o+D\frac{C_{x+\Delta x}}{\Delta x}}{\frac{D}{\Delta x}+v} \qquad 4.33$$

4.3.6 Validation of T-KIM

In order to validate the accuracy of the transport aspect of the numerical model, it was compared to well accepted analytical models. The Ogata-Banks analytical model (Ogata and Banks, 1961) (Equations 4.34 and Appendix G) assumes a first type boundary condition with $C(0,t)=C_o$,

$$C(x,t)=\frac{C_0}{2}\left[erfc\left(\frac{x-vt}{2\sqrt{Dt}}\right)+exp\left(\frac{vx}{D}\right)*erfc\left(\frac{x+vt}{2\sqrt{Dt}}\right)\right] \qquad 4.34$$

where C is the aqueous concentration (M/L^3), C_o is the source concentration (M/L^3), v is average linear velocity (m s^{-1}), D is the dispersion coefficient (m^2 s^{-1}), x is distance from the source (L) and t is time (T).

Another analytical solution to the ADE, this time accounting for retardation and reaction, and referred to here as BearPE, was also compared to T-KIM (Equation 4.2) (Bear, 1979). BearPE was developed with a third type boundary,

$$-D\frac{\partial C}{\partial x}+vc=vC_0$$

and has the form

$$C(x,t) = \frac{C_0}{2}\left\{\exp\left[\frac{vx}{2D}\left(1-\sqrt{1+\frac{4k_{obs}D}{v^2}}\right)\right] erfc\left[\frac{Rx - vt\sqrt{1+\frac{4k_{obs}D}{v^2}}}{2\sqrt{DRt}}\right]\right\} \quad 4.35$$

where R is retardation factor, k_{obs} is an observed first order rate constant (min^{-1}).

4.4 Results and Discussion

4.4.1 Conservative Transport

Breakthrough of a nonreacting and nonsorbing solute from a hypothetical column was modeled with T-KIM and the Ogata-Banks analytical solution (Equation 4.31, Table 4.1 and Figure 4.1). Since the Ogata-Banks solution assumes a first type boundary condition, T-KIM was also executed assuming a first type boundary. A comparison of the two curves shows very good agreement. A small amount of numerical dispersion is present in the T-KIM solution, leading to systematic but minor error in the solution. These results verify that the basic transport functions of the T-KIM model perform as intended.

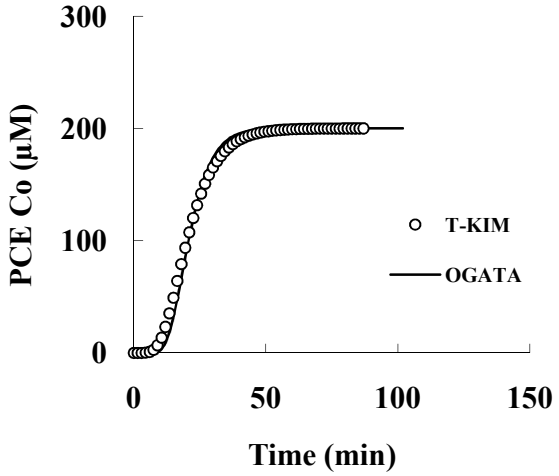

Figure 4.1: Conservative solute transport through an 18 cm long column data with C_o at 200 µM.

Table 4.1 Input parameter values for the comparison of models

	T-KIM	OGATA	BearPE	KIM	Langmuir Sorption Isotherm
v (cm/min)	0.82	0.82	0.82	0.82	
D (cm^2/min)	0.82	0.82	0.82		
Fe/V (g/L)	4192			4192	4192
k_{obs} (min^{-1})	k_{obs}=0 (compare to OGATA), otherwise calculated by KIM		k_{obs}=0.044 (C_o=30 μM), k_{obs}=0.04(C_o=60 μM), k_{obs}=0.035 (C_o=100 μM), k_{obs} =0.026 (C_o=200 μM)) (Figure 4.2), k_{obs}=0.016 (C_o=400 μM), k_{obs} =0.012 (C_o=600 μM), k_{obs}=0.01(C_o=800 μM)		
R_f	R_f=1 (compare to OGATA); R_f=7.79 (C_o=30 μM), R_f=7.44 (C_o=60 μM), R_f=6.89 (C_o=100 μM), R_f =5.67 (C_o=200 μM) (Figure 4.2), R_f=4 (C_o=400 μM), R_f=3.16 (C_o=600 μM), R_f= 2.69(C_o=800 μM)		R_f=7.55 (C_o=30 μM), R_f=7.08 (C_o=60 μM), R_f=6.60 (C_o=100 μM), R_f =5.52 (C_o=200 μM) (Figure 4.2), R_f=4 (C_o=400 μM), R_f=3.33 (C_o=600 μM), R_f= 2.84(C_o=800 μM)		R_f=7.35 (C_o=30 μM), R_f=7.08 (C_o=60 μM), R_f=6.7 (C_o=100 μM), R_f=5.73 (C_o=200 μM), R_f=4.19 (C_o=400 μM), R_f=3.24 (C_o=600 μM), R_f= 2.64 (C_o=800 μM))
$C_{1/2}$ (μM)					6.11 (C_o=30 μM), 13.28. (C_o=60 μM), 24.35 (C_o=100 μM), 58.05 (C_o=200 μM), 140.5 (C_o=400 μM), 230.75 (C_o=600 μM), 324 (C_o=800 μM)
w	0.5				
K_{PCE} (min^{-1})	0.07			0.07	
C^S_{maxTOT} (μM/g)	0.5				0.506
C^R_{maxTOT} (μM/g)	0.026			0.029	
J^R (L/μM)1	0.018			0.011	
J^S (L/μM)	0.0035				0.0031

4.4.2 Reactive Transport

In order to assess the validity of the terms accounting for nonreactive sorption and degradation, another hypothetical column experiment was simulated this time with input parameters representative of PCE transported through a granular iron medium. The basic

transport parameters, velocity and dispersion, were not changed from the conservative solution simulation above. The T-KIM solution was compared to BearPE, an analytical solution with retardation and reaction, and assuming a third type boundary (Bear, 1979). In this simulation, T-KIM was executed with a third type boundary, a fixed retardation factor and a fixed first order rate constant (Table 4.1 and Figure 4.2).

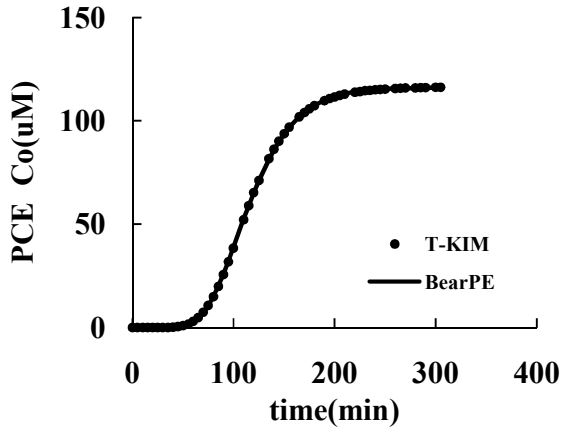

Figure 4.2: PCE transported through a hypothetical 18 cm long column with C_o = 200 µM. Other inputs are specified in Table 4.1.

Once again the agreement between T-KIM and the analytical solution is close. The agreement between the two solutions appears to be better than the previous case because an extra measure of dispersion, introduced by the third type boundary, reduces the error due to numerical dispersion. Use of a third type boundary not only improves the accuracy of the numerical model, it is considered to be a more realistic boundary condition since it conserves mass at the boundary while a first type boundary does not (Batu, 2010).

4.4.3 Assessing Reactive Site Parameter Estimation Accuracy

To assess the functionality of the terms accounting for competition in the T-KIM code, a series of synthetic column breakthrough curves with increasing C_o was calculated

by T-KIM with retardation factors and first order rate constants varying due to competition. These synthetic data were analyzed using the techniques introduced by Marietta and Devlin (2005) and Bi *et al*. (2010) to solve the inverse problem. If the model functioned correctly, the analysis was expected to produce parameters that matched the model input (Table 4.1 and Figure 4.3). This fit accurately estimated the reactive site sorption and reaction parameters used in the T-KIM simulations showing that T-KIM was calculating the processes as intended (Table 4.1). Note that for the purposes of this assessment the highest value of C_o considered was 800 μM, higher than what was considered in experimental data sets. This was done with emphasis on capturing the widest range of rate behavior in the assessment, not to faithfully reproduce experimental data sets.

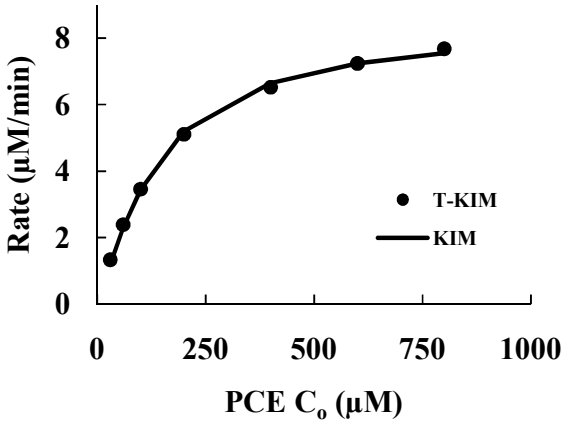

Figure 4.3: Fitting of T-KIM concentration dependent rate data with KIM.

The fitted KIM resulted in estimates of k, C^R_{max}, and J^R that closely matched the input to T-KIM (Table 4.1). On the basis of this result, the processes of competition simulated in T-KIM were considered to be functioning as intended.

4.4.4 Assessing Nonreactive Site Parameter Estimation Accuracy

T-KIM also estimated R_f as a time- and location-specific quantity for each synthetic column experiment. Apparent R_f values, representing weighted column-wide averages, were estimated by BearPE as discussed by Bi *et al.* (2010), and used to estimate Langmuir isotherm parameters for nonreactive sites. Therefore direct comparisons between BearPE R_f values and those calculated by T-KIM were not possible for every data point in the synthetic breakthrough curves. Instead, a single point R_f was selected from each breakthrough curve in the T-KIM data for comparison with the corresponding BearPE R_f. The T-KIM point-specific retardation factors, $R_f^{T\text{-}KIM}$, selected for comparison with the BearPE values were chosen for time, t, corresponding to concentrations halfway between the initial concentrations in the columns (= 0 μM in this case) and the steady state concentrations. The T-KIM calculated results matched the BearPE calculated retardation factors very well (Table 4.1 and Figure 4.4). This exercise showed that BearPE can be used to accurately estimate effective retardation factors reproducible from the T-KIM data.

Langmuir isotherm parameters for the nonreactive sites were estimated by fitting $R_f^{T\text{-}KIM}$ to the theoretical Langmuir sorption isotherm derived retardation factor equation (Equation 4.7). This fitting process resulted in nonreactive sorption parameters that matched the T-KIM input very well, showing that the nonreactive competition processes were being calculated by the model as intended (Table 4.1 and Figure 4.4).

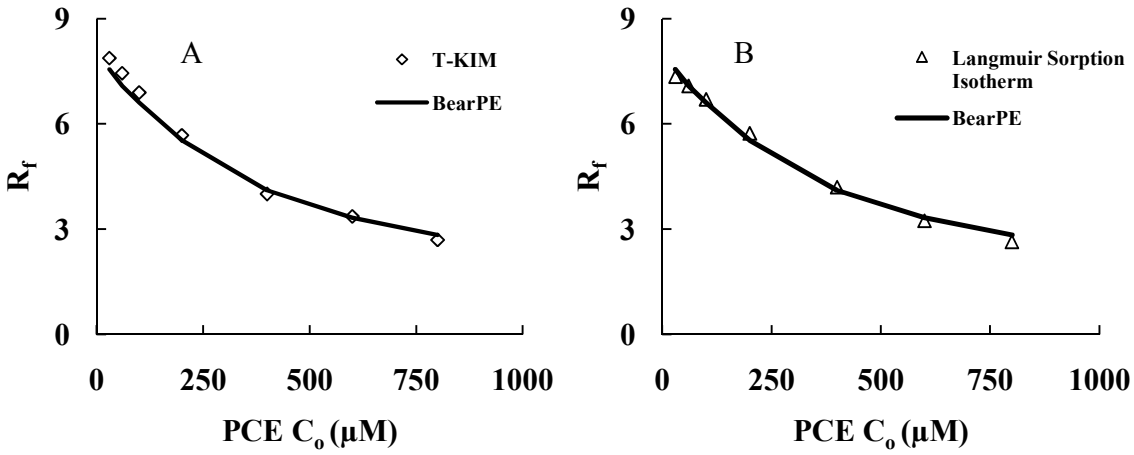

Figure 4.4: Comparison of R_f calculated byT-KIM, fitted by BearPE and calculated by Langmuir sorption isotherm for PCE synthetic column experiments.

4.4.5 Competition on Solid Surface

Having established the validity of the transport, reaction and competition functions of the T-KIM code, a preliminary assessment of interspecies competition under the conditions of the experiments reported in the earlier chapters of this thesis was undertaken (Figure 4.5). In the PCE column experiments, TCE was the only daughter product detected, suggesting that only TCE was present in the columns with concentrations sufficient for inter-species competition. However, competition of 'other' daughter products was also considered by T-KIM. Since the detected TCE concentration is very low, it is possible that PCE was mostly converted to other products, so the proportion parameter, p, applied in T-KIM for TCE was estimated to be 0.1, and q for other products was estimated to be 0.9.

The PCE and TCE curves could be reasonably reproduced in the model using parameter values determined experimentally. Under these conditions, the degradation curve for PCE accounting for TCE production and competition is virtually indistinguishable from the curve produced ignoring competition effects from TCE. It is concluded that the presence of TCE in the columns investigated in this work had no

measurable effect on PCE disappearance. It remains a possibility that other, undetected compounds were present in the column and competed with PCE for the iron surface. These might include the acetylene compounds, *cis*-dichloroethene, and chloroethene. Further more detailed work is needed to evaluate this possibility.

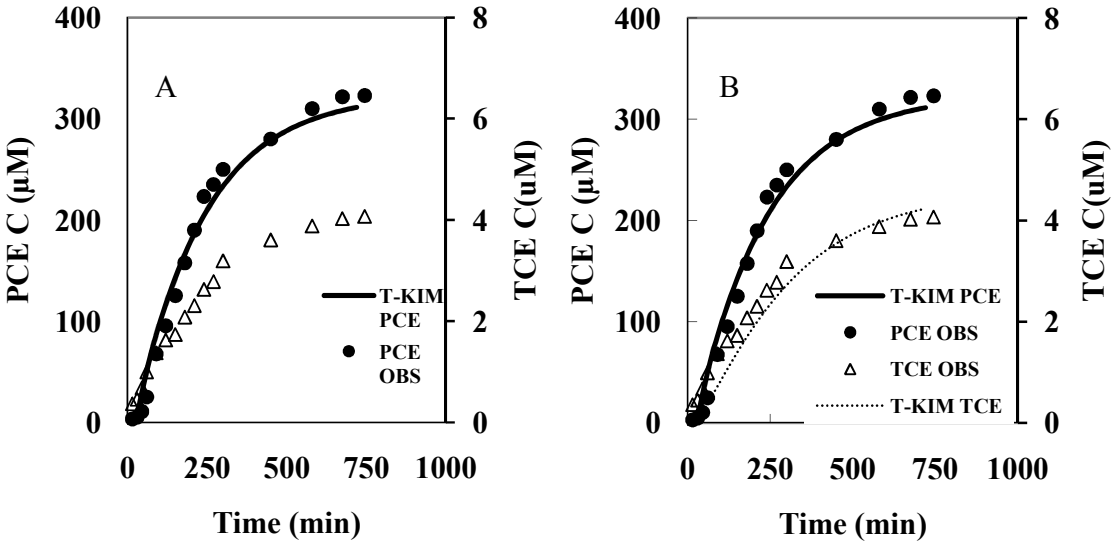

Figure 4.5: PCE column experimental data (C20) fitted with T-KIM without TCE competition (A), and with TCE and other products competing for iron surface (B). The initial concentration of PCE was 380 µM. The initial concentration of TCE for both simulations was set at 0.0001 µM, representing an arbitrarily low concentration.

At low TCE concentrations, the competition on reactive sites and non-reactive sites between TCE and PCE was not noticeable. In order to observe a noticeable competition effect on PCE degradation rate, the initial concentration of TCE had to be increased to a value over 100 µM (Figure 4.6).

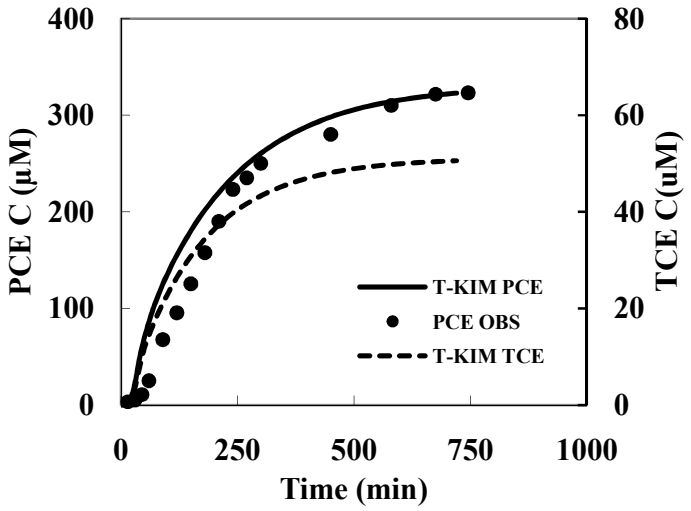

Figure 4.6: PCE column experimental data (C20) fitted with T-KIM with TCE competing for iron surface. The initial concentration of TCE was set at 100 µM.

4.5 Conclusion

A one dimensional finite difference numerical transport model incorporating surface limited reaction and nonlinear sorption to reactive and nonreactive sites, and interspecies competition, was evaluated against 2 analytical solutions to the transport equation. The model was found to agree well with the analytical solutions for cases involving first and third type boundaries, and for linear sorption and first order reaction kinetics. The nonlinear functions of the model were validated by using recently developed methods to solve the inverse problem and showing that fitted and input parameters agreed well. Preliminary calculations showed that levels of TCE detected in the column experiments reported in chapters 2 to 3 were insufficient to cause measurable competition effects in the degradation of PCE.

References

Allen-King, R. M., R. M. Halket and D. R. Burris (1997). "Reductive Transformation and Sorption of Cis-and Trans-1,2-Dichloroethene in A Metallic Iron-Water System." Environmental toxicology and chemistry 16(3): 424-429.

Arnold, W. A. and A. L. Roberts (2000a). "Inter- and Intraspecies Competitive Effects in Reactions of Chlorinated Ethylenes with Zero-Valent Iron in Column Reactors." Environmental Engineering Science 17(5): 291-302.

Arnold, W. A. and A. L. Roberts (2000b). "Pathways and Kinetics of Chlorinated Ethylene and Chlorinated Acetylene Reaction with Fe(0) Particles." Environmental Science & Technology 34(9): 1794-1805.

Batu, V. (2010). "Estimation of Degradation Rates by Satisfying Mass Balance at the Inlet." Ground Water 48(4): 560-568.

Bear, J. (1979). Hydraulics of Groundwater (Mcgraw-Hill Series in Water Resources and Environmental Engineering) New York, McGraw-Hill Companies.

Bi, E., J. F. Devlin and B. Huang (2009). "Effects of Mixing Granular Iron with Sand on the Kinetics of Trichloroethylene Reduction." Ground Water Monitoring and Remediation 29(2): 56-62.

Bi, E., J.F.Devlin, B. Huang and R. Firdous (2010). "Transport and Kinetic Studies To Characterize Reactive and Nonreactive Sites on Granular Iron." Environmental Science and Technology 44(14): 5564-5569.

Burris, D. R., T. J.Campbell and V. S.Manoranjan (1995). "Sorption of Trichloroethylene and Tetrachloroethylene in A Batch Reactive Metallic Iron-water System." Environmental Science and Technology 29(11): 2850-2855.

Campbell, T. J., D. R. Burris, A. L. Roberts and J. R. Wells (1997). "Trichloroethylene and Tetrachloroethylene Reduction in A Metallic Iron-Water-Vapor Batch System." Environmental Toxicology and Chemistry 16(4): 625-630.

Devlin, J. F. (2009). "Development and Assessment of A Rate Equation for Chemical Transformations in Reactive Porous Media." Environmental Science and Technology.

Dries, J., L. Bastiaens, D. Springael, A. Spiros N and L. Diels (2004). "Competition for Sorption and Degradation of Chlorinated Ethenes in Batch Zero-valent Iron Systems." Environmental Science and Technology 38: 2879-2884.

EPA (1999). Field Applications of In Situ Remediation Technologies: Permeable Reactive Barriers. E. U. S. E. P. Agency). 542-R-99-002.

Farrell, J., M. Kason, N. Melitas and T. Li (2000). "Investigation of the Long-term Performance of Zero-valent Iron for Reductive Dechlorination of Trichloroethylene." Environmental Science and Technology 34: 514-521.

Flury, B., J. Frommer, U. Eggenberger, U. Mader, M. Nachtegaal and R. Ketzschmar (2009). "Assessment of Long-term Performance and Chromate Reduction Mechanisms in

A Field Scale Permeable Reactive Barrier." Environmental Science and Technology 43(17): 6786-6792.

Johnson, T. L., W. Fish, Y. A. Gorby and P. G. Tratnyek (1998). "Degradation of carbon tetrachloride by iron metal: Complexation effects on the oxide surface." journal of contaminant hydrology 29(4): 379-398.

Lee, W. and B. Batchelor (2002). "Abiotic reductive dechlorination of chlorinated ethylenes by iron-bearing soil minerals. 1. Pyrite and magnetite." Environmental Science & Technology 36(23): 5147-5154.

Liang, L., G. R. Moline, W. Kamolpornwijit and O. R. West (2005). "Influence of Hydrogeochemical Processes on Zero-valent Iron Reactive Barrier Performance: A Field Investigation." Journal of Contaminant Hydrology 78: 291-312.

Marietta, M. and J. F. Devlin (2005). Separating the Kinetic and Sorption Parameters of Nitroaromatic Compounds in Contact with Granular Iron. 4th International Groundwater Quality Conference. waterloo, canada**:** 6.

Matheson, L. J. and P. G. Tratnyek (1994). "Reductive Dehalogenation of Chlorinated Methanes by Iron Metal." Environmental Science and Technology 28(12): 8.

Miehr, R., P. G. Tratnyek, J. Z. Bandstra, M. M. Scherer, M. J. Alowitz and E. J. Bylaska (2004). "Diversity of Contaminant Reduction Reactions by Zerovalent Iron: Role of the Reductate." Environmental Science and Technology(38): 139-147.

O'Hannesin, S. F. and R. W. Gillham (1998). "Long-term performance of an in situ "iron wall" for remediation of VOCs." Ground Water 36(1): 164-170.

Ogata, A. and R. B. Banks (1961). A solution of the Differential Equation of Longitudinal Dispersion in Porous Media U. S. G. S. P. Paper**:** 411-A, 417.

Pulsa, R. W., C. J. Paula and R. M. Powell (1999). "The Application of In Situ Permeable Reactive (Zero-Valent Iron) Barrier Technology for the Remediation of Chromate-Contaminated Groundwater: A Field Test." Applied Geochemistry 14(8): 11.

Rodriguez-Maroto, J. M., F. Garcia-Herruzo, A. Garcia-Rubio, C. Gomez-Lahoz and C. Vereda-Alonso (2009). "Kinetics of the chemical reduction of nitrate by zero-valent iron." Chemosphere 74(6): 804-809.

Schäfer, D., R. Köber and A. Dahmke (2003). "Competing TCE and cis-DCE Degredation Kinetics by Zero-valent Iron-Experimental Results and Numerical Simulation." Journal of Contaminant Hydrology 65: 183-202.

Su, C. and R. W. Puls (1999). "Kinetics of Trichloroethene Reduction by Zerovalent Iron and Tin: Pretreatment Effect, Apparent Activation Energy, and Intermediate Products." Environmental Science and Technology 33(1): 163-168.

Wüst, W. F., R. Kober, O. Schlicker and A. Dahmke (1999). "Combined Zero- and First-order Kinetic Model of the Degradation of TCE and Cis-DCE with Commercial Iron." Environmental Science and Technology 33: 4304-4309.

5 Kinetic Experiments to Determine the Control on Reaction Rates for Two Forms of Granular Iron

5.1 Abstract

Two types of granular iron, Connelly and QMP, were used in batch experiments reacting with 4-chloronitrobenzene (4ClNB) at various temperatures to determine the activation energies of the reactions on the two metals. Previous work indicated that when Connelly iron was used the disappearance of 4ClNB was a combined result of reaction and adsorption with minimal mass transfer effects. The activity energies, E_a, for the reduction reaction was calculated with the Arrhenius equation to determine if mass transfer was more important in reactions with the QMP iron, which was manufactured in a fashion that might have produced relatively large internal porosity. The Connelly iron was found to exhibit a faster reaction rate compared to QMP iron, most likely because it possessed a greater sorption capacity. Nevertheless, based on the E_a values calculated in this study (40.87 kJ mole^{-1} for QMP and 51.7 kJ mole^{-1} for Connelly irons), the reaction mechanism for Connelly iron and QMP iron were both primarily controlled by electron transfer within the temperature range of 23 ºC to 60 ºC. The activation energy for the reduction of 4ClNB by QMP iron was slightly lower than by Connelly iron, most likely related to the less oxidized nature of the QMP iron surfaces at the beginning of the tests.

5.2 Introduction

Granular iron is being used increasingly as a cost-effective groundwater remediation alternative with its capability of reducing a variety of important pollutants (Zhuang *et al.*, 2008). Abundant research has been carried out to improve our understanding of the interactivity between iron and contaminants in PRB systems (Burris

et al., 1998; Dries *et al.*, 2004; Miehr *et al.*, 2004). Various forms of granular iron have been investigated, and differences have been documented. Most importantly, different iron products vary in price, reactivity, and possibly in their longevity in the subsurface (Burris *et al.*, 1998; Su and Puls, 1999; Tamara and Butler, 2004). Therefore, newly introduced forms of iron should be compared with well established brands of commercial granular iron to assess their potential as PRB packing materials.

QMP iron is a recent commercial product under consideration for use in PRBs. Preliminary laboratory studies were performed by EnviroMetal Technologies Inc. The material is manufactured by quenching fine droplets of molten iron in a water mist. The surface oxide phases on the material are similar to those on more conventional forms of granular iron, for example Connelly and Peerless, and the product has been shown to reduce chlorinated solvents dissolved in water. However, the preliminary work indicated that the QMP iron was not consistently as reactive as the other commercial products. It was hypothesized that the quenching process may have created micro pores within the solid grains, creating a dual porosity medium subject to mass transport control on the reaction rates. The purpose of this work was to perform experiments that might permit a distinction to be made between reaction and diffusion as primary controls on reaction rates for QMP and a control, Connelly iron, which is thought to react at rates primarily controlled by electron transfer.

Lab experiments have shown that increasing temperatures affect the sorption and dechlorination reaction rates on solid metal surfaces, including iron (Fang and Al-Abed, 2008). For example, increasing temperature was found to increase the maximum sorption capacity of hydrogen on copper and iron (Bransfield *et al.*, 2007). Since diffusion

requires less energy to occur than electron transfer, the activation energy, E_a, for diffusion is expected to be less than that for electron transfer. Therefore, E_a might be useful in determining whether electron transfer or mass transfer controls a reaction rate (Su and Puls, 1998; Lai and Lo, 2007; Fang and Al-Abed, 2008). E_a is commonly determined from the slope (Equation 5.1) of the Arrhenius equation (Equation 5.2). The data necessary for this type of analysis come from kinetic experiments performed at different temperatures (constant pressure) (Lasaga *et al.*, 1981; Laidler, 1987; Sparks, 1989).

$$E_a = -R\left[\frac{\partial(\ln k)}{\partial\left(\frac{1}{T}\right)}\right]_P \qquad 5.1$$

$$\ln k = -\frac{E_a}{R}\frac{1}{T} + \ln A \qquad 5.2$$

where k is the rate constant (T^{-1}), T is temperature (K); R is the gas constant (8.314 J/mol/K); A is a constant sometimes referred to as a frequency factor, because it is related to the frequency of collisions and the probability that the collisions are favorably oriented for reaction.

Several studies have reported E_a for chlorinated organics reduced by various iron solids (Table 5.1). The energies reported for trichloroethene (TCE) and tetrachloroethene (PCE) were in the range 25 kJ/mole to 70 kJ/mole, reflecting wide variations in the experimental conditions, and the possibility that in some cases reactions were mass transfer controlled and in others they were electron transfer controlled.

Table 5.1: Reported activity energy of granular iron reacting with chlorinated compounds

mass Loading (g/L)	Iron	Pre treatment	Experiment	Contaminant	C_o (μM)	*Ea* (kJ mole^{-1})	Temp Range (ºC)	Reference
250 or 205	VWR Coarse Iron	None	Batch and Column	Chlorinated Ethene (TCE, cis-DCE, trans-DCE, 1,1-DCE, VC)	194 - 352	15.12-18.06	10-34	(Sivavec *et al.*, 1996)
250	Fisher, Aldrich, Peerless, Master Builders	None	Batch	TCE	15.2	32.2-39.4	10-55	(Su and Puls, 1999)
250	Master Builders, Peer, Aldrich	Acid washed	Batch	TCE	15.2	25.8-81.8	25-55	(Su and Puls, 1999)
2728-2862	Connelly	None	Column	TCE	629-679.8	70.3	10-23	(Lai and Lo, 2007)
2728-2862	Connelly	None	Column	PCE	475.9-540.9	38.6	10-23	(Lai and Lo, 2007)
2.5	Fe/Pd, Fisher Fe and 0.585% GFS Pd	Acid washed	Batch	2-chlorobiphenyl	2-19	20±4	4-60	(Fang and Al-Abed, 2008)
2.5	Fe/Pd, Fisher Fe and 0.585% GFS Pd	Acid washed	Batch	2-chlorobiphenyl	2-19	17±7	4-51	(Fang and Al-Abed, 2008)
41.7	Fluka Fe^0 filings	None	Batch	CCl4	85	55.9 ±12.0	4-45	(Scherer *et al.*, 1997)
41.7	Fluka Fe^0 filings	None	Batch	Hexachloroethane	85	40.5±4.1	4-45	(Scherer *et al.*, 1997)
			Gas phase	Polyvinylchloride (PVC)	30 mg solid	116.5	80-280	(Yoshioka *et al.*, 2005)
			Gas phase	Polyvinylchloride (PVC)	30 mg solid	15	300-400	(Yoshioka *et al.*, 2005)

There is no consensus in the literature on the specific magnitude of E_a that distinguishes between mass transfer and electron transfer control (Table 5.2). Sparks (1989) places the upper limit on diffusion control at <42 kJ mole^{-1} while Scherer *et al*. (1997) place the upper limit as low as 10 kJ mole^{-1}. Su and Puls (1999) reported that the most commonly cited limit is about 15 k J mole^{-1}. Among the studies directly concerned with chlorinated solvent reactions with iron, the indications are that activation energies greater than 10 to 15 kJ/mole most likely be indicative of reaction controlled kinetics (Su and Puls, 1999; Lim and Lastoskie, 2009).

Table 5.2: Estimated value of activity energy to determine the mechanism of dechlorination process

Ea (kJ mole^{-1})	Mechanism	Contaminants	Iron	Experiment	Reference
>9.9	Reaction controlled	PCE, TCE, cis-DCE	Fe 110	Gas phase	(Lim and Lastoskie, 2009)
15.12-18.06	Diffusion limited	Chlorinated Ethene (TCE, cis-DCE, trans-DCE,1,1-DCE, VC)	VWR Coarse Iron	Batch and Column	(Sivavec *et al.*, 1996)
>21	Reaction controlled	general	general	general	(Lasaga *et al.*, 1981)
<15	Diffusion controlled	TCE	Acid washed Fisher, Aldrich, Peerless, Master Builders iron	Batch	(Su and Puls, 1999)
70.3 (TCE) 38.6 (PCE)	Reaction controlled	TCE and PCE	Connelly	Column	(Lai and Lo, 2007)
116.5	Reaction controlled	Polyvinylchloride (PVC) powder		Gas phase	(Yoshioka *et al.*, 2005)
15	Heat transfer controlled	Polyvinylchloride (PVC) powder		Gas phase	(Yoshioka *et al.*, 2005)
<21	Mass transport controlled	general	general	general	(Laidler, 1987)
15	Diffusion controlled	general	general	general	(Pilling and Seakins, 1996)
<42	Diffusion controlled	general	general	general	(Sparks, 1989)
<10-16	Mass transport controlled	hexachloroethane and CCl4	Fluka Fe^0 filings	Batch	(Scherer *et al.*, 1997)

Dechlorination of organics by granular iron is thought to occur by several mechanisms. Hydrogenolysis, β-elimination, reductive α-elimination, and hydrogenation are all recognized reactions that can occur with zero valent iron (Lim and Lastoskie, 2009). Observed reaction rates are combined rates involving one or more of these mechanisms in some proportion. The complicated nature of this system, combined with the complex nature of the granular iron surface, have led some to postulate that diffusion ultimately controls reaction rates (Ebert *et al.*, 2006). However, others have collected experimental evidence that the reaction rates are electron transfer controlled. These studies involved polished iron or acid washed iron samples (Su and Puls, 1999), and

untreated Fe^0 particles (Scherer *et al.*, 1997; Lai and Lo, 2007). The rate control in PRB settings has yet to be definitively determined.

To calculate the E_a from the slope of an Arrhenius plot, one of three rate constant terms can be used. The parameter k_{obs} (T^{-1}), is used assuming first order kinetic behavior (Sivavec *et al.*, 1996; Su and Puls, 1998); k_{SA} ($T^{-1}m^{-2}$ L) can be used, again assuming first order behavior, this time explicitly accounting for the contribution of iron surface area to the observed reaction rates (Lai and Lo, 2007); or kC_{max}, can be used assuming Langmuir Hinshelwood kinetics apply (Equation 5.3).

$$\left(\frac{dC}{dt}\right)_0 = -\left(\frac{kC_{max}\frac{Fe}{V}}{\frac{1}{J}+C_0}\right)C_0 \qquad 5.3$$

where C_0 is aqueous concentration of 4ClNB (M/L^3) at the beginning of each experiment, Fe is iron mass (M), V is volume of water (L^3), C_{max} is the surface capacity for sorption (M/M_{solid}), J is the Langmuir sorption parameter describing affinity of solute for solid (L^3/M), k is the first-order rate constant for the reaction on the iron surface (T^{-1}), t is time (T).

However, since both k_{obs} and k_{SA} are parameters that lump the sorption and reaction processes together, neither can be reliably used to estimate E_a for the electron transfer, independent of sorption, in granular iron systems. For example, if both Langmuir sorption and Langmuir-Hinshelwood kinetics apply, and use first order kinetics to get observed rate constant, then k_{obs} is a lumped parameter given by equation 5.4.

$$k_{obs} = \frac{k\frac{Fe}{V}JC_{\max}}{1+JC} \qquad 5.4$$

Inserting this into the Arrhenius equation,

$$\ln\left[\frac{k\frac{Fe}{V}JC_{\max}}{1+JC}\right]=-\frac{E_a}{R}\frac{1}{T}+\ln A \qquad 5.5$$

rearranging,

$$\ln k=-\frac{E_a}{R}\frac{1}{T}+\ln A'(1+JC) \qquad 5.6$$

where $A' = A/((Fe/V)\,JC_{max})$. Here it is seen that the intercept is concentration dependent and this introduces a degree of nonlinearity to the equation (unless C is held perfectly constant).

On the other hand, if both Langmuir sorption and Langmuir-Hinshelwood kinetics apply, and Langmuir-Hinshelwood kinetics are used to interpret the rate data, sorption can be partially separated from reaction through the isolation of the affinity parameter J, as outlined in Devlin and Allin (2005) and the rate constant can be represented by the lumped parameter kC_{max},

$$\ln kC_{\max}=-\frac{E_a}{R}\frac{1}{T}+\ln A$$

rearranging,

$$\ln k+\ln C_{\max}=-\frac{E_a}{R}\frac{1}{T}+\ln A$$

simplifying, we get:

$$\ln k=-\frac{E_a}{R}\frac{1}{T}+\ln\frac{A}{C_{\max}} \qquad 5.7$$

Now it is seen that the intercept is only affected by a constant, C_{max}, so no nonlinearities are introduced to the analysis and estimation of E_a.

5.3 Materials and Methods

The materials and experimental methods employed were identical to those described in Appendix A, with the exception of using 4-chloronitrobenzene (4CLNB) instead of TCE or PCE to monitor iron reactivity. All chemicals including 4ClNB,

methanol and acetonitrile were obtained in the highest purity available from Aldrich and used without additional purification. Spike solutions of 4ClNB were prepared in methanol (HPLC grade). Aqueous solutions of 4ClNB were prepared in deoxygenated 8 mM $NaClO_4$ solution at pH 10 for consistency with previous experiments and to approximate conditions in the middle of a granular iron PRB. The perchlorate solution was selected to maintain an ionic strength of 8 mM, similar to that of groundwater without affecting the iron reactivity substantially (Devlin and Allin, 2005). Deoxygenation of the solution was achieved by sparging it with ultra high purity nitrogen gas for 20 minutes. This procedure was verified to reduce the dissolved oxygen (DO) concentration below 0.2 mg/L in the solution, based on analysis using a Chemetrics DO kit (K-7512 and K-7501).

The batch tests were performed using the glass encased magnetic (GEM) system to optimize mixing and minimize the possibility of mass transfer limitations in the experiments (Devlin and Allin, 2005). Briefly, each GEM was filled without headspace with about 170 ml of deoxygenated $NaClO_4$ solution at pH 10. Connelly iron flakes sieved to the particle size range 710 μm to 2 mm were used in the experiments without any pretreatment. The Brunauer, Emmett and Teller (BET) surface area (Brunauer *et al.*, 1938) for the iron was determined to be 0.76 m^2/g for the iron used in these experiments (Devlin and Allin, 2005). QMP iron powder (supplied by ETI Co.) with grain size range 46 μm to 600 μm was used as received. All experiments were conducted with 2.5±0.05 g of iron in the GEM reactors.

The GEM reactors were spiked at the beginning of each experiment to achieve the desired initial concentrations. Resultant methanol concentrations in the reactors were

always below 10^{-4} mol fraction, avoiding co-solvency effects and interferences (Munz and Roberts, 1986; Burris *et al.*, 1998).

Prior to the first experiment in any series (series consisted of experiments with increasing initial concentrations), the GEM was flushed with contaminant-free perchlorate solution and allowed to stand for 2 days, after which it was rinsed again 3 times with about 500 mL of fresh solution. GEM reactors were flushed twice between experiments in order to remove any remaining 4ClNB or its transformation products, particularly 4-chloroaniline, from the iron surface and the reactor (Marietta and Devlin, 2005). The GEM reactors were stirred at 300 rpm with a polytetrafluoroethene (PTFE) coated magnetic stir bar, both during the rinses and the experiments.

Experiments were performed over a range of initial concentrations from 10 to 500 μM. Each experiment lasted 90 minutes. Samples of about 1.0 mL to 2.0 mL were collected and transferred into 2.0 mL vials with glass syringes. Samples were taken every 5 minutes for the first 30 minutes, and then every 15 minutes for the next 60 minutes. To maintain anoxic conditions inside the GEM reactor, headspace was minimized and 2 mL of deoxygenated $NaClO_4$ solution at pH 10 was added to the reactor as each sample was withdrawn.

All experiments were conducted in duplicate. Declining concentrations over time were fitted with the first-order kinetic equation, yielding estimates of k_{obs} and C_o from which initial rates $(dC/dt)_o = k_{obs}C_o$ were calculated. The Langmuir-Hinshelwood kinetic model (Equation 5.3) was fitted to the initial rate data (plotted against C_o) to obtain estimates of the lumped parameter kC_{max} and the affinity parameter J, for each series (Devlin and Allin, 2005).

All the samples and calibration standards were analyzed within 24 hours of collection. Calibration standards were prepared fresh daily from the stock solution. Aqueous samples were analyzed by HPLC as described by Marietta and Devlin (Marietta and Devlin, 2005). Calibration of the instrument was conducted for each run as described by Devlin (Devlin, 1996).

5.4 Results and Discussion

The disappearance of 4ClNB in the presence of both Connelly and QMP iron followed first order kinetic curves from which pseudo-first order rate constants, k_{obs}, and C_o could be estimated (Figure 5.1). QMP iron was associated with slower 4CLNB reduction rates, compared to Connelly iron, at all temperatures and initial concentrations tested. The same trends were visible when the data were plotted in *rate-*C_o space (Figure 5.3). The reactivity of both Connelly and QMP iron both increased with temperature. These graphs also revealed that the rate differences appear to be less pronounced between room temperature (23 ^{o}C) and 40 ^{o}C than between 40 ^{o}C and 60 ^{o}C. Another noticeable difference in the two rate trends is that a rate plateau is more convincingly achieved with QMP iron than with Connelly, which suggested the kC_{max} parameter for the Connelly iron was larger than that for QMP.

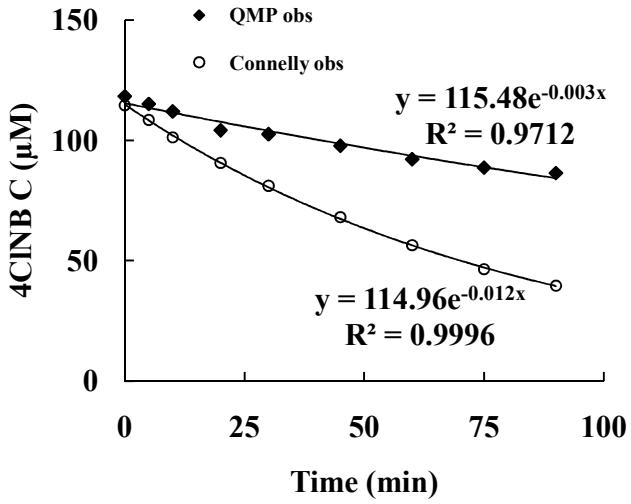

Figure 5.1: Batch experimental data fitted with the first order kinetic model (solid line) for the reaction of Connelly iron (o) and QMP (♦) iron reacting with 4ClNB at 40 ºC. Estimated k_{obs} and initial concentrations are 0.003 min^{-1} and 115.48 µM for QMP iron, 0.012 min^{-1} and 114.96 µM for Connelly iron.

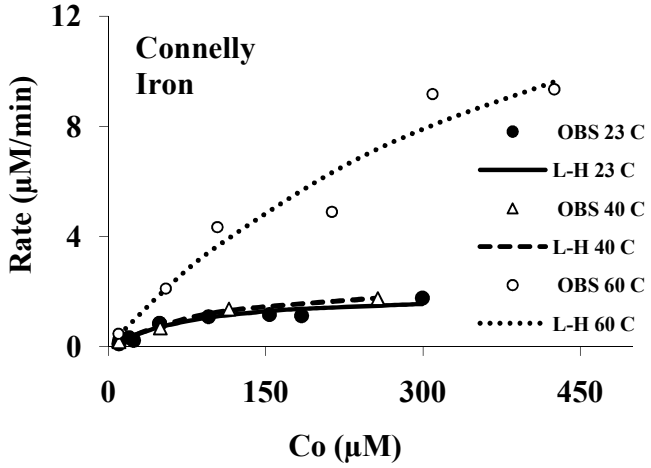

Figure 5.2: Observed rate constants plotted with the initial concentrations for the reaction of Connelly iron with 4ClNB at different temperatures.

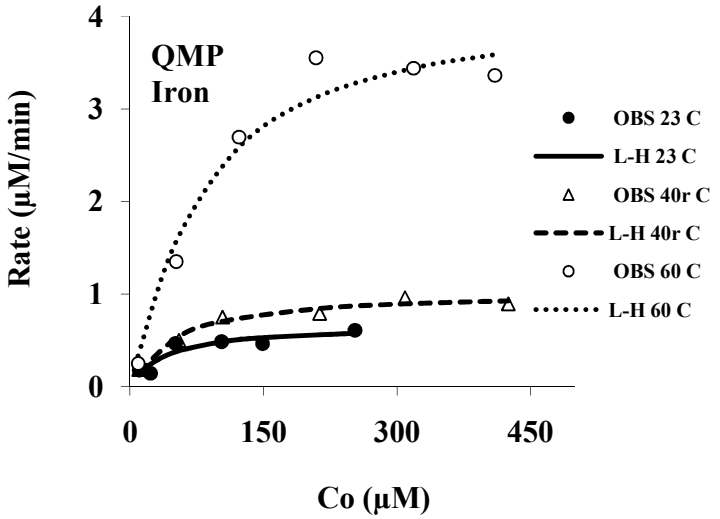

Figure 5.3: Observed rate constants plotted with the initial concentrations for the reaction of QMP iron with 4ClNB at different temperatures.

Observed data sets plotted as initial rates ($(dC/dt)_o = k_{obs}C_o$) versus C_o were fitted by the L-H model to get estimated values of kC_{max} and J. As temperature was increased, the magnitude of J appeared to decrease slightly while kC_{max} was found to increase (Figure 5.4). The results for J suggest that sorption is either little affected or diminished by temperature increases. The effect of temperature on kC_{max} is difficult to parse, but it is expected that some of the increase in this lumped value is due to increases in k because the electron transfer rates generally increase with heating. To better understand the temperature effect on the iron reacting with 4ClNB and the reaction mechanism, column experiments are needed to generate experimental data that can be fitted with kinetic iron model (KIM) (Devlin, 2009), which is capable of separating the parameters k and C_{max}.

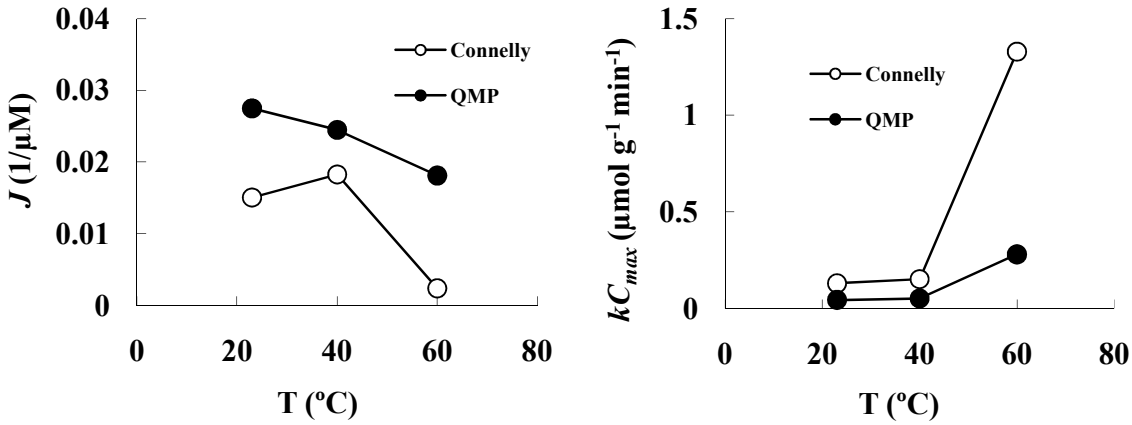

Figure 5.4: Effects of temperature on the Langmuir-Hinshelwood parameters *J* and kC_{max}.

Once kC_{max} was estimated, it was used in an Arrhenius plot to obtain estimates of E_a (Figure 5.5). The estimated E_a for Connelly iron reacting with 4ClNB is 51.7 kJ/mole, for QMP iron is 40.87 kJ/mole. The slope estimated with ±1 standard error for Connelly iron is -6222.7±3010, and for QMP iron it is -4915.5±2670. For neither Connelly nor QMP iron did the $ln(kC_{max})$ vs. $1/T$ data points fall perfectly on a straight line, as predicted by equation 1.5. This could be attributed to either experimental noise or a systematic change in the mechanism (hence E_a) by which 4ClNB was reduced. Additional work aimed at better defining the line is required to resolve these possibilities. Until this resolution can be achieved, it will be assumed that the data do represent straight line trends and the associated E_a values can be calculated. The estimated E_a values for Connelly iron and QMP iron reacting with 4ClNB over the temperature range 23 ºC to 60 ºC are greater than 10 to 15 kJ/mole, suggesting that the reactions with both iron types were electron transfer controlled in these experiments (Figure 5.5).

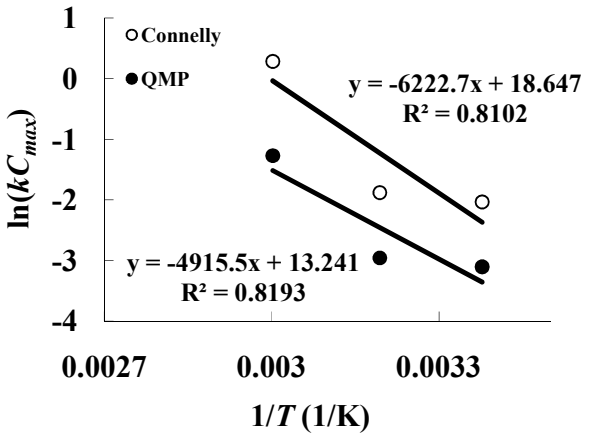

Figure 5.5; Plotting $ln(kC_{max})$ vs. 1/T for Connelly and QMP iron reacting with 4CLNB.

The different activity energy values determined for QMP and Connelly iron could be a result of various surface conditions, such as available number of reactive sites on the iron surface, impurities, lattice structures of the iron (Bransfield *et al.*, 2007), diffusion limited access to the reactive sites (Burris *et al.*, 1998), and the presence or absence of carbon, a sorptive species sometimes assumed to be sorptive but nonreactive (Burris *et al.*, 1998). It was noted by visual inspection that Connelly iron had a surface that was more oxidized – indicated by an orange-yellow coloration – than that of fresh QMP iron, which appeared to be black in color and exhibited less oxidized coatings on the metal surface. The grain size of QMP was also observed to be smaller than Connelly iron, indicating a likely higher surface area.

Based on the lower estimated value of E_a for QMP compared to Connelly iron, and the higher surface area of QMP, it might be expected that QMP iron would be more reactive with 4ClNB than Connelly iron. Experimentally, however, Connelly iron exhibited the higher overall reactivity. An obvious explanation for this is that the QMP oxide coatings were more effective at passivating the metal surface than the Connelly

coatings. Since preliminary analyses found the oxides to be same mineralogically, the differences might be in the uniformity of the coatings, or their integrity. Alternatively, the data can be explained if the sorption capacity of Connelly iron (for 4ClNB) is greater than that of QMP iron. Note that the estimates of J were generally similar in magnitude for QMP and Connelly irons (in fact J_{QMP} was slightly greater than $J_{Connelly}$), so any sorption difference would have to have been in the C_{max} term, reflecting the sorption capacity. Since these experiments did not uniquely identify the parameters k and C_{max}, further work is needed to verify this hypothesis.

The estimated E_a values for Connelly and QMP irons reacting with 4ClNB in this research were estimated to be 40.87 and 51.7 kJ mole^{-1}, respectively. The literature reports similar estimates of E_a for TCE and PCE, which are known to react considerably more slowly with granular iron than 4ClNB. In the cases of TCE and PCE, the E_a values are usually less than 40 kJ mole^{-1} (Figure 5.5 and Table 5.1). This result suggests that many of the earlier studies reported E_a values strongly affected by mass transport limitations. Given the mixing methods used, mainly rolling or shaking, and the high iron loadings in the batch tests (>200 g/L for TCE, see Table 5.1), which could have restricted solution mixing, mass transport limitations might reasonably be expected in those experiments. Note that this is less likely in the GEM experiments, which were well mixed with good solution-iron contact (Garvin and Devlin, 2006).

It should also be noted that previously reported E_a values were calculated using k_{obs}, the pseudo-first order rate constant. As discussed above in section 5.2, E_a estimated in this way might be affected by Fe/V, C_{max}, and the magnitude of C_o. As shown in Table

5.1, the values of concentration in previously reported experiments were quite variable, so reported E_a values may be considered quite uncertain.

5.5 Conclusions

The reduction of 4ClNB results from the combined effects of reaction and adsorption. Based on the E_a values calculated in this work, the reaction mechanism for Connelly iron and QMP iron were both primarily controlled by electron transfer within the temperature range of 23 ºC to 60 ºC. The activation energy for the reduction of 4ClNB could be slightly lower for reactions with QMP iron than Connelly with ±1 standard error, perhaps related to the less oxidized nature of the QMP iron surface initially. Nevertheless, reactions with Connelly iron were faster than those with QMP iron most likely because the sorption capacity for 4ClNB was greater on Connelly iron than it was on QMP iron. More detailed investigations are needed to resolve these issues completely.

References

Bransfield, S. J., D. M. Cwiertny, K. Livi and D. H. Fairbrother (2007). "Influence of Transition Metal Additives and Temperature on the Rate of Organohalide Reduction by Granular Iron: Implications for Reaction Mechanisms." Applied Catalysis B: Environmental 76: 8.

Brunauer, S., P. H. Emmett and E. Teller (1938). "Adsorption of Gases in Multimolecular Layers." Journal of American Chemical Society 60(2): 309-319.

Burris, D. R., R. M. Allen-King, V. S. Manoranjan, T. J. Campbell, G. A. Loraine and B. Deng (1998). "Chlorinated Ethene Reduction by Cast Iron: Sorption and Mass Transfer." Journal of Environmental Engineering 7: 1012-1019.

Devlin, J. F. (1996). "A Method to Assess Analytical Uncertainties over Large Concentration Ranges with Reference to Volatile Organics in Water." Ground Water Monitoring and Remediation: 179-185.

Devlin, J. F. (2009). "Development and Assessment of A Rate Equation for Chemical Transformations in Reactive Porous Media." Environmental Science and Technology.

Devlin, J. F. and K. O. Allin (2005). "Major Anion Effects on the Kinetics and Reactivity of Granular Iron in Glass-encased Magnet Batch Reactor Experiments." Environmental Science and Technology 39: 1868-1874.

Dries, J., L. Bastiaens, D. Springael, A. Spiros N and L. Diels (2004). "Competition for Sorption and Degradation of Chlorinated Ethenes in Batch Zero-valent Iron Systems." Environmental Science and Technology 38: 2879-2884.

Ebert, M., R. Kober, A. Parbs, V. Plagentz, D. Schafer and A. Dahmke (2006). "Assessing Degradation Rates of Chlorinated Ethylenes in Column Experiments with Commercial Iron Materials Used in Permeable Reactive Barriers." Environmental Science and Technology 40: 2004-2010.

Fang, Y. X. and S. R. Al-Abed (2008). "Dechlorination kinetics of monochlorobiphenyls by Fe/Pd: Effects of solvent, temperature, and PCB concentration." Applied Catalysis B-Environmental 78(3-4): 371-380.

Garvin, N. L. and J. F. Devlin (2006). "Minimizing mass transfer effects in granular iron batch tests using GEM reactors." Journal of Environmental Engineering-Asce 132(12): 1673-1676.

Lai, K. C. K. and I. M. C. Lo (2007). "Effects of seepage velocity and temperature on the dechlorination of chlorinated aliphatic hydrocarbons." Journal of Environmental Engineering-Asce 133(9): 859-868.

Laidler, K. J. (1987). Chemical kinetics. New York, Harper Collins Publishers.

Lasaga, A. C., R. A. Berner, G. W. Fisher, D. E. Anderson and R. J. Kirkpatrick (1981). Reviews in Mineralogy Volume 8 Kinetics of Geochemical Processes. Chelsea, Michigan, BookCrafters, Inc. .

Lim, D. H. and C. M. Lastoskie (2009). "Density Functional Theory Studies on the Relative Reactivity of Chloroethenes on Zerovalent Iron." Environmental Science & Technology 43(14): 5443-5448.

Marietta, M. and J. F. Devlin (2005). Separating the Kinetic and Sorption Parameters of Nitroaromatic Compounds in Contact with Granular Iron. 4th International Groundwater Quality Conference. waterloo, canada**:** 6.

Miehr, R., P. G. Tratnyek, J. Z. Bandstra, M. M. Scherer, M. J. Alowitz and E. J. Bylaska (2004). "Diversity of Contaminant Reduction Reactions by Zerovalent Iron: Role of the Reductate." Environmental Science and Technology(38): 139-147.

Munz, C. and P. V. Roberts (1986). "Effects of Solute Concentration and Cosolvents on the aqueous activity-Coefficient of Halogenated Hydrocarbons." Environmental Science and Technology 20(8): 6.

Pilling, M. J. and P. W. Seakins (1996). Reaction Kinetics Oxford University Press, USA.

Scherer, M. M., J. C. Westall, M. Ziomek-Moroz and P. G. Tratnyek (1997). "Kinetics of Carbon Tetrachloride Reduction at An Oxide-free Iron Electrode." Environmental Science and Technology 31(8): 6.

Sivavec, T. M., D. P. Horney and S. S. Baghel (1996). Reductive Dechlorination of Chlorinated Ethenes by Iron Metal and Iron Sulfide Minerals. American Chemical Society Extended Abstract, Industrial and Engineering Chemestry Division**:** 42-45.

Sparks, D. L. (1989). Kinetics of Soil Chemical Processes. San Diago, Academic Press.

Su, C. and R. W. Puls (1998). Temperature Effect on Reductive Dechlorination of Trichloethene by Zero-Valent Metals. Wickramanayake GB, Hinchee RE, eds. Physical, Chemical, and Thermal Technologies: Proceeding of the First International Conference on Remediation of Chlorinated and Recalcitrant Compounds. Monterey, CA, Battelle Press. Columbus, OH. 1(5)**:** 317-322.

Su, C. and R. W. Puls (1999). "Kinetics of Trichloroethene Reduction by Zerovalent Iron and Tin: Pretreatment Effect, Apparent Activation Energy, and Intermediate Products." Environmental Science and Technology 33(1): 163-168.

Tamara, M. L. and E. C. Butler (2004). "Effects of Iron Purity and Groundwater Characteristics on Rates and Products in the Degradation of Carbon Tetrachloride by Iron Metal." Environmental Science & Technology 38(6): 1866-1876.

Yoshioka, T., N. Saitoh and A. Okuwaki (2005). "Temperature dependence on the activation energy of dechlorination in thermal degradation of polyvinylchloride." Chemistry Letters 34(1): 70-71.

Zhuang, L., L. Gui and R. W. Gillham (2008). "Degradation of pentaerythritol tetranitrate (PETN) by granular iron." Environmental Science & Technology 42(12): 4534-4539.

6 Summary, Conclusions and Suggestions for Future Work

Previous work introduced the KIM, showing it was useful for isolating the contributions of sorption and reaction parameters to reactivity. Analysis of the sorption to reactive and nonreactive sites on granular iron was made possible with this mathematical tool. In this work, the use of the KIM was extended to define the contributions of these processes to reactivity as iron ages and across two organic compound classes. It was found that iron exposed to oxidizing organics lost reactivity from the of rate of electron transfer, but gained sorption capacity, increasing overall reaction rates temporarily.

The degree to which KIM parameters might be fitting parameters was assessed by comparing reduction kinetics from two classes of organics. The nitroaromatic compounds tested included 4ClNB and 4AcNB, and both reacted faster than the chlorinated solvents tested, PCE and TCE. As expected, the rate difference was found to be related to the rate constant parameter, k, suggesting electron transfer was faster in the nitroaromatic reductions than in the chlorinated solvent reductions.

A one dimensional transport model with Langmuir sorption kinetics and KIM kinetics, using it to generate synthetic column data, and then analyzing the data as reported in the laboratory work for the sorption and kinetic constants. The model was also used to assess the possibility of interspecies competition between TCE and PCE in the column experiments.

Previous work established that well mixed reactors and column tests with high Connelly iron loadings (>85% by weight porous medium), exhibited kinetics that were not strongly influenced by the rate of contaminant mass transport to the solid surface. A new type of granular iron, QMP, manufactured by spray cooling molten iron droplets,

exhibited reaction rates that were slower than Connelly iron. Prior to conducting KIM related experiments on QMP to assess reaction vs. sorption, the metal was evaluated for the possibility that internal grain porosity was introducing a mass transport limitation to the observed kinetics. This was investigated by measuring the activation energy of the 4ClNB-QMP reaction and comparing the result with the activation energy for diffusion limited reactions. The conclusions of this work are summarized below.

6.1 Longevity of Zero-Valent Iron

It is concluded that the iron surface loses fast reactive sites and gains slow reactive sites as a result of its exposure to water and contaminants. The kinetics of young iron with a fresh surface is dominated by a relatively small number of fast reactive sites. Older iron reacts with kinetics dominated by a larger number of slow reactive sites. The two trends offset one another so granular iron maintains its effectiveness longer than might be anticipated. This phenomenon was revealed for both TCE and PCE reduction experiments, adding credence to the conclusion. The chemical nature of the sorption sites, reactive and nonreactive, was not determined in this work, but may be related to the presence of carbon on the iron surface on the basis of reports by others.

The reactive sites only occupied a small proportion of iron surface; this work found the percentage of sorption sites that were reactive to be about 2%, in agreement with two published studies. It is also concluded that although reactivity is maintained by kinetics dominated by a large number of relatively low reactivity sites, the number of fast reactive sites on the iron surface decreases with iron age. This does not directly affect reactivity, but may signal processes that will ultimately affect reactivity and decide the longevity of

granular iron. These processes may include loss of reactive sites by corrosion and burial under precipitate coatings.

6.2 Reaction Kinetics with Separated Sorption and Reaction Parameters

Application of KIM enabled a comparison of sorption and reaction parameters for chlorinated and nitroaromatic compounds. These classes of compounds were known to react with granular iron at very different rates, and based on thermodynamic data (one electron reduction potentials) the differences were thought to be due to electron transfer control. Rate data fitted with KIM, and using a Monte Carlo algorithm to evaluate parameter uncertainty, confirmed that the rate differences between the two classes were due to electron transfer kinetics and not sorption.

Within the compound classes, other expectations were realized. PCE is known to be more hydrophobic than TCE, and KIM analysis indicated that the relative rates of PCE and TCE reduction with iron were largely due to this property. PCE was shown to sorb to the iron surface to a greater extent than TCE, and this increased sorption is believed to have increased the likelihood of reactions, explaining the faster PCE reduction rates. The trends in sorption for the nitroaromatic compounds was less certain, possibly because the rates were so fast that the method was insufficiently sensitive to discern the parameters precisely.

6.3 Competition Reaction

KIM was incorporated into a one dimensional numerical reactive transport model, T-KIM, which is capable of describing inter- and intra-species competition between TCE, PCE and other products on the iron surface. T-KIM was validated against two analytical transport models. The first, OGATA, was based on the analytical solution published by

Ogata and Banks (Ogata and Banks, 1961), which assumed a first-type boundary condition and transport with neither sorption nor reaction. The second, BEARPE, was published by Bear (Bear, 1979), and assumed a third type boundary, a first order reaction term and instructions for the incorporation of sorption into the solution. T-KIM was also found to return nearly identical estimates of retardation factors and first order rate constants as the analytical solutions when it was used to fit experimental data.

T-KIM was used to investigate the magnitude of competition between PCE and its reduction product, TCE, in the experiments reported in this work. The results showed unequivocally that the TCE concentrations were too low at all times to introduce a competition effect with PCE. Further work is needed to evaluate the possibility of competition from other substances.

6.4 Assessment of the KIM Analysis Methodology

Prior to this work, only experimental data had been analyzed using the methodology that permitted the KIM parameters to be uniquely determined. In those cases, the correct values of the parameters could not be known in advance so the estimated values of *J, k,* and C_{max} could not be independently verified. In this work, a synthetic data set for which KIM parameters were known was generated and analyzed, as previously done with the experimental data sets. The correct identification of the parameters from this synthetic data set proved that the methodology accurately estimates the KIM parameters. One caveat must be added to this conclusion: the numerical model used to generate the synthetic data was based assumptions of equilibrium sorption and rates determined by electron transfer, as is KIM. Therefore, real systems that depart from these basic assumptions will not be reliably interpreted with KIM.

6.5 Evaluation of QMP Granular Iron

Connelly iron has been well investigated in the past and is thought to react with 4ClNB without measurable mass transport limitations in well-mixed systems. The rate controlling processes for QMP iron were not well known, so they were investigated by comparing reaction activation energies for 4ClNB reduction with the two types of iron. Activation energies, E_a, were determined from temperature dependent kinetics of 4ClNB reduction with QMP and Connelly irons.

Based on the estimated E_a values for the chemical reductions, which were consistently greater than E_a values associated with mass transport, the reaction mechanism(s) for 4ClNB transformation on Connelly iron and QMP iron is electron transfer controlled. This suggests that differences in transformation rates are due to factors related to the solid surfaces themselves. For example, the reason Connelly iron reacts faster than QMP iron might be due to a larger sorption capacity on its surface. This could result from a lower carbon presence on the QMP surface. However, future work will have to resolve this possibility with the fact that QMP exhibited a slightly greater sorption affinity, J, for 4ClNB than did Connelly iron.

Both batch and column systems from the literature were examined with equal or higher iron loadings than those used here. Since some of those studies calculated similar or lower E_a values than those found for 4ClNB, which is known to react very rapidly with granular iron, the possibility is raised that mass transfer played a significant role in the earlier observed transformation rates. This is particularly likely in the case of batch studies that were mixed by rotary shaking or rolling, two methods demonstrated to be problematic in achieving adequate mixing in granular iron systems. Previous column tests conducted to estimate activation energies may have been biased by the assumption of

simple first order kinetics when the initial concentrations were above the levels required for saturation effects to be observed.

6.6 Suggestions for Future Research

Longer term column experiments with iron continuously exposed to TCE, PCE and other contaminants are needed to further validate the conclusions of this work. Experiments with higher initial concentrations of competing background contaminants, such as TCE, PCE and other organics, are necessary to further investigate the competition phenomenon.

To improve the estimates of E_a, additional batch testing at different temperatures, is needed. If these experiments are extended to include column tests, it may be possible to perform temperature sensitive analyses of the sorption and reaction parameters via the KIM analysis.

The parameters discussed and estimated in this work represent macroscopic averaged parameters that are representative of iron grain surfaces. Work is needed to examine the grain surfaces microscopically in order to look for systematic changes that might correspond with the observed changes in the macroscopic parameters.

The program T-KIM was written on a spreadsheet and as such was limited to solving for three species simultaneously. The code should be transferred to a scripted language, such as VBA or FORTRAN, and expanded to include an indefinite number of species.

Reference

Bear, J. (1979). Hydraulics of Groundwater (Mcgraw-Hill Series in Water Resources and Environmental Engineering) New York, McGraw-Hill Companies.

Bransfield, S. J., D. M. Cwiertny, K. Livi and D. H. Fairbrother (2007). "Influence of Transition Metal Additives and Temperature on the Rate of Organohalide Reduction by Granular Iron: Implications for Reaction Mechanisms." Applied Catalysis B: Environmental 76: 8.

Burris, D. R., R. M. Allen-King, V. S. Manoranjan, T. J. Campbell, G. A. Loraine and B. Deng (1998). "Chlorinated Ethene Reduction by Cast Iron: Sorption and Mass Transfer." Journal of Environmental Engineering 7: 1012-1019.

Garvin, N. L. and J. F. Devlin (2006). "Minimizing mass transfer effects in granular iron batch tests using GEM reactors." Journal of Environmental Engineering-Asce 132(12): 1673-1676.

Ogata, A. and R. B. Banks (1961). A solution of the Differential Equation of Longitudinal Dispersion in Porous Media U. S. G. S. P. Paper: 411-A, 417.

Appendix A Batch Test Methodology

Batch tests were conducted in glass encased magnet (GEM) reactors (Devlin and Allin, 2005) to achieve good mixing, and minimal abrasion (Garvin and Devlin, 2006). In order to achieve reasonable reaction times with the chlorinated solvents, the GEM reactors were modified to contain up to 40 g of granular iron (compared to 2.5 g previously reported for reactions involving nitroaromatics). The internal hanging magnetic bar was replaced with four magnetic buttons positioned on the perimeter of the beaker. The iron grains were arranged around the inside perimeter of the beaker to accommodate the greater amount of solid.

Each reactor was filled with about 170 ml of deoxygenated $NaClO_4$ solution at pH 10, with little or no headspace (Figure A.1). Prior to the first experiment of any series, the iron-filled reactor was flushed with approximately 500 mL deoxygenated $NaClO_4$ (pH 10) three times with 1 to 2 days interval between flushes, to permit some equilibration of the surface with the background solution. Contaminant spikes were introduced directly to the GEM reactors via glass micro-liter syringes (Fisher Scientific) to achieve the desired concentrations. To minimize mass transfer effects, the GEM systems were stirred at 300 revolutions per minute (RPM) with a Teflon®-coated magnetic stir bar.

Each series of experiments involved stepping up of the starting concentration beginning with low concentrations (~10 μM) and ending with high concentrations (~450 μM). Samples were collected at regular times for about 1.5 hours with increasing intervals between samples. To maintain minimal headspace and anoxic conditions inside the GEM reactor, 2 mL fresh deoxygenated $NaClO_4$ solution at pH 10 was added into GEM reactor after each sample was collected. The vials were centrifuged using an IEC

Micromax centrifuge (model OM 3590) for 5 minutes at 12000 rpm to minimize the suspended particles prior to analysis by HPLC.

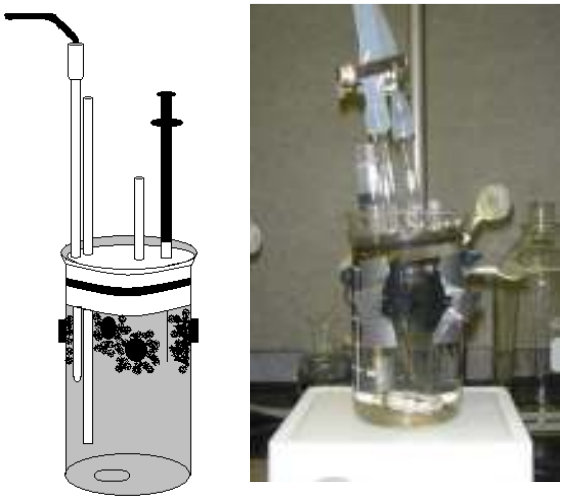

Figure A.1: Modified Glass Encased Magnetic (GEM) Reactor. Left figure is sketch of GEM reactor. Right figure is experimental set of GEM with about 30 g of Connelly iron inside.

To remove excess reactant and reaction products from the iron surface and reactor between experiments, the GEM reactors were flushed with 500 mL deoxygenated $NaClO_4$ solution at pH 10 three times with a 1 day interval between flushes. Preliminary testing indicated this procedure removed all but trace amount of TCE or PCE from the reactors. Chlorinated compounds other than PCE and TCE were not analyzed in this work due to instrument limitations. Nevertheless, since less chlorinated compounds are less hydrophobic than either TCE or PCE (Schwille, 1988), they are more readily flushed out of the reactor than either PCE and TCE. So interferences from these lesser chlorinated compounds were considered negligible in this study.

Batch tests exhibited TCE and PCE disappearances that corresponded to a first order kinetic model (Figure A.2 and Figure A.3). The solid line is an exponential trend line, reflecting a pseudo-first order kinetic model that fit observed data well. By fitting

the observed data with a pseudo-first order kinetic model. Therefore, it is possible to estimate an apparent rate constant, k_{obs}, and initial concentration, C_o, for each batch experiment.

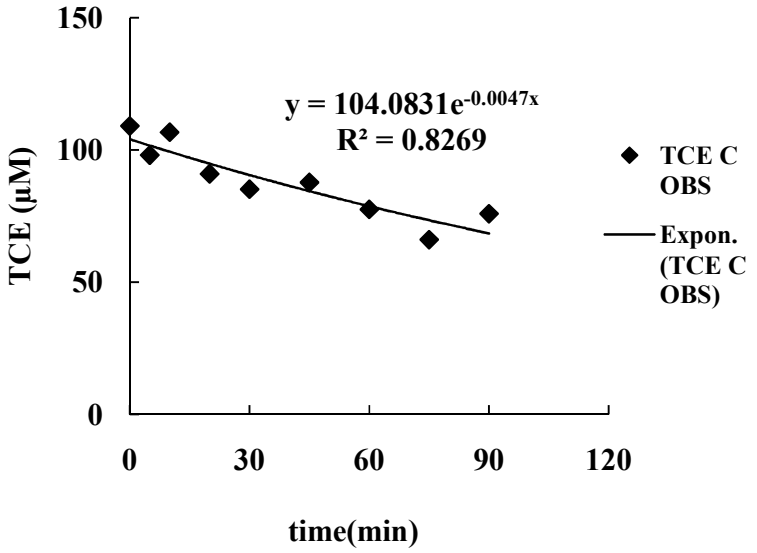

Figure A.2: TCE batch experiment observed data with Fe/V at 120.7 g/L and 17 days aged. This was the third experiment of GEM #23.

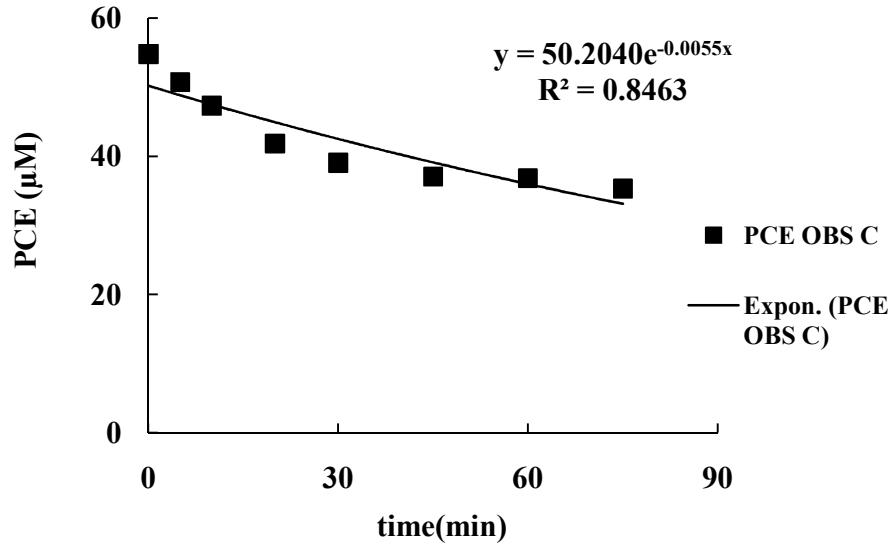

Figure A.3: PCE batch experiment observed data with Fe/V at 121.6 g/L and 8 days aged. This was the second experiment of GEM #27.

High performance liquid chromatography (HPLC) was used to analyze TCE, PCE and 4ClNB samples. The HPLC settings were: an injection volume of 30 μL, flow speed of 1m/min, stop time was 5.5 minutes, post time was 0 minutes. The mobile phase was 40% water, 30% acetonitrile (Yabusaki *et al.*) and 30% methanol. The maximum fluid pressure was 40 bars, the minimum fluid pressure was 0 bars. The detection wavelength was 254 nm, and the reference wavelength was 360 nm. Detection limit is about 1 μM.

Appendix B BearPE Fitting of Tracer Test Result

Column experimental data were fitted using BearPE (a FORTRAN code for the nonlinear fitting of data to the advection dispersion equation with reaction and sorption) to get an estimate of k_{obs}, the initial concentration, C_o, and the retardation factor, R_f. To test the accuracy of the BearPE estimates of k_{obs}, R_f, and C_o, a tracer test was conducted and analyzed by BearPE.

Initial guesses of parameters are: the flow velocity at 0.1376E-3 (m/sec), the dispersivity at 0.5E-3 (m), the retardation factor was fixed at 1, the first order decay constant was fixed at an arbitrarily low value of 0.1E-4 (sec^{-1}). Tracer test results confirm that BearPE solution is capable of estimating C_o and velocity of column experiment accurately.

Table B.1: Comparison the result of tracer test with BearPE fitting.

	Q(mL/min)	A(cm^2)	porosity	Velocity	
				(m/sec)	(cm/min)
Tracer Test	1.14	1.77	0.69	0.941	0.000156
BearPE				0.984	0.000164

Table B.2: Tracer test result.

	First tracer test			Second tracer test	
time(min)	Drops of silver nitrate titrant	Cl^{-1}(mg/L)	time(min)	Drops of silver nitrate titrant	Cl^{-1}(mg/L)
0	0	0	0	0	0
3	0	0	3	0	0
6	1	52.5	6	1	52.5
10	2	105	10	2	105
14	2.5	131.25	14	2.5	131.25
15	3	157.5	18	3	157.5
22	4	210	22	4	210
26	5	262.5	26	5	262.5
30	6	315	30	6	315
40	7	367.5	40	7	367.5
50	7	367.5	50	7	367.5
60	7	367.5	60	7	367.5

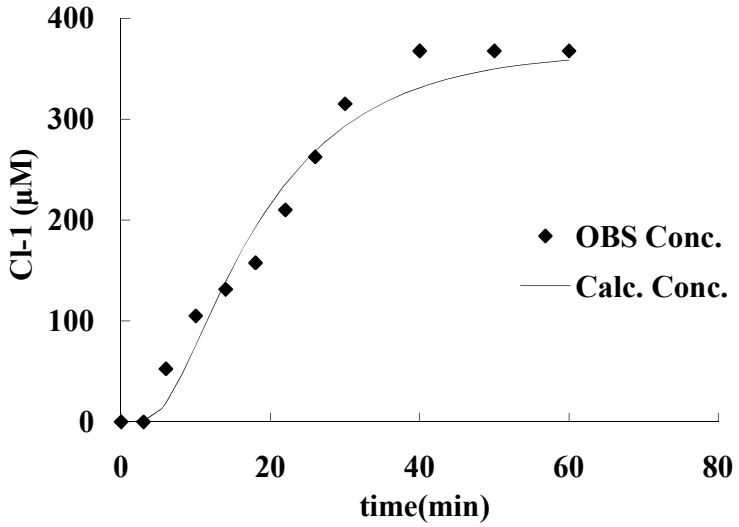

Figure B.1: BearPE fitting for the chloride tracer test.

Appendix C Effect of Metal Loading and pH

Iron loading is one of the most significant experimental variables that can influence reaction rates of dehalogenation (Matheson and Tratnyek, 1994). It is believed that the reaction rate is proportional to the iron loading. Some researchers have hypothesized that a non-linear relationship between iron loading and reactivity might be caused by a shift from kinetic to mass transfer control (Gotpagar *et al.*, 1997; Arnold, 1999; Friis *et al.*, 2007b). Gotpagar *et al.* (1997)used 40 mesh (0.354 mm) and 100 mesh (0.149 mm) iron reacting with 80 mg/L TCE at pH 6.25. Their study demonstrated the reaction rate is not linearly relative to metal loading or surface area when the iron water ratio was bigger than 250 g/L (Gotpagar *et al.*, 1997).

Some studies showed a linear relationship between reaction rates and iron loading (or surface area) (Matheson and Tratnyek, 1994; Sivavec *et al.*, 1996; Arnold, 1999; Deng *et al.*, 1999; Su and Puls, 1999; Moore *et al.*, 2003). Matheson and Tratnyek (Matheson and Tratnyek, 1994) even obtained a linear regression line of k_{obs} (T^{-1}) versus surface area concentration for dechlorination by Fisher granular iron:

$$K_{obs}=0.0025(\pm 0.0002)\ [\text{Fe surface area}]+0.017(\pm 0.005) \qquad \text{C.1}$$

Hence it is necessary to test if iron loading could affect the reaction rate. In this study, the effect of different iron loadings was carried by conducting a series of runs at an initial TCE concentration of 20.5±3 μM but with various amounts of iron in different GEM systems (Figure C.1).

As Figure C.1 reveals, the pseudo-first order reaction rate is proportional to iron loading. In the respect, this study's results are consistent with other studies. Re-expressing the L-H kinetic model to equation C.2 as a transformed pseudo-first order

kinetic model, reveals that for same reactant, the reaction rate of batch experiment should have a linear relationship with initial concentration, when C_o is low.

$$\frac{dC_0}{dt} = -\left(\frac{kC_{max}}{\frac{1}{J} + C_0}\right)\frac{Fe}{V}C_0 \qquad \text{C.2}$$

Also some researchers proposed a possibility that there are reactive sites and non-reactive sites on the solid surface, based on nonlinear adsorption behaviors observed for TCE and PCE (Burris *et al.*, 1998; Bi *et al.*, 2009b). It is probable that there is a constant proportion of TCE and PCE sorbed to reactive sites over non-reactive sties. Increasing iron loading or solid surface area will increase the total number of reactive and non-reactive sites, and the total mass sorbed on the reactive and non-reactive sites. So at the same initial concentration, increasing iron loading will increase the reaction rate.

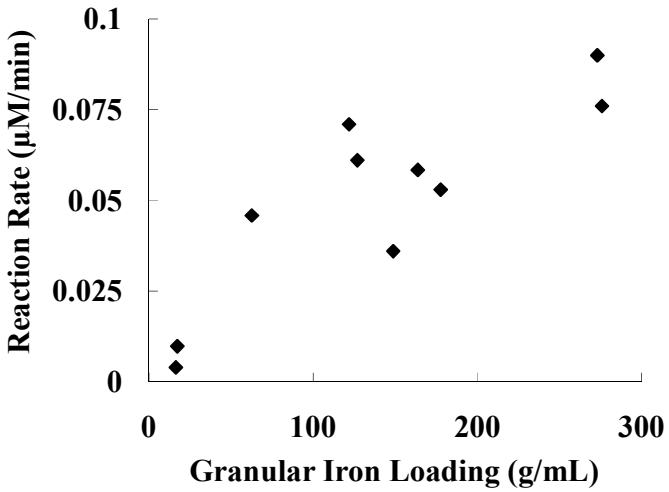

Figure C.1: Effect of metal loading on TCE reacting with granular iron in GEM. Initial concentrations of TCE were 20.5±3 µM. Experiments were conducted same as described in Appendix A.

The pH of the NaClO4 solution introduced to the GEM reactors was 10±0.05. Aqueous samples taken at the end of three TCE batch experiments and two column

experiments declined in pH as low as 8.8±0.2. Although granular iron contacted water commonly has a pH between 8 and 10 (Pulsa *et al.*, 1999; Klausen *et al.*, 2003; McMahon *et al.*, May 1999), a decreasing pH is unusual but has also been reported in other studies, especially when TCE is at high concentrations (Matheson and Tratnyek, 1994); (Grant and Kueper, 2004; Bi *et al.*, 2009b).

Appendix D Calculation of KIM Parameters

To obtain the value of parameters J and the lumped parameters k^*C_{max}, pseudo-first-order kinetic was re-expressed with L-H kinetic model for all set of batch tests, as showed in equation D.1:

$$\frac{dC_0}{dt} = -\left(\frac{kC_{max}\frac{Fe}{V}}{\frac{1}{J}+C_0}\right)C_0 = -K'C_0 \qquad \text{D.1}$$

where Fe/V is iron water ratio (M/L^3), C_{max} is the surface capacity for sorption (M/M_{solid}), J is the Langmuir sorption parameter describing affinity of solute for solid (L^3/M), k is first-order rate constant (T^{-1}), k' is the pseudo-first order reaction rate constant (T^{-1}).

Fitting experimental data with the L-H model can be done with linearized versions of nonlinear rate equations. However, linearization procedures alter the error distribution of data sets and change the relationship that is assumed to exist between dependent and independent variables (Garfinkel *et al.*, 1977; Marietta and Devlin, 2005). Therefore, parameter estimates based on multiple sets of batch and column experimental result can be inaccurate. A nonlinear simplex optimization was applied to obtain best fit parameters for unweighted reaction rates and initial concentrations of all batch and column experiments (Devlin, 1994).

Rearranging equation D.1 and assembling all of the equations of a suite into a matrix form, as introduced by Devlin and Allin (Devlin and Allin, 2005):

$$\begin{bmatrix} -1 & \frac{\left(\frac{Fe}{V}\right)_1}{k_1'} \\ -1 & \frac{\left(\frac{Fe}{V}\right)_2}{k_2'} \\ \vdots & \vdots \\ -1 & \frac{(\frac{Fe}{V})_n}{k_n'} \end{bmatrix} \begin{bmatrix} 1/J \\ kC_{max} \end{bmatrix} = \begin{bmatrix} Co_1 \\ Co_2 \\ \vdots \\ Co_n \end{bmatrix} \quad \text{D.2}$$

where n is the number of batch experiments in the suite. Since C_{on} and k_n' of batch experiments were estimated by pseudo-first order kinetic model, and *Fe/V* was measured, equation D.2 can be solved and yield the value of parameters *J* and k^*C_{max}. Normally a set of unique estimates of *J* and k^*C_{max} can be calculated with equation D.2 for each species.

To separate the lumped parameters kC_{max}, the KIM model was applied to fit with column experimental data. It was assumed that sorption affinity (*J*) was the same for batch and column experimental systems. By assuming zero as the initial background concentration, and no production of solute, a solution of advection-dispersion equation with first order reaction (Equation D.3) was applied to estimate the column reaction rate and initial concentration C_o (Bear, 1979; Van Genuchten and Alves., 1982):

$$C(x,t) = \frac{C_0}{2}\left[exp\left\{\frac{Vx}{2D}(1 - \sqrt{1 + \frac{4kD}{V^2}})\right\} erfc\left\{\frac{Rx - Vt\sqrt{1 + \frac{4kD}{V^2}}}{2\sqrt{DRt}}\right\} + exp\left\{\frac{Vx}{2D}(1 + \sqrt{1 + \frac{4kD}{V^2}})\right\} erfc\left\{\frac{Rx + Vt\sqrt{1 + \frac{4kD}{V^2}}}{2\sqrt{DRt}}\right\}\right] \quad \text{D.3}$$

where k is pseudo-first order rate constant (T^{-1}); V is flow velocity (L/T); R is a retardation factor (dimensionless); x is distance (L); t it time (T); C_o is the initial concentration (M/L^3); D is the dispersion coefficient (L^2/T), which is calculated by equation D.4:

$$D = aV + D^*/n \qquad \text{D.4}$$

where α is dispersivity (L), n is porosity (dimensionless), D^* is molecular diffusion coefficient (L^2/T). The column data were then processed with a linearized form of equation

D.5 to calculate the best fit estimated of k and C_{max} for each reactant.

$$\begin{bmatrix} \frac{(\frac{Fe}{V})_1 k'_1}{1+JCo_1} & (\frac{Fe}{V})_1 Co_1 \\ \frac{(\frac{Fe}{V})_2 k'_2}{1+JCo_2} & (\frac{Fe}{V})_2 Co_2 \\ \vdots & \vdots \\ \frac{(\frac{Fe}{V})_n k'_n}{1+JCo_n} & \left(\frac{Fe}{V}\right)_n Co_n \end{bmatrix} \begin{bmatrix} C_{max} \\ kC_{max} \end{bmatrix} = \begin{bmatrix} -k'_1(Co_1 + \frac{1}{J}) \\ -k'_2(Co_2 + \frac{1}{J}) \\ \vdots \\ -k'_n(Co_n + \frac{1}{J}) \end{bmatrix} \qquad \text{D.5}$$

In equation D.2 and

D.5, each matrix row represents an experiment with a specific initial concentration C_o. With the KIM model, the parameter values of k, C_{max} and J were obtained for each reactant.

Appendix E Customized FORTRAN Program

The kinetic modeling for both batch and column experimental data were performed using a customized FORTRAN program (KIM2P and KIMPE) programmed by Devlin. The three kinetic and adsorption parameters k, C_{max} and J could be obtained in a single fitting process based on observed batch and column experimental data sets of k_{obs} and initial concentration C_o estimated with a first order kinetic model.

The input parameters for KIMPE are the surface rate constant, k (1/T), the maximum sorption concentration, C_{max} (M/M), and the Langmuir parameter, J (L^3/M). Example of using the customized FORTRAN program for column experimental set is given at followed (Figure E.1). In this example, input parameters for KIMPE are k at 0.2 min^{-1}, C_{max} at 0.004 μM/g and J at 0.023 L/μM. The synthetic data set is calculated using T-KIM with k at 0.2 min^{-1}, C_{max} at 0.004 μM/g and J at 0.02 L/μM. The fitting of KIMPE gives a residual sum of squares at 0.1214, which is considered quite good.

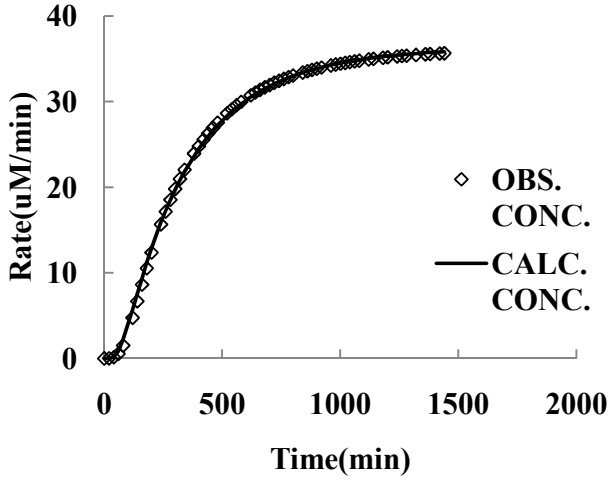

Figure E.1: KIMPE fitting for synthetic column experimental data sets.

Appendix F Analyzing Granular Iron Aging Effects on the Kinetics of Tetrachloroethylene (PCE) Reduction

Chapter 2 analyzed the kinetic parameters for granular columns of different ages reacting with TCE solution. It was concluded that increases in the column exposure time decreased the rate constant and increased the capacity of surface sorption. This research also analyzed an aged granular iron column reacting with PCE. Comparing the changes of kinetic and sorption parameters during column aging following exposure to (and degradation of) TCE and PCE (Table F.1, Figure F.1, Figure F.2, Figure F.3 and Figure F.4), both TCE and PCE aged columns revealed the same trends of deceasing rate constants and increasing sorption capacities. As in the case of the TCE column, the aged PCE column changes were interpreted as occurring due to the loss of fast reactive sites and the gain of slower reactive sites.

Table F.1: Ranges of sorption and kinetic parameters for different aged PCE columns

	Column23	Column 20	Column 25		
Experiment	1-7 days	0-30 days	1-9 days	28-43 days	64-84 days
	Figure F.1		Figure F.2	Figure F.3	Figure F.4
$k(\text{min}^{-1})$	0.08-0.29	0.03-0.2	0.11-0.23	0.04-0.15	0.01-0.03
$C_{max}(\mu\text{mol g}^{-1})$	0.01-0.03	0.03-0.11	0.01	0.01-0.05	0.03-0.05
$J(\mu\text{M}^{-1})$	0.01-0.07	0.01-0.11	0.01-0.04	0.01-0.03	0.04-0.07

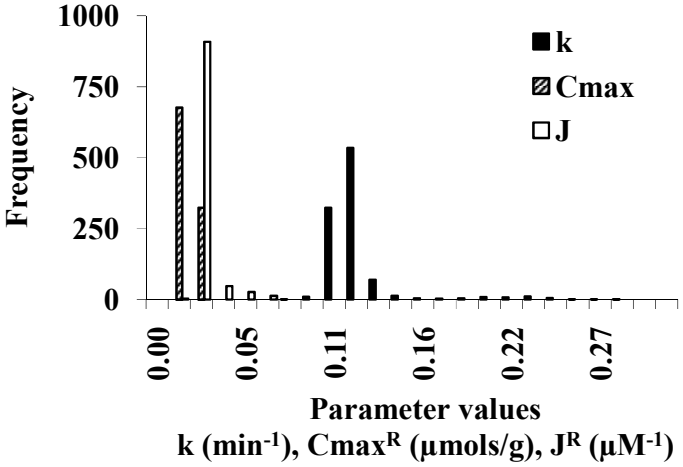

Figure F.1: Frequency of *k*, C_{max} and *J* for PCE contacted iron 1-7 days exposure time (column 23).

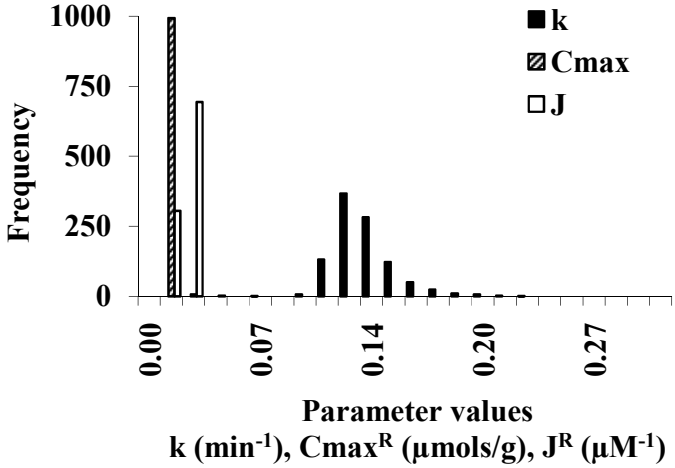

Figure F.2: Frequency of *k*, C_{max} and *J* for PCE contacted iron 1-9 days exposure time (column 25).

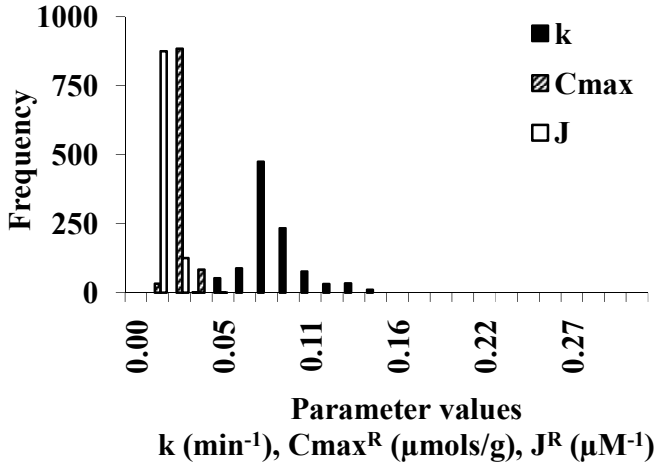

Figure F.3: Frequency of *k*, C_{max} and *J* for PCE contacted iron experiment on day 28-43 (column 25).

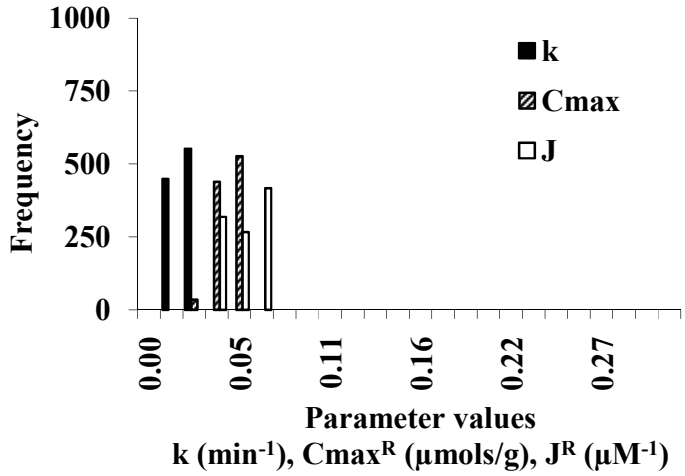

Figure F.4: Frequency of *k*, C_{max} and *J* for PCE contacted iron experiment on day 64-84 (column 25).

Appendix G Comparison of T-KIM and van Genuchten-Alves Analytical Solution

The van Genuchten-Alves analytical solution to the advection dispersion equation considered retardation and (first order) reaction (Genuchten and Alves, 1982) (Equation G.1). van Genuchten-Alves applied a third type boundary condition with C(0,0)=C_o and C(0,t)=C_i). To compare with van Genuchten-Alves, T-KIM was executed with a third type boundary condition, and with a fixed retardation factor and first order rate constant.

$$C(x,t) = \frac{C_0}{2}\left[exp\left\{\frac{vx}{2D}\left(1 - \sqrt{1+\frac{4k_{obs}D}{v^2}}\right)\right\} erfc\left\{\frac{Rx - vt\sqrt{1+\frac{4k_{obs}D}{v^2}}}{2\sqrt{DRt}}\right\} + exp\left\{\frac{vx}{2D}\left(1 + \sqrt{1+\frac{4k_{obs}D}{v^2}}\right)\right\} erfc\left\{\frac{Rx + vt\sqrt{1+\frac{4k_{obs}D}{v^2}}}{2\sqrt{DRt}}\right\}\right] \quad \text{G.1}$$

where C is the aqueous concentration (M/L^3), C_0 is the initial aqueous concentration (M/L^3), v is the pore water velocity (m s^{-1}), D is the dispersion coefficient (m^2 s^{-1}), R is the retardation factor, k_{obs} is the observed rate constant (min^{-1}), x is distance (L) and t is time (T).

The breakthrough curve of a synthetic column experimental data calculated by T-KIM was fitted with van Genuchten-Alves analytical solution for contaminant transport with retardation and reaction. The numerical calculation result of T-KIM is consistent with the result of van Genuchten-Alves analytical solutions (Figure G.1).

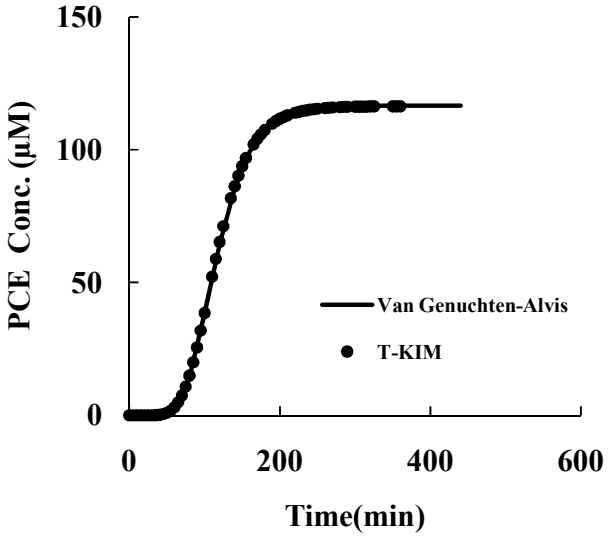

Figure G.1: Synthetic PCE 18 cm long column experimental data C_o at 200 µM was fitted by T-KIM, and van Genuchten-Alvis with fixed retardation factor and rate constant

The breakthrough curves of a synthetic experimental data set were fitted with van Genuchten-Alvis to obtain retardation factors. T-KIM also estimated R_f at specific time and length for each synthetic column experiments. The T-KIM calculated results are well fitted by the analytical model calculated retardation (Figure G.2).

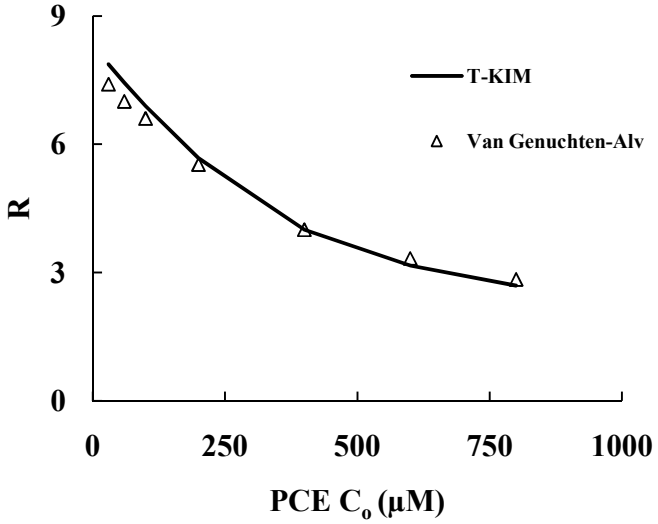

Figure G.2: Compare of T-KIM calculated retardation factor (Rf) (solid line) and van Genuchten-Alv is fitted Rf of PCE synthetic column experiments.

Appendix H Coding the Transport Kinetic Iron Model in Excel

The transport model for PCE is written,

$$\frac{\partial C_{PCE}}{\partial t} = \frac{D_{PCE}}{R_{PCE}}\frac{\partial^2 C_{PCE}}{\partial x^2} - \frac{v}{R_{PCE}}\frac{\partial C_{PCE}}{\partial x} - \frac{\dfrac{k_{PCE}C^R_{max,PCE}(Fe/V)}{\dfrac{1}{J^R_{PCE}} + \dfrac{C^R_{max,PCE}(Fe/V)}{1+J^R_{PCE}} + C_{PCE}}}{R_{PCE}} C_{PCE} - \frac{C_{PCE}}{\dfrac{1+J^S_{PCE}C_{PCE}}{\dfrac{\rho b}{\theta}J^S_{PCE}} + \dfrac{\Gamma^S_{max,PCE}}{1+J^S_{PCE}C_{PCE}}}\frac{\partial \Gamma^S_{max,PCE}}{\partial t} \quad \text{H.1}$$

where *Fe* is iron mass (M); *V* is the volume of water (L^3), and *Fe/V* is equal to ρ_b/θ in 100% packed granular iron medium. C_{PCE} is the aqueous concentration (M/L^3); $C^R_{max,PCE}$ is the capacity of the solid surface to sorb the solute of PCE to reactive sites (M/M_{solid}); J^R_{PCE} is a sorption parameter related to the affinity of PCE for reactive sites (L^3/M); k_{PCE} is the rate constant for the reactions of PCE on the solid surface (T^{-1}); *t* is time (T); *v* is pore water velocity (cm min^{-1}), D_{PCE} is dispersion coefficient (cm^2 min^{-1}) ($D= v\alpha+D^*$, where α is dispersivity (cm), D^* is effective diffusion coefficient (cm^2 min^{-1})); Γ is the concentration of sorbed mass of interest on solid surface (M/M) (note: generalized units are given where *M* is mass or moles, *L* is length and T is time). As showed in equation H.1, the first order observed rate constant is calculated with KIM kinetic parameters.

In equation H.1, D_{PCE}, *Fe/V, v,* J^R_{PCE}, J^S_{PCE} and k_{PCE} were set as constant values. Similarly, TCE and other products were described by D_{TCE}, D_{other}, *Fe/V, v,* $J^R_{TCE,}$ J^R_{other}, J^S_{TCE}, J^S_{other}, k_{TCE} and k_{other} also set as constant values. All other parameters were variable with changing distance *x* and time *t*. The calculations of concentrations (Equation H.11), observed first order rate constant calculated with KIM parameters (Equations H.9 and

H.10), retardation factors (Equation H.2), concentration of sorbed mass of interest on iron surface (Equations H.3, H.4, H.5, H.6, H.7 and H.8) are shown as follows.

$$R_f = 1 + \frac{\rho_b}{\theta} \frac{J^S C^S_{max}}{\left(1 + J^S C\right)^2} \quad \text{H.2}$$

The maximum concentration of sorbed mass of interest on solid surface (M/M) can be calculated as follows.

$$\Gamma^S_{max\ PCE} = C^S_{maxTOT} - \Gamma^S_{TCE} - \Gamma^S_{other} \quad \text{H.3}$$

$$\Gamma^S_{max\ TCE} = C^S_{maxTOT} - \Gamma^S_{PCE} - \Gamma^S_{other} \quad \text{H.4}$$

$$\Gamma^S_{max\ other} = C^S_{maxTOT} - \Gamma^S_{PCE} - \Gamma^S_{TCE} \quad \text{H.5}$$

Equations H.6, H.7 and H.8 were used to calculate Γ^S_{PCE}, Γ^S_{TCE} and Γ^S_{other} at specific time and position.

$$\Gamma^S_{PCE} = \frac{C^S_{\max PCE} C_{PCE}}{\frac{1}{J^S_{PCE}} + C_{PCE}} \quad \text{H.6}$$

$$\Gamma^S_{TCE} = \frac{C^S_{\max TCE} C_{TCE}}{\frac{1}{J^S_{TCE}} + C_{TCE}} \quad \text{H.7}$$

$$\Gamma^S_{other} = \frac{C^S_{\max other} C_{other}}{\frac{1}{J^S_{other}} + C_{other}} \quad \text{H.8}$$

where C^S_{maxPCE} is the nonreactive sorption capacity for PCE (M/M), J^S_{PCE} is sorption parameter related to the affinity of PCE for nonreactive sites (L^3/M), C_{PCE} is the aqueous concentration of PCE (M/L^3). Other parameters are similarly defined for the subscripted substances.

The first order rate constant can be calculated as follows with KIM (Equation H.9) kinetic parameters.

$$\frac{dC}{dt} = -\frac{kC_{max}^{R}(Fe/V)C}{\frac{1}{J^R} + \frac{C_{max}^{R}(Fe/V)}{1+J^R} + C} \qquad \text{H.9}$$

$$k_{obs} = \frac{kC_{max}^{R}(Fe/V)}{\frac{1}{J^R} + \frac{C_{max}^{R}(Fe/V)}{1+J^R} + C} \qquad \text{H.10}$$

A finite difference scheme was employed to solve concentration part of equation H.1 numerically. The combined implicit and explicit solution with the weighting factor is written as equation H.11.

$$C_{x,t} = \gamma(\alpha C_{x+\Delta x,t} + bC_{x-\Delta x,t} + \alpha(\frac{1-\omega}{\omega})C_{x+\Delta x,t-\Delta t} + b(\frac{1-\omega}{\omega})C_{x-\Delta x,t-\Delta t} + eC_{x,t-\Delta t}) - \gamma\delta(\Gamma^{S}{}_{\max x,t} - \Gamma^{S}{}_{\max x,t-\Delta t}) \qquad \text{H.11}$$

Where,

$$\alpha = \frac{\omega D\Delta t}{\Delta x^2 R}$$

$$b = \alpha + \frac{\omega v\Delta t}{R\Delta x}$$

$$e = 1 - \frac{2(1-\omega)D\Delta t}{R\Delta x^2} - \frac{(1-\omega)v\Delta t}{R\Delta x} - \frac{(1-\omega)k\Delta t}{R}$$

$$\gamma = \frac{\Delta x^2}{\left(\Delta x^2 + \frac{2\omega D \Delta t}{R} + \frac{\omega v \Delta t \Delta x}{R} + \frac{\omega k \Delta t \Delta x^2}{R} \right)}$$

$$\delta = \frac{\omega C_{x,t}}{\frac{1 + J^S C_{x,t}}{\frac{Fe}{V} J^S} + \frac{\Gamma^S_{\max,x,t}}{1 + J^S C_{x,t}}} + \frac{(1-\omega) C_{x,t-\Delta t}}{\frac{1 + J^S C_{x,t-\Delta t}}{\frac{Fe}{V} J^S} + \frac{\Gamma^S_{\max x,t-\Delta t}}{1 + J^S C_{x,t-\Delta t}}}$$

To code the T-KIM model into Excel, the concentrations, retardation factors, concentration of sorbed mass of interest on iron surface concentration and first order rate constant parts must be available. Each of these equations was given an identical grid, 52 cells by 73 cells in this calculation. Figure H.1 illustrates the appearance of these grid clusters, which have been placed below the input table and the output graph (generated by plotting the grid of the global equation for PCE). The input parameters have been named are showed in Table H.1.

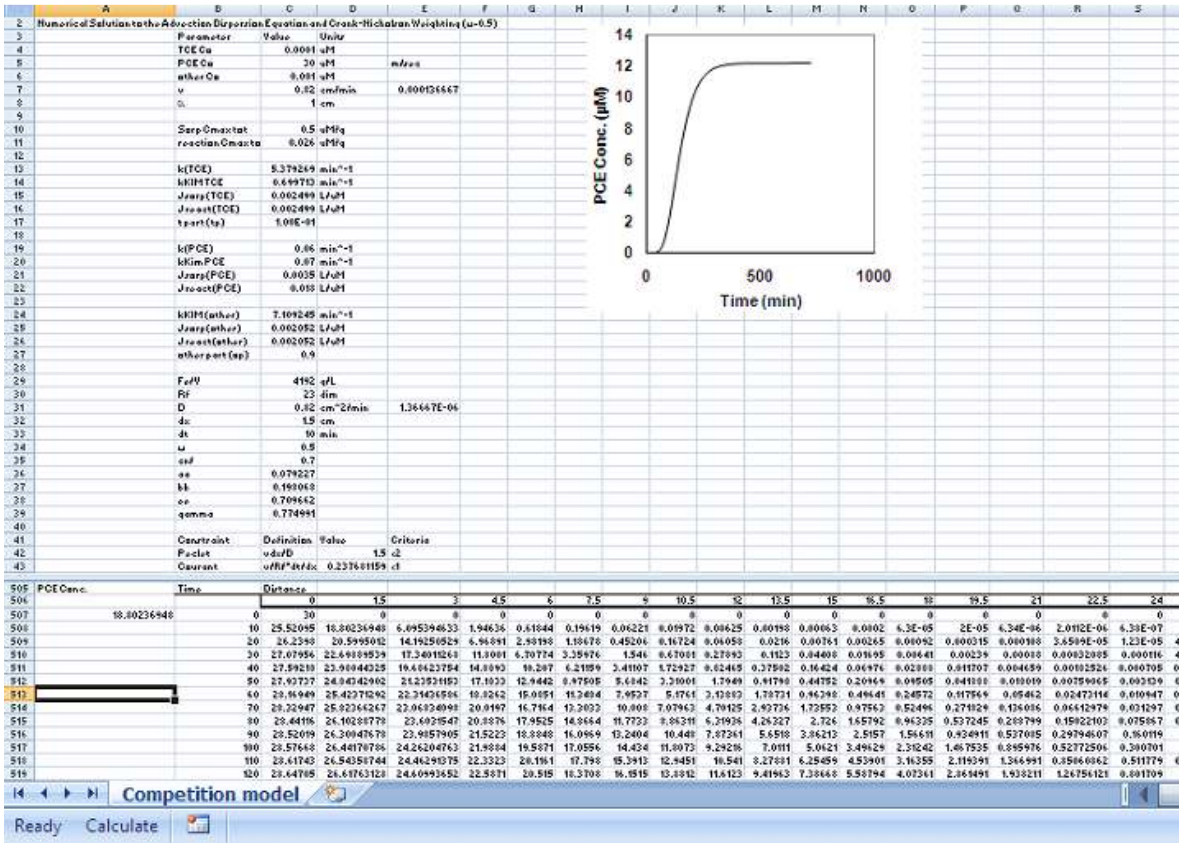

Figure H.1: T-KIM numerical model spreadsheet layout. The calculations for PCE concentration grids and input parameters are shown. The remaining 35 term grids are below or above the visible area.

Table H.1: Input parameters for T-KIM calculation in Excel.

Input Parameter		Units	Named in Excel
TCE Co	Initial concentration of TCE	uM	tcec0
PCE Co	Initial concentration of PCE	uM	Co
other Co	Initial concentration of other products	uM	otherco
ν	velocity	cm/min	v
α	dispersivity	cm	a
Sorp Cmax tot	Maximum sorption capacity for non-reactive sites	uM/g	cmaxtot
reaction Cmax tot	Maximum sorption capacity for reactive sites	uM/g	cmaxtotre
k_{TCE}	rate constant for the reactions of TCE on the solid surface	min^-1	kKIMt
J sorp(TCE)	sorption parameter related to the affinity of TCE for non-reactive sites	L/uM	jt
J react(TCE)	sorption parameter related to the affinity of TCE for reactive sites	L/uM	jrtce

q	Proportion for TCE as daughter products of PCE	dimensionless	tp
k_{PCE}	rate constant for the reactions of PCE on the solid surface	min^-1	kKimp
J sorp(PCE)	sorption parameter related to the affinity of PCE for non-reactive sites	L/uM	jp
J react(PCE)	sorption parameter related to the affinity of PCE for reactive sites	L/uM	jrpce
k_{other}	rate constant for the reactions of other products on the solid surface	min^-1	kkimo
J sorp(other)	sorption parameter related to the affinity of other products for non-reactive sites	L/uM	Jo
J react(other)	sorption parameter related to the affinity of other products for reactive sites	L/uM	jrother
p	Proportion for other products as daughter products of PCE	dimensionless	op
Fe/V	Iron loading	g/L	fev
D	Dispersion coefficient	cm^2/min	D
w	Crank-Nicholson weight	dimensionless	w
bn	Boundary conditions (bn=1 is first type boundary condition, bn=3 is third type boundary condition)	dimensionless	bn

Assuming the same layout as indicated in Figure H.1, the excel equations used to calculate compound input parameters are showed in Table H.2. The T-KIM can be finalized in Excel as showed in Table H.3 with a list of the formulas that should be typed into the top left cell in each grid except boundary condition was changed

Table H.2 Equations to calculate compound input parameters in T-KIM.

Term	Excel input Equation	Remarks
D	=α*ν	
Peclet	=ν*dx/D	
Courant	=ν /R_f*dt/dx	R_f is a value calculated from $C_{1/2}$

Table H.3 Final touches to T-KIM in Excel with typed formulas at top left cell in each grid at time 0 and distance 0 (except the cells at specific x and t).

parameter	Excel Equation	
$R_{f,\,PCE}$	1+fev*C812*jp/(1+jp*C508)^2	
α PCE	w*D*dt/(dx^2*C126)	
b PCE	C202+w*v*dt/(dx*C126)	
c PCE	1-2*(1-w)*D*dt/(dx^2*C126)-(1-w)*v*dt/(dx*C126)-(1-w)*C1805*dt/C126	
γ PCE	dx^2/(dx^2+2*w*D*dt/C126+w*v*dt*dx/C126+w*dt*dx^2*C1805/C126)	
C PCE	$C_{o,PCE}$	x=0, t=0
	IF(bn=1, (1/(D/dx+v)*(v*Co+D*D508/dx)), Co)	x=0, t>0
	0	x>0, t=0
	IF(D431*(D203*E508+D279*C508+D203*(1-w)/w*E507+D279*(1-w)/w*C507+D355*D507)-D431*D1421<0,0,D431*(D203*E508+D279*C508+D203*(1-w)/w*E507+D279*(1-w)/w*C507+D355*D507)-D431*D1421)	x>0, t>0
C TCE	$C_{o,TCE}$	X≥0, t=0
	IF(bn=1, (1/(D/dx+v)*(v*tcec0+D*D584/dx)), tcec0)	X=0, t>0
Γ^{S}_{TCE}	C887*C583/(1/jt+C583)*A735	
C^{S}_{maxPCE}	IF(cmaxtot-C735-C2414>cmaxtot,cmaxtot,IF(cmaxtot-C735-C2414<0,0,cmaxtot-C735-C2414))	
C^{S}_{maxTCE}	IF(A888=1,IF(cmaxtot-C659-C2414>cmaxtot,cmaxtot,IF(cmaxtot-C659-C2414<0,0,cmaxtot-C659-C2414)),cmaxtot)	
$R_{f,TCE}$	1+fev*C887*jt/(1+jt*C583)^2	
α TCE	w*D*dt/(dx^2*C963)	
b TCE	C1040+w*v*dt/(dx*C964)	
c TCE	1-2*(1-w)*D*dt/(dx^2*C963)-(1-w)*v*dt/(C963*dx)-(1-w)*C1881*dt/C963	
γ TCE	dx^2/(dx^2+2*w*D*dt/C963+w*v*dt*dx/C963+w*kt*C1881*dx^2/C963)	

Table H.3: (continued) Final touches to T-KIM in Excel with typed formulas at top left cell in each grid at time 0 and distance 0 (except the cells at specific x and t).

δ TCE	0.0001	x≥0, t=0
	(w*C584/((1+jt*C584)/(fev*jt)+C888/(1+jt*C584))+(1-w)*C583/((1+jt*C583)/(fev*jt)+C887/(1+jt*C583)))*(C888-C887)*A1344	x≥0, t>0
δ PCE	0.0001	x≥0, t=0
	(w*C508/((1+jp*C508)/(fev*jp)+C812/(1+jp*C508))+(1-w)*C507/((1+jp*C507)/(fev*jp)+C811/(1+jp*C507)))*(C812-C811)*A1421	x≥0, t>0
Γ^R_{TCE}	C1574*C583/(1/jrtce+C583)	
Γ^R_{PCE}	C1728*C507/(1/jrpce+C507)	
C^R_{maxPCE}	IF(cmaxtotre-C1497-C2643>cmaxtotre, cmaxtotre, IF(cmaxtotre-C1497-C2643<0, 0, cmaxtotre-C1497-C2643))	
C^R_{maxTCE}	IF(cmaxtotre-C1651-C2643>cmaxtotre, cmaxtotre, IF(cmaxtotre-C1651-C2643<0,0,cmaxtotre-C1651-C2643))	
$k_{obs,\ PCE}$	kKimp*C1728*fev/(1/jrpce+C1728*fev/(1+jrpce)+C507)	
$k_{obs,\ TCE}$	kKIMt*C1574*fev/(1/jrtce+C1574*fev/(1+jrtce)+C583)	
$R_{f,\ other}$	1+fev*jo*C2490/(1+jo*C2338)^2	
α other	w*D*dt/(dx^2*C1958)	
b other	C2034+w*v*dt/(C1958*dx)	
c other	1-2*(1-w)*D*dt/(C1958*dx^2)-(1-w)*v*dt/(C1958*dx)-(1-w)*C2795*dt/C1958	
	IF(D509*tp*D1807/D965+D1269*(D1041*E585+D1117*C585+D1041*(1-w)/w*E584+D1117*(1-w)/w*C584+D1193*D584)-D1269*D1345<0,0, D509*tp*D1807/D965+D1269*(D1041*E585+D1117*C585+D1041*(1-w)/w*E584+D1117*(1-w)/w*C584+D1193*D584)-D1269*D1345)	x>0, t>0
Γ^S_{PCE}	C811*C507/(1/jp+C507)	
γ other	dx^2/(dx^2+2*w*D*dt/C1958+w*v*dt*dx/C1958+w*C2795*dt*dx^2/C1958)	
δ other	0.0001	x≥0, t=0 and x=0, t≥0

Table H.3 (continued) Final touches to T-KIM in Excel with typed formulas at top left cell in each grid at time 0 and distance 0 (except the cells at specific x and t).

	(D2491-D2490)*(w*D2339/((1+jo*D2339)/(fev*jo)+D2491/(1+jo*D2339))+(1-w)*D2338/((1+jo*D2338)/(fev*jo)+D2490/(1+jo*D2338)))	x>0, t>0
C other	0.0001	X≥0, t=0
	IF(bn=1, (1/(D/dx+v)*(v*otherco+D*D584/dx)), otherco)	X=0, t>0
	IF((D1806*op*D508/D1959+D2263*(D2035*E2339+D2111*C2339+D2035*(1-w)/w*E2338+D2111*(1-w)/w*C2338+D2187*D2338)-D2263*D2568)<0, 0, (D1806*op*D508/D1959+D2263*(D2035*E2339+D2111*C2339+D2035*(1-w)/w*E2338+D2111*(1-w)/w*C2338+D2187*D2338)-D2263*D2568))	x>0, t>0
Γ^{S}_{other}	C2490*C2338/(1/jo+C2338)	
$C^{S}_{max,\ other}$	IF((cmaxtot-C659-C735)>cmaxtot, cmaxtot, IF((cmaxtot-C659-C735)<0, 0, cmaxtot-C735-C659))	
Γ^{R}_{other}	C2719*C2338/(1/jrother+C2338)	
$C^{R}_{max,\ other}$	IF(cmaxtotre-C1497-C1651>cmaxtotre, cmaxtotre, IF(cmaxtotre-C1497-C1651<0, 0, cmaxtotre-C1497-C1651))	
$k_{obs,\ other}$	kkimo*C2719*fev/(1/jrother+C2719*fev/(1+jrother)+C2338)	

Appendix I Comparison of Connelly Iron and QMP Iron

Batch experimental data were fitted with a first order kinetic model from which an apparent rate constant, k_{obs}, and the initial concentration, C_o, were obtained for each experiment. Activation energy was then calculated using the k_{obs} values (Table I.1). Because of the scattering of original experimental results, it is not able to estimate the activity energy at some sections. The E_a of the reaction between Connelly iron and 4ClNB ranged from 1.4-54.5 KJ/μM, E_a of the reaction between QMP iron and 4ClNB are ranged from 5.52-66.1 KJ/μM. It is difficult to decide if the degradation was diffusion controlled or not based on the wide range of E_a. Following an aqueous temperature change from 40 ºC to 60 ºC, both dechlorination of Connelly iron and QMP iron exhibited substantial increases in E_a, indicating the dechlorination reactions were probably controlled by electron transfer.

Table I.1: Activity energy calculated with k_{obs} of the reaction between Connelly or QMP iron and 4ClNB at different initial concentrations and temperatures.

		Connelly iron		QMP iron	
4ClNB (μM/L)	T (C°)	k_{obs} (min^{-1})	E_a (KJ/μM)	k_{obs} (min^{-1})	E_a (KJ/μM)
10	23	0.02	1.4	0.017	5.52
	40	0.023	33.9	0.019	15.26
	60	0.05		0.027	
50	23	0.017		0.006	17.4
	40	0.014	44.6	0.009	45.5
	60	0.039		0.026	
100	23	0.011	1.95	0.005	19.34
	40	0.012	54.5	0.007	48.43
	60	0.042		0.022	
200-250	23	0.006	29.41		
	40	0.007	12.99	0.004	66.11
	60	0.023		0.017	
300	23				
	40			0.003	54.11
	60	0.03		0.011	
425	23				
	40			0.002	59.06
	60	0.022		0.008	

Observed data sets of k_{obs} and C_w were fitted with the L-H model to obtain the kinetic parameters k^*C_{max} and J. Activity energy was then calculated using the k^*C_{max} values (Table I.2). E_a increased with increasing temperature, which confirmed that activity energy was temperature dependent.

Table I.2: Activity energy calculated with k^*C_{max} of the reaction of Connelly or QMP iron reacting with 4ClNB at different initial concentration and temperature.

	T (ºC)	J ($L\mu M^{-1}$)	k^*C_{max} ($\mu Mg^{-1}min^{-1}$)	E_a ($KJ\mu M^{-1}$)
Connelly iron	23	0.015	0.13	7.04
	40	0.018	0.15	93.85
	60	0.002	1.33	
QMP iron	23	0.027	0.05	6.61
	40	0.024	0.05	67.9
	60	0.253	0.25	

Appendix J Long Term Sample Storage Test and Blank Test for GEM and Column Reactors

Since samples from GEM and column experiments were stored up to 24 hours before analysis, it is necessary to test the effect of sample storage on sample integrity. TCE aqueous solutions (2 mL) were prepared in deionized water and kept in sample vials without headspace, in a fashion similar to the samples from experiments. These TCE solutions were prepared with initial concentrations of about 600 μM and were kept in a refrigerator for up to 48 hours. The results (Figure J.1), confirmed that for at least 48 hours, there was no significant change in concentration for these aqueous samples..

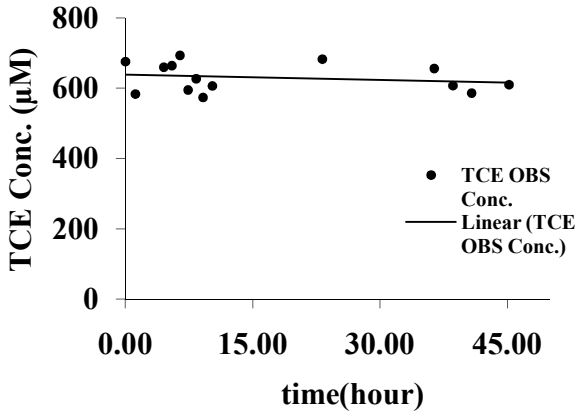

Figure J.1: Long term sample storage test.

Blank tests for the GEM and column reactors were also performed. GEM reactors the same as described in Appendix A were used, but were prepared without any iron added to the reactor. The procedure of the blank tests was the same as that used in the other experiments. In each blank GEM test, a stock solution of TCE or PCE was mixed with about 170 ml of 8 mM $NaClO_4$ solution. Samples were taken at predetermined intervals. Low and high initial concentrations were tested to better represent the range of

concentrations used in actual experiments. The standard 90-minute (or longer) test period was applied in the blank tests. The results confirmed that no considerable mass loss occurred in the reactors during the tests for either TCE or PCE (Figure J.2).

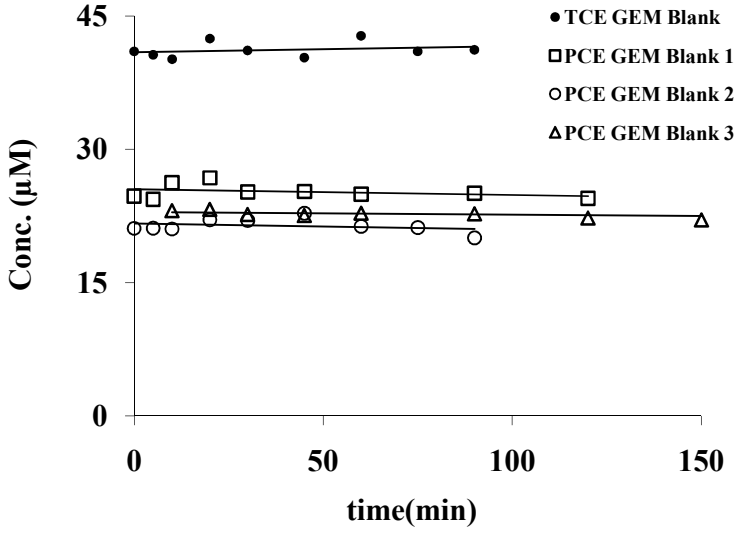

Figure J.2: GEM blank test for TCE and PCE at low initial concentration at standard test period. Lines are linear trend line for observed points.

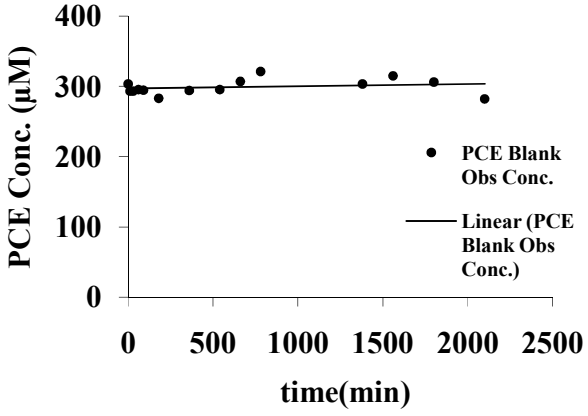

Figure J.3: GEM blank test for PCE at higher initial concentration and longer period. Solid round points represent GEM blank test for PCE (C_o=300 µM).

A blank TCE column test was also performed in this study. Again, the same experimental method as that used in non-blank tests was used, as described in Chapter 2.

A glass column was filled with 50.66 g of glass beads. The column was 17.66 cm in length and was found to have a porosity of 47% gravimetrically. The feed solution (120 μM TCE) was prepared in a Teflon bag and connected to the glass column with Viton tubing. The pumping speed was set to 1 mL/min. A breakthrough curve was generated from which it was determined that there was no noticeable mass loss inside the reservoir, tubing, or column (Figure J.4).

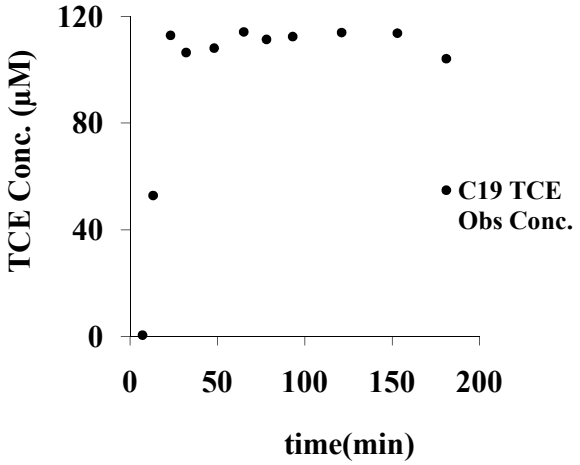

Figure J.4: Column blank test for TCE with glass beads and C_o at 120 μM.

References

Arnold, W. A. (1999). Kinetics and Pathways of Chlorinated Ethylene and Chlorinated Ethane Reaction with Zero-Valent Metals. Department of Geography and Environmental Engineering. Baltimore, Maryland Johns Hopkins University. PhD.

Bear, J. (1979). Hydraulics of Groundwater (Mcgraw-Hill Series in Water Resources and Environmental Engineering) New York, McGraw-Hill Companies.

Bi, E., J. F. Devlin and B. Huang (2009). "Effects of Mixing Granular Iron with Sand on the Kinetics of Trichloroethylene Reduction." Ground Water Monitoring and Remediation 29(2): 56-62.

Burris, D. R., R. M. Allen-King, V. S. Manoranjan, T. J. Campbell, G. A. Loraine and B. Deng (1998). "Chlorinated Ethene Reduction by Cast Iron: Sorption and Mass Transfer." Journal of Environmental Engineering 7: 1012-1019.

Deng, B., D. R. Burris and T. J. Campbell (1999). "Reduction of Vinyl Chloride in Metallic Iron-Water Systems." Environmental Science & Technology 33(15): 2651-2656.

Devlin, J. F. (1994). "A SIMPLE AND POWERFUL METHOD OF PARAMETER-ESTIMATION USING SIMPLEX OPTIMIZATION." Ground Water 32(2): 323-327.

Devlin, J. F. and K. O. Allin (2005). "Major Anion Effects on the Kinetics and Reactivity of Granular Iron in Glass-encased Magnet Batch Reactor Experiments." Environmental Science and Technology 39: 1868-1874.

Friis, A. K., A. C. Heimann, R. Jakobsen, H. J. Albrechtsen, E. Cox and P. L. Bjerg (2007). "Temperature dependence of anaerobic TCE-dechlorination in a highly enriched Dehalococcoides-containing culture." Water Research 41(2): 355-364.

Garfinkel, L., M. C. Kohn, D. Garfinkel and L. Endrenyi (1977). "SYSTEMS-ANALYSIS IN ENZYME-KINETICS." Crc Critical Reviews in Bioengineering 2(4): 329-361.

Garvin, N. L. and J. F. Devlin (2006). "Minimizing mass transfer effects in granular iron batch tests using GEM reactors." Journal of Environmental Engineering-Asce 132(12): 1673-1676.

Genuchten, V. and W. J. Alves (1982). Analytical Solutions of the One-Dimentional Convective-Dispersive Solute Transport Equation. A. R. S. United States Department of Agriculture.

Gotpagar, J., E. Grulke, T. Tsang and D. Bhattacharyya (1997). "Reductive dehalogenation of trichloroethylene using zero-valent iron." Environmental Progress 16(2): 137-143.

Grant, G. P. and B. H. Kueper (2004). "The Influence of High Initial Concentration Aqueous-phase TCE on the Performance of Iron Wall Systems " Journal of Contaminant Hydrology 74: 13.

Klausen, J., P. J. Vikesland, T. Kohn, D. R. Burris, W. P. Ball and A. L. Roberts (2003). "Longevity of Granular Iron in Groundwater Treatment Processes: Solution Composition Effects on Reduction of Organohalides and Nitroaromatic compounds " Environmental Science and Technology 37: 1208-1218.

Marietta, M. and J. F. Devlin (2005). Separating the Kinetic and Sorption Parameters of Nitroaromatic Compounds in Contact with Granular Iron. 4th International Groundwater Quality Conference. waterloo, canada**:** 6.

Matheson, L. J. and P. G. Tratnyek (1994). "Reductive Dehalogenation of Chlorinated Methanes by Iron Metal." Environmental Science and Technology 28(12): 8.

McMahon, P. B., K. F. Dennehy and M. W. Sandstrom (May 1999). "Hydraulic and Geochemical Performance of a Permeable Reactive Barrier Containing Zero-Valent Iron, Denver Federal Center." Ground Water 37(3): 8.

Moore, A. M., C. H. D. Leon and T. M. Young (2003). "Rate and Extent of Aqueous Perchlorate Removal by Iron Surfaces." Environmental Science & Technology 37(14): 3189-3198.

Pulsa, R. W., C. J. Paula and R. M. Powell (1999). "The Application of In Situ Permeable Reactive (Zero-Valent Iron) Barrier Technology for the Remediation of Chromate-Contaminated Groundwater: A Field Test." Applied Geochemistry 14(8): 11.

Schwille, F. (1988). Dense Chlorinated Solvents in Porous and Fractured Media Model Experiments.

Sivavec, T. M., D. P. Horney and S. S. Baghel (1996). Reductive Dechlorination of Chlorinated Ethenes by Iron Metal and Iron Sulfide Minerals. American Chemical Society Extended Abstract, Industrial and Engineering Chemestry Division**:** 42-45.

Su, C. and R. W. Puls (1999). "Kinetics of Trichloroethene Reduction by Zerovalent Iron and Tin: Pretreatment Effect, Apparent Activation Energy, and Intermediate Products." Environmental Science and Technology 33(1): 163-168.

van Genuchten, M. T. and W. J. Alves. (1982). Analytical Solutions of the One-Dimensional Convective-Dispersive Solute Transport Equation. Riverside, CA 92501.

Yabusaki, S., K. Cantrell, B. Sass and C. Steefel (2001). "Multicomponent reactive transport in an in situ zero-valent iron cell." Environmental Science & Technology 35(7): 1493-1503.